

DISSERTATION

STUDIES ON INTERSPECIES INTERACTIONS DRIVEN BY MICROBIAL INVASION  
THAT SHAPE THE STABILITY AND FUNCTION OF PLANT ASSOCIATED  
MICROBIOMS

Submitted by

Jeongyun Choi

Department of Agricultural Biology

In partial fulfillment of the requirements

For the Degree of Doctor of Philosophy

Colorado State University

Fort Collins, Colorado

Spring, 2026

Doctoral Committee:

Advisor : Jan E. Leach

Pankaj Trivedi

Goutam Gupta

Joshua Chan

Copyright by Jeongyun Choi 2026

All Rights Reserved

## ABSTRACT

### STUDIES ON INTERSPECIES INTERACTIONS DRIVEN BY MICROBIAL INVASION THAT SHAPE THE STABILITY AND FUNCTION OF PLANT ASSOCIATED

Despite increasing recognition of the importance of plant microbiomes in agricultural systems, the mechanisms through which microbial invasions and interspecies interactions influence microbiome stability and functional outputs remain poorly understood. This dissertation investigates how microbial invasions, pathogen suppression, and interbacterial interactions shape microbial community dynamics and functions in plant.

Chapters 2–4 collectively examine how microbial invasion, pathogen suppression, and interbacterial interactions contribute to microbiome stability and function. Chapters 2 and 3 focus on pathogen invasion and subsequent suppression, demonstrating how targeted antimicrobial strategies can not only reduce pathogen titre but also influence microbiome structure and recovery in plant-associated systems. In contrast, Chapter 4 shifts to a controlled synthetic community to dissect how interbacterial interactions drive functional outcomes, independent of pathogen presence.

Chapter 2 evaluates the efficacy of a host-derived chimeric antimicrobial peptide (UGK17) in suppressing *Candidatus Liberibacter asiaticus*, while assessing its impact on the citrus phyllosphere microbiome. This chapter suggests that targeted antimicrobial strategies can control plant pathogens while minimizing unintended disruption of beneficial microbiota.

Chapter 3 further investigates the ecological consequences of pathogen suppression in the field by examining the elimination of *Xylella fastidiosa* in grapevine leaves using the chimeric

antimicrobial peptide UGK17. This chapter highlights that selective pathogen suppression can facilitate microbiome restoration.

Chapter 4 explores how microbial interactions influence functional outputs within microbial communities using a synthetic bacterial community composed of xylanase producing bacteria. This chapter suggests that interbacterial interactions shift in response to neighboring species and that community complexity can contribute to more stable functional outcomes.

Together, these studies provide new insights into how microbial invasions and interspecies interactions shape microbiome stability and function. Understanding these processes will facilitate the development of microbiome-based strategies to improve plant health, enhance crop productivity, and promote resilient agricultural ecosystems.

## ACKNOWLEDGEMENTS

I would like to express my deepest gratitude to my advisor, Dr. Pankaj Trivedi. From the moment you picked me up at Denver Airport on the coldest day, to the day of my dissertation defense, you have been there for me at every important moment throughout my PhD Journey. When I felt overwhelmed and doubted whether I could finish my PhD before my defense, your encouragement kept me going. If you didn't say you believe in me in one of that calls, I would not have made it to the end. I hope to continue growing as a researcher and to meet you often in the scientific community, both of us smiling more along the way.

I would also like to sincerely thank my committee members, Dr. Jan Leach, Dr. Goutam Gupta, and Dr. Joshua Chan, for your support, thoughtful advice, and valuable feedback throughout my PhD journey. Dr. Jan Leach, I am truly looking forward to new journey with you. Dr. Goutam Gupta, I deeply appreciate for providing the AMP which allow me to initiate my research projects. Dr. Joshua Chan, I am sincerely grateful for your patience and for working with me to find solutions during the long period when I struggled to obtain clear results.

To my first lab mate, who showed me that research is fun, Dr. Aritra Roy Choudhury. Thank you for believing in me even more than I believe in myself when I was unsure about starting my PhD. When we first met, we were both young and so broken, and we both have families, and I can finally become a doctor. It feels incredible. Thank you for being like an older brother and best friend to me!

To my friends, Yehwa and Yujin, thank you for always answering my calls from Korea whenever I felt homesick. Because of you, I was able to settle down here and make it through this journey.

To my family, Mom, Dad, and my younger brother Suo, my forever supporters. I love you so much and miss you! Please stay healthy and happy!

To my best, amazing, beautiful, sweet, cuty husband, Brian, You always take care of me even when I didn't realize how tired I was. I am so excited for our future together, filled with more joy and laughter. I love you!

And finally, to my dog Lucy, who stayed by my side through all those log nights. Thank you! I promise I will stay up less now. Let's stay healthy and happy together for many more years. I love you!

## TABLE OF CONTENTS

ABSTRACT.....	ii
ACKNOWLEDGEMENTS.....	iv
CHAPTER 1: INTRODUCTION.....	1
1.1 Potential sources and pathways of microbiome invaders.....	1
1.2 Impact of invaders on the microbiome.....	3
1.3 Mechanisms Behind Microbiome Responses .....	7
1.4 Consequences of microbial interactions.....	13
1.5 Research gaps and scope of the dissertation .....	17
REFERENCES.....	20
CHAPTER 2: A host-derived chimeric peptide protects citrus against Huanglongbing without threatening the native microbial community of the phyllosphere .....	27
2.1 OVERVIEW.....	27
2.2 INTRODUCTION.....	28
2.3 MATERIALS AND METHODS .....	32
2.4 RESULTS AND DISCUSSION .....	38
2.5 CONCLUSION .....	46
REFERENCES.....	48
CHAPTER 3: The elimination of the <i>Xylella fastidiosa</i> in the grapevine by using the chimeric antimicrobial peptide and its impact on the native microbiome .....	55
3.1 OVERVIEW.....	55
3.2 INTRODUCTION.....	56
3.3 MATERIALS AND METHODS .....	58
3.4 RESULT AND DISCUSSION.....	64
3.5 CONCLUSION .....	76
REFERENCE .....	77
CHAPTER 4: Interbacterial interactions determine functional shifts in Xylan degradation.....	81
4.1 OVERVIEW.....	81
4.2 INTRODUCTION.....	82
4.3 MATERIAL AND METHOD .....	84
4.4 RESULT AND DISCUSSION.....	90

4.5 CONCLUSION .....	101
REFERENCES.....	102
CHAPTER 5: CONCLUSION AND FUTURE DIRECTIONS.....	105
APPENDIX.....	108

## CHAPTER 1: INTRODUCTION

The health and stability of these microbiomes are crucial for the overall well-being of their respective ecosystems (J. Suman et al., 2022). However, microbiomes are highly sensitive and can be easily disrupted by various factors, including the introduction of external invaders.

Microbial pathogens disrupt the native microbial balance and reshaping the structure, with cascading effects on ecosystem functionality. For instance, bacteria modify the peptidoglycan in their cell wall to defend against biotic and abiotic threats (Yadav et al., 2018). Also, bacteria can adjust their metabolism based on the surrounding conditions to maximize their proliferation, which may change the beneficial bacteria into pathogens. For example, Getzke et al (2024) showed that osmotic stress enhances the activity of the exometabolite brassicapeptin A in *Pseudomonas brassicacearum*, which disrupts plant cell membranes and shifts the bacterium from a beneficial or non-pathogenic state to a disease-causing one. Invaders have diverse strategies to colonize in new environments by suppressing potential stressors such as antimicrobial molecules, antagonistic microbes, and host immune responses (Trivedi et al., 2020; Weiland-Bräuer, 2021) or by making favorable conditions such as increasing access to limiting nutrients, forming protective biofilms, or altering physicochemical conditions (Barber & Fitzgerald, 2024; Weiland-Bräuer, 2021). Additionally, invaders may have rapid reproductive cycles, enabling them to establish a foothold quickly before native microbes mount significant resistance (Buffie & Pamer, 2013).

### 1.1 Potential sources and pathways of microbiome invaders

Invaders can enter the ecosystem through multiple pathways, ranging from human activities to natural environmental changes. Each pathway has significant impact on invasion dynamics

and can stimulate the invasion in various directions. To prevent or mitigate microbial invaders, it is important to understand the potential sources and pathways.

Invaders can be dispersed by natural mechanisms such as wind, water, or animal and insect vectors. Wind and water can transmit the invaders over vast distances and introduce them to new environments or hosts. For example, contaminated irrigation water can introduce bacterial pathogens such as *Salmonella* or *Escherichia coli* into soil and plant microbiomes, causing downstream effects on human and animal health. Furthermore, this contaminated water can flow into rivers and oceans, potentially influencing aquatic microbiomes and altering microbial community composition in these environments (Rusiñol et al., 2020). Also, bioaerosols generated by wastewater treatment plants contain microorganisms and components of the microbial cells and these can be easily transferred to new environments (Kataki et al., 2022). Additionally, insects can transmit pathogens by injecting bacteria or bacteriophage to various hosts while animals disperse gut microbes through excrement (Rocklöv & Dubrow, 2020). Climate change can accelerate transmission and proliferation of invaders through increased temperatures and extreme fluctuations of weather, which create favorable conditions for establishment of invaders, and through increased migration of insects and plant vectors to new ecosystems (Rocklöv & Dubrow, 2020).

Anthropogenic factors including agricultural practice and global trade have significantly increased the frequency and extent of microbial invasions. Agriculture is a major source of microbiome invaders. The use of microbial inoculants as biofertilizers or biocontrol agents introduces beneficial microbes such as nitrogen-fixing bacteria and mycorrhizal fungi (Hao et al., 2021; Liu et al., 2022). Global trade and transportation move microbial invaders faster and further (Banks et al., 2015). Transport of goods, plants, animals, and even humans can move

microbial invaders, across borders and into new environments and. can facilitate migration of insects or plants which can introduce new microbes into the system or shape their own microbiome (Coats & Rumpho, 2014).

## **1.2 Impact of invaders on the microbiome**

The introduction of invaders can rapidly alter microbial diversity and structure. These changes vary based on the type of invader, its interaction with native microbes, and the plant tissues where the microbiomes reside. Generally, open environments such as rhizosphere have more diverse and dynamic microbial communities compared to host-dependent environments like the endosphere due to their varied niches, nutrients, and exposure to fluctuating environmental factors like temperature, humidity, and nutrient availability. In contrast, host-dependent environments tend to have more host-adapted microbiota as they contain limited resources and dedicated interaction between hosts and microbiota. However, under these limited conditions, high diversity of the microbiome makes it difficult for invaders to colonize due to greater competition for resources and niches (Van Elsas et al., 2012). Also, more complex microbiomes may have higher resource utilization efficiency, leaving fewer resources for the potential invaders (Chen et al., 2022). Although invaders may suppress one microbial group, their function can be supplemented by another group which has similar capabilities. As a result, the native microbiome may experience temporary fluctuations but eventually return to its prior state more quickly and push out the invaders from the communities.

Overall, open environments tend to respond gradually and heterogeneously to invasion, and this change in invasion can be highly affected by the environmental factors and nutrient dynamics. In contrast, host-related environments, react more rapidly and noticeably because host-associated microbiomes are sensitive to the host physiology, tightly regulated by the host's

immune system, and have limited nutrients and niches. Even within the same environment, different types of invaders may show various immediate and long-term consequences since they have distinct interactions with the microbiome.

### **1.2.1 Immediate Effects on Microbial Diversity and Composition**

When the bacterial invaders such as pathogens and bioinoculants are introduced into microbial communities, they initially compete with native microbes for resources and niches, resulting in immediate alterations in microbial community structures. This phenomenon is frequently observed with pathogens. Many studies have shown that the invasion of bacterial pathogens into the soil or plant causes declines in microbial diversity and shifts the community structure, in particular, resulting in a decrease of *Actinobacteria* and *Firmicutes* and an increase of *Proteobacteria* (Gu et al., 2016; Lee et al., 2021). To successfully colonize an environment, bacterial pathogens suppress native bacterial groups by resource depletion or antagonistic interactions (George et al., 2022; Lee et al., 2021). Also, they modify the environment to create favorable conditions to colonize in the host. For example, in the gut, once pathogens recognize that they are in the right place to colonize by recognizing specific molecules, they change the pH of surrounding environment or create new niches for themselves by penetrating host cells, promoting their proliferation and reducing the abundance of beneficial microbes (Woodward et al., 2024).

In contrast to pathogens, the invasion of beneficial bacteria increases microbial diversity, even though they initially may face challenges due to competition and ecological resistance. Their invasion may amend the beneficial microbiota increasing the bacterial richness. Also, their abilities to improve soil fertility by producing organic acids and extracellular polymeric substances (EPS) enhance the nutrient availability to plants and microbiota in soil (Suman et al.,

2022). Moreover, the antimicrobial compounds beneficial bacteria produced suppresses pathogens (Suman et al., 2022). Collectively, these can increase niches and nutrients for the low abundance beneficial and commensal bacteria, promoting a diverse and complex microbial network.

However, beneficial bacteria face greater difficulties in invading the host-related microbiome compared to an open environment due to the host immune system and intense competition. For example, *Pseudomonas fluorescence* can easily colonize in the bulk soil by outcompeting pathogens while its invasion is more dependent on the host such as root exudate or host conditions (Vishnevskaya et al., 2020). The disturbance of the native microbiome by beneficial bacterial invasion is greater when the plant is under stress compared to the normal condition (Martínez-Arias et al., 2022). Harsh environmental conditions for host plants may strengthen the relation between host and invader.

Interestingly, microbial communities react differently to fungal invasion compared to bacteria. Several studies have shown that the invasion of fungal pathogens increases bacterial diversity in the host-related environment (Mendes et al., 2023; Sam et al., 2017; Wan et al., 2024). When pepper is infected by the fungal pathogen such as *Fusarium* wilt disease, plants enrich the abundance of protozoa in the rhizosphere, resulting in an increase of predation within the microbial community (Gao et al., 2024). This puts selective pressure on the community, increasing bacterial diversity by providing niches and resources to less dominant bacterial groups. In the study of Mehmood et al. (2020) demonstrated that although the application of sclerotia of *Sclerotinia sclerotium* decrease the richness and evenness of bacterial and fungal diversity, it could suppress plant pathogens and enrich beneficial microbes in the soil. In this study, declined microbial diversity due to the *Sclerotinia sclerotium* has been recovered over 2

months, suggesting that the microbial community gradually recovered as the fungal colonization progressed and the plant–microbe interactions stabilized.

However, beneficial fungi, such as arbuscular mycorrhizal fungi (AMF), exhibit a completely different impact on the microbiome depending on the environmental condition especially pollution. For example, AMF inoculation increased the bacterial diversity in the rhizosphere under high heavy metal conditions but the diversity decreased without the heavy metal (Hao et al., 2021). This may be because plants may “Cry for help” to the AMF, stimulating colonization by AMF under stressed conditions. The successful colonization of AMF may increase microbial diversity by encouraging plant growth promoting microbes as well as introducing AMF-associated bacteria (Ujvári et al., 2021). However, healthy plants may recognize the invasion of AMF as an attack and trigger the immune system, thereby reducing microbial diversity.

Other invaders, such as bacteriophage and protozoa, also play significant roles in shaping microbiomes. Despite their importance, their impacts on microbiomes are not well studied. As they are difficult to culture and to get a common gene sequence for the amplicon sequencing, the studies on them are biased to the culturable members (Guzzo et al., 2022). Although, bacteriophage are hard to study because they mutate rapidly and have high diversity in their small gene content, their invasion significantly impacts bacterial communities. However, disturbance of bacterial communities due to bacteriophage is not consistent since each bacteriophage targets a specific bacterial group (Li et al., 2019).

Invasion of protozoa tends to increase bacterial diversity (Chabé et al., 2017; Mawarda et al., 2022). Protozoa selectively prey on specific microbial taxa, altering the composition and diversity of microbial communities. Grazing dominant bacterial species can release nutrients and increase ecological niches for less competitive taxa, resulting in promotion of dynamic and

balanced microbial environments (Mawarda et al., 2022). Also, increased predation can enhance the microbial network complexity and stability which can protect hosts from the pathogenic invaders by supporting the native microbiota (Guo et al., 2023; Liu et al., 2024).

### **1.2.2 Long-Term Consequences for Microbial Community Structure**

Microbial communities adapt to the structural changes imposed by long-term invaders with altered functions. The contrasting short-term effects caused by pathogenic and beneficial bacterial invaders may ultimately lead to different long-term outcomes in microbial community structure and function. Microbial communities with pathogens may become dominated by other pathogenic bacteria and deficient to commensal and beneficial bacteria. Eventually, the microbial communities may have balance between the pathogen and the bacteria producing antifungal and antibacterial compounds while it may limit the presence of sensitive native microbes, creating a narrower community diversity. Such shifts may decrease resilience and alter ecosystem functions (Liu & Salles, 2024).

Conversely, the invasion of beneficial microbes can lead to sustained enhancements in microbial diversity and function. In soil, it can encourage stable populations of nutrient-cycling microbes such a nitrogen-fixers and decomposers, creating a complex microbial network that supports plant growth and soil fertility (Poppeliers et al., 2023). This can also enhance the stability and resilience of microbial diversity.

## **1.3 Mechanisms Behind Microbiome Responses**

### **1.3.1 Interaction Dynamics Among Microbial Species**

The response of microbial communities to invaders is governed by the complex interplays of interactions among inherent and invading microbes. When an invader enters a microbial

community, interactions between microbes are disrupted, leading to cascading effects on community structure and function. Understanding the mechanisms behind their responses to invasions is critical for predicting and managing the effects of invaders on microbiome structure and function. These dynamics include competitive strategies, communication systems, genetic exchanges, and physical interactions, all of which contribute to the resistance, adaptation, or transformation of the microbiome.

### **Competition between microbes**

Microbial competition plays a critical role in determining the success of invaders and the resilience of the native community. Competition occurs over limited resources such as nutrients and niches. Bacteria employ a variety of competitive mechanisms, including the secretion of antimicrobial compounds like bacteriocins and antibiotics that inhibit competitors (Palmer & Foster, 2022). For instance, *Pseudomonas fluorescens* produce cyclic lipopeptides and hydrogen cyanide to suppress competitors in both soil and the rhizosphere (Sarkar et al., 2022). Competition can also involve the production of mycotoxins or other secondary metabolites that suppress the bacterial competitors as well as fungi (Venkatesh & Keller, 2019).

In addition, direct interactions facilitated by the type VI secretion system (T6SS) represent a critical mechanism for microbial competition and invasion. The T6SS is a molecular weapon that allows bacteria to inject toxic effectors into adjacent cells, killing competitors or impairing their growth. This system plays a pivotal role in shaping microbial communities and colonization of invaders, particularly in host-associated environments. For example, the T6SS of *P. fluorescence* F113 disrupts native microbial communities by eliminating competitors (Durán et al., 2021). Similarly, *P. protegens*, a promising candidate for controlling plant pest insects that can colonize in insect guts, creates a niche by targeting *Enterobacteriaceae* with T6SS (Vacheron et al., 2019).

## **Quorum sensing and signaling molecules**

Quorum sensing is a cell-to-cell communication system based on the production and detection of signaling molecules, enhancing microbial virulence, biofilm formation, and resource acquisition (Law & Tan, 2022). As cell density rises, the signaling molecules called autoinducers also become concentrated. When the concentration of the autoinducers is over a threshold, expression of a number of genes is activated (Hartmann et al., 2024). The resulting upregulated functions could be beneficial or detrimental to the host, depending on the bacterial species (Hartmann et al., 2024). Invaders can disrupt the quorum sensing of native species, either by producing quorum quenching molecules such as lactonases or competing signals to manipulate the community (Gonzales et al., 2024). The quorum sensing is not limited between bacteria. *P.s aeruginosa* produces homoserine lactone, which inhibits hyphal and biofilm formation in *Candida albicans*, an opportunistic fungal pathogen. (Grainha et al., 2020).

Fungi produce signaling metabolites such as tyrosol and farnesol which influence interactions with bacteria and other fungi. Tyrosol is a secondary metabolite, promoting germ tube, hyphal development and biofilm formation. Interestingly, fungi produce another signaling molecule, farnesol, which inhibits hyphal and biofilm development, effectively regulating fungal virulence (Rodrigues & Černáková, 2020). Some bacteriophage contain genes encoding quorum sensing components that regulate the lysis-lysogeny decision through integration of host cell density information (Silpe et al., 2020). Also, phage promote biofilm formation by enhancing the bacterial quorum sensing signals to increase their chances of spreading to a new host.

## **Biofilm formation**

Biofilms include structured microbial extracellular polymeric substances (EPS), representing

a key adaptive strategy in competitive environments. Biofilms enhance microbial survival by providing physical protection, nutrient trapping, and increased resistance to antimicrobial molecules (Flemming & Wingender, 2010). Invaders may produce biofilms to integrate into the native microbiome or outcompete resident microbes. In open environments such as water and soil, bacterial invaders form mixed-species biofilms so that they can interact more efficiently with native microbes via horizontal gene transfer or the type VI secretion system (Flemming et al., 2023).

### **Lateral gene transfer (LGT)**

Lateral gene transfer is a gene exchange between organisms across species barriers and even between different kingdoms (Emamalipour et al., 2020). Thus, it distinguishes from the traditional parent to offspring inheritance. This process is important to microbial evolution and interactions, enabling microbes to adapt to a new environment rapidly by acquiring beneficial traits like antibiotic resistance, metabolic capabilities, and pathogenicity factors (Emamalipour et al., 2020). Conversely, native microbes may also acquire genes from invaders. Le et al. (2018) found that *Rhizophagus irregularis*, an AMF, has taken some genes from plants and endophytes which may enhance hyphal development, showing that LGT plays a critical role in building symbiosis between AMF-plants-endophytes.

Horizontal gene transfer (HGT) occurs between bacteria via transformation, conjugation, and transduction (Arnold et al., 2022). Through HGT, bacteria can exchange their genes by taking up free DNA fragments from the environment, connecting physically via pilus, or through infection by bacteriophage. Additionally, Phage-mediated transfer of CRISPR-associated genes equips bacteria with tools to resist future phage infections (Jiang & Doudna, 2017). This dynamic coevolution maintains microbial diversity and stability. As biofilms can increase the cell density,

they can enhance interactions between the species leading to HGT.

### **1.3.2 Impacts of host on invasion into microbiome**

The host plays a critical role in shaping microbial community dynamics during an invasion. Hosts, like plants, animals, or humans, influence both the establishment and persistence of invaders in their associated microbiomes, either directly through immune responses and physiological adaptations or indirectly through changes in nutrient availability and habitat conditions. These interactions determine the outcomes of invasion, impacting not only the microbiome but also the host's health.

The host immune system acts as a primary barrier to microbial invasion. Invaders, whether pathogens or beneficial organisms, must navigate this defense system to colonize the host microbiome. In the plant, the innate immune system recognizes microbial invaders using pattern recognition receptors (PRRs), which identify microbe-associated molecular patterns (MAMPs) (Wang et al., 2022). Invaders can bypass this immune response by secreting effectors or plant-resembling plant-associated and root-associated domains (PREPARADOs) (Trivedi et al., 2020). These strategies help the invaders to suppress the plant immune response or mimic plant functions to facilitate a beneficial relationship with the plant (Trivedi et al., 2020).

On the other hand, hosts can regulate microbial invasion by altering nutrient availability and habitat conditions. Plant root exudates selectively promote beneficial microbes under environmentally stressed conditions (Xu & Coleman-Derr, 2019). Under drought conditions, plants release carbon-rich exudates such as malic acid to attract beneficial microbes (Fuchslueger et al., 2014).

Additionally, the different response of microbiomes among the type of invaders may be due

to host recognition. When hosts recognize pathogen infection, they detect molecular markers. For instance, fungi can be detected by the chitin comprising their cell walls while the bacteria are detected by the lipopolysaccharides on their outer membrane. Also, hosts, especially plants, use different strategies to defend against infection. To combat the fungal and bacterial pathogens, plants can produce antimicrobial compounds (Baindara & Mandal, 2022). These can be specific to bacteria or fungi or broadly effective, i.e., suppress both types of pathogens. Therefore, the different impact on the microbiome by the invasion of bacteria and fungi may be driven by the different characteristics between them and host distinguishing the organisms.

### **1.3.3 Environmental and anthropogenic factors influencing microbiome response**

Microbial invasions are influenced by environmental conditions and human activities, with factors such as climate change, pollutants, and agricultural practices. These factors can either facilitate or hinder the success of invaders, depending on the specific contexts of the invasion and the ecosystems involved.

Climate change is one of the major drivers of microbial invasions, and it includes temperature fluctuation, precipitation patterns, and extreme weather events. Higher temperatures may create favorable conditions for invaders or stress native microbes, reducing competition and opening niches for invaders (Li et al., 2023). Zhang et al. (Zhang et al., 2016) showed AMF colonization increases under higher temperatures. Also, exposure to long and extreme heat may decrease the microbial diversity, making the plants more susceptible to invaders (Greenspan et al., 2020). Elevated temperature often brings drought stress to the plant and the native microbial communities, reducing diversity and resilience (Greenspan et al., 2020).

On the other hand, pollutants such as nanoparticles and nanoplastics also significantly affect

invasion and microbiome. Nanoparticles such as metal oxides exhibit antimicrobial properties, selectively suppressing native microbes such as *Actinobacteria* (Moorcroft et al., 2020).

Conversely, nanoplastics can serve as surfaces for microbial colonization, acting as vectors that carry invaders into new environments. For example, *P. aeruginosa* has been shown to colonize plastic particles, facilitating its spread into aquatic ecosystems (Guan et al., 2024). Furthermore, nanoplastics often absorb nutrients and contaminants, creating microenvironments that may favor certain invasive species (Guan et al., 2024).

Lastly, human-driven cultivation practices can influence microbial invasions. Monocropping and intensive farming often reduce microbial diversity, weakening native microbial networks and resilience and making them more vulnerable to invasion (Shu et al., 2024). Also, overuse of pesticides can suppress beneficial native microbes and significantly down-regulate the expression of nitrogen fixation gene such as *nifH* (Walder et al., 2022). Therefore, crop rotation and using bioinoculants, which enhance microbial diversity and resilience and reduce invasion, are considered best practices (Zhou et al., 2023).

## **1.4 Consequences of microbial interactions**

### **1.4.1 Impact on the invader's survival and evolution**

The most critical factors determining whether the invaders survive or are eliminated from the community are the microbial community diversity and host. Liu et al. (2012) showed that microbial diversity is more important in determining colonization and survival of invaders than nutrient availability. In highly diverse microbial communities, the invaders may be eliminated because of community's high resilience, even though they colonized the community (Van Elsas

et al., 2012). However, in low diversity microbial communities, the invaders can survive longer and can eventually change the whole structure and function of the microbial communities (Hu et al., 2022).

The interaction between hosts and invaders may be another important factor to survive. Pathogens often establish stable populations in host-related environments by facilitating plant hormone synthesis to take more nutrients. *Agrobacterium tumefaciens* induces galls on plants by injecting a tumor inducing plasmid (Ti plasmid) into the plant cell. The Ti plasmid contains biosynthetic genes for auxins, cytokinins, and opines, which when expressed, cause the plant cell to divide uncontrollably and synthesize nutrients (opines) that are used by the pathogen (Sakakibara et al., 2005). *P. syringae* produces effector proteins like HrpP that activate salicylic acid signaling and suppress jasmonic acid signaling, thereby suppressing pattern-triggered immunity (PTI), a primary plant immune response (Jin et al., 2023).

Several studies have shown that bioinoculants have short persistence in the soil or rhizosphere, even though they show enhancement of plant immune responses and suppression of pathogenesis (Poppeliers et al., 2023). Darbon and his team (2024) tracked the residence of four different beneficial bacterial strains in the potato roots for 3 years after inoculation. All the strains showed suppression of pathogenic symptoms, but only *Pseudomonas brassicacearum* was detected after 3 years.

Pathogens are more dependent on the host compared to the beneficial bacteria. Therefore, they have evolved to activate host hormone production or suppress its immune system to colonize and survive in the host while beneficial microbes can independently survive and establish symbiosis with the host.

### **1.4.2 Effects on the stability and resilience of the microbial community**

Microbial communities with higher diversity and complex networks exhibit greater resilience to invasion despite its initial disturbance (Shade et al., 2012). This resilience is attributed to the redundancy within the community, where specific taxa performing similar ecological functions can compensate for the suppression or loss of others. This functional redundancy may allow the community to maintain stability and recover from disturbances. However, pathogen invasions can significantly alter microbial community structure and lead to diverse outcomes. Interestingly, the skin microbiota when disturbed by disinfectant recovers its structure after removing the treatment (SanMiguel et al., 2018); however, when the skin microbiota is disturbed by antibiotic treatment, it is replaced by a completely different microbial structure (Proença et al., 2021).

These observations align with the Anna Karenina Principle (AKP) as applied to microbial communities. AKP suggests that "healthy microbial communities are similar in their structure and functionality, whereas disrupted communities diverge in unpredictable ways." This principle highlights how resilient communities maintain stable interactions and resist invasion, while disrupted ones exhibit divergent and often destabilizing responses (Arnault et al., 2023; Zaneveld et al., 2017).

### **1.4.3 Outcomes for the host organism and the environment**

Microbiomes are important to maintain ecosystem functions such as nutrient cycling, protection of host health, and carbon sequestration. When microbial invaders disrupt these communities, each change in the microbiome can cascade through the ecosystem, leading to function alteration or even a complete shift in ecosystem dynamics. First, in the open environment, such as soil and aquatic ecosystems, microbial communities are essential for

nutrient cycling. Invaders can interfere with native microbial processes. For example, pathogenic invaders disrupt the nitrogen cycle by reducing populations of nitrogen fixing bacteria like *Rhizobium* or *Azotobacter* through competition or antagonism (Cao et al., 2024). Conversely, beneficial bacterial invaders, like bioinoculants containing *Pseudomonas fluorescens* or *Bacillus subtilis*, can enhance nutrient availability by promoting the solubilization of phosphates and producing extracellular enzymes such as xylanase (Poppeliers et al., 2023). However, the effects can vary with environmental conditions. In the stressed environments, such as soils polluted with heavy metals, the invasion of AMF can improve nutrient cycling by enhancing the plant growth promoting bacteria and stabilizing toxic ions while disrupting the microbial community without the pollutants (Hao et al., 2021).

While invaders can enhance nutrient availability to the host, pathogen suppression is another important function of microbiome to maintain the host health and enhance its growth. Native microbial communities can suppress pathogenic organisms through competition, predation, and production of antimicrobial compounds. Invaders can strengthen or destabilize these controls. Beneficial microbes such as *Streptomyces* and *Trichoderma* produce antimicrobial compounds including antibiotics such as streptomycin, tetracycline, and gliotoxin and cell wall degrading enzymes such as chitinases and glucanases that suppress pathogenic fungi and bacteria (Khan et al., 2023; Poveda & Eugui, 2022). However, this might affect the pathogen near these invaders rather than entire community because these antimicrobial compounds can impact other microbes. In contrast, pathogens such as *Fusarium* in the rhizosphere or *Clostridium difficile* in the gut, outcompete beneficial microbes, leading to infection and dysbiosis of microbial community (Mendes et al., 2023).

The reason why pathogen suppression is important in the ecosystem is that not only the

microbiome itself but also plant growth promotion is essential for carbon sequestration. Indeed, microbiomes are involved in carbon storage dynamics, and invasion can alter that ability (Chauhan et al., 2023). In contrast, the increased abundance of beneficial bacteria due to invasion can enhance carbon sequestration by stimulating plant growth and increasing root biomass (Liu et al., 2022).

Microbial invasions can cause regime shifts where ecosystems transition to an entirely different functional state. In agricultural systems, invasive pathogens can degrade soil health, reducing crop productivity and carbon sequestration, and resulting in the need for increased use of chemical fertilizers and pesticides. In ecosystems, such shifts can lead to the loss of biodiversity and diminished ecosystem functions.

### **1.5 Research gaps and scope of the dissertation**

While many studies have documented changes in microbial diversity and community composition following invasion, the consequences of these changes for microbial functions and ecosystem processes remain poorly understood. In particular, the mechanisms through which microbial interactions determine invasion outcomes and influence functional responses of microbial communities remain unclear.

In plant associated microbiomes, pathogen invasion represents one of the major disturbances that can alter microbial community dynamics and host health. Although numerous studies have investigated how pathogens disrupt microbial communities, less is known about how microbial communities respond when pathogens are selectively suppressed. Furthermore, microbial functions within communities are often shaped by interactions among microbial species, including competition, metabolic exchange, and cooperative behaviors. However, the extent to

which these interbacterial interactions influence functional outputs within microbial communities remains poorly understood.

To address these knowledge gaps, this dissertation aims to

- Determine how targeted suppression of plant pathogens influences the structure and diversity of plant-associated microbiomes.
- Investigate whether pathogen suppression promotes recovery of native microbial communities.
- Examine how interbacterial interactions influence microbial functional outputs within microbial communities.

This work is divided into three main chapters.

Chapter 2, *A host-derived chimeric peptide protects citrus against Huanglongbing without threatening the native microbial community of the phyllosphere*, evaluates the efficacy of a host-derived antimicrobial peptide in suppressing *Candidatus Liberibacter asiaticus*, the causal agent of citrus Huanglongbing disease. In addition, this chapter investigates the potential impact of pathogen suppression on the structure and diversity of the citrus phyllosphere microbiome.

Chapter 3, *The elimination of Xylella fastidiosa in grapevine using a chimeric antimicrobial peptide and its impact on the native microbiome*, examines how targeted suppression of the bacterial pathogen *Xylella fastidiosa* influences microbial community dynamics in the grapevine leaf microbiome. This chapter focuses on determining whether removal of a pathogen can mitigate pathogen-driven disruptions of microbial communities and promote microbiome recovery.

Chapter 4, *Interbacterial interactions determine functional shifts in xylan degradation*,

investigates how microbial interactions influence functional outputs within microbial communities. Using a synthetic microbial community model consisting of xylanase producing bacteria, this chapter examines how interactions among microbial species influence extracellular enzyme production and community level functional responses.

Together, these studies provide insights into how microbial invasion and microbial interactions shape microbiome stability, function, and ecosystem processes. Understanding these mechanisms may contribute to the development of strategies for managing microbiomes in agricultural systems and improving plant health through targeted manipulation of microbial communities.

## REFERENCES

- Arnault, G., Mony, C., & Vandenkoornhuysse, P. (2023). Plant microbiota dysbiosis and the Anna Karenina Principle. *Trends in Plant Science*, 28(1), 18–30.
- Arnold, B. J., Huang, I.-T., & Hanage, W. P. (2022). Horizontal gene transfer and adaptive evolution in bacteria. *Nature Reviews Microbiology*, 20(4), 206–218.
- Baindara, P., & Mandal, S. M. (2022). Plant-derived antimicrobial peptides: novel preservatives for the food industry. *Foods*, 11(16), 2415.
- Banks, N. C., Paini, D. R., Bayliss, K. L., & Hodda, M. (2015). The role of global trade and transport network topology in the human-mediated dispersal of alien species. *Ecology Letters*, 18(2), 188–199.
- Barber, M. F., & Fitzgerald, J. R. (2024). Mechanisms of host adaptation by bacterial pathogens. *FEMS Microbiology Reviews*, 48(4), fuae019.
- Buffie, C. G., & Pamer, E. G. (2013). Microbiota-mediated colonization resistance against intestinal pathogens. *Nature Reviews Immunology*, 13(11), 790–801.
- Cao, M., Huang, S., Li, J., Zhang, X., Zhu, Y., Sun, J., Zhu, L., Deng, Y., Xu, J., & Zhang, Z. (2024). Disease-induced changes in bacterial and fungal communities from plant below-and aboveground compartments. *Applied Microbiology and Biotechnology*, 108(1), 315.
- Chabé, M., Lokmer, A., & Ségurel, L. (2017). Gut protozoa: friends or foes of the human gut microbiota? *Trends in Parasitology*, 33(12), 925–934.
- Chauhan, P., Sharma, N., Tapwal, A., Kumar, A., Verma, G. S., Meena, M., Seth, C. S., & Swapnil, P. (2023). Soil microbiome: diversity, benefits and interactions with plants. *Sustainability*, 15(19), 14643.
- Chen, W., Wang, J., Chen, X., Meng, Z., Xu, R., Duoqi, D., Zhang, J., He, J., Wang, Z., & Chen, J. (2022). Soil microbial network complexity predicts ecosystem function along elevation gradients on the Tibetan Plateau. *Soil Biology and Biochemistry*, 172, 108766.
- Coats, V. C., & Rumpho, M. E. (2014). The rhizosphere microbiota of plant invaders: an overview of recent advances in the microbiomics of invasive plants. *Frontiers in Microbiology*, 5, 368.
- Darbon, G., Declerck, S., Riot, G., Doubell, M., & Dupuis, B. (2024). Inoculation and tracking of beneficial microbes reveal they can establish in field-grown potato roots and decrease blemish diseases. *Biology and Fertility of Soils*, 1–14.

- Durán, D., Bernal, P., Vazquez-Arias, D., Blanco-Romero, E., Garrido-Sanz, D., Redondo-Nieto, M., Rivilla, R., & Martín, M. (2021). *Pseudomonas fluorescens* F113 type VI secretion systems mediate bacterial killing and adaptation to the rhizosphere microbiome. *Scientific Reports*, 11(1), 5772.
- Emamalipour, M., Seidi, K., Zununi Vahed, S., Jahanban-Esfahlan, A., Jaymand, M., Majdi, H., Amoozgar, Z., Chitkushev, L., Javaheri, T., & Jahanban-Esfahlan, R. (2020). Horizontal gene transfer: from evolutionary flexibility to disease progression. *Frontiers in Cell and Developmental Biology*, 8, 229.
- Flemming, H.-C., van Hullebusch, E. D., Neu, T. R., Nielsen, P. H., Seviour, T., Stoodley, P., Wingender, J., & Wuertz, S. (2023). The biofilm matrix: multitasking in a shared space. *Nature Reviews Microbiology*, 21(2), 70–86.
- Flemming, H.-C., & Wingender, J. (2010). The biofilm matrix. *Nature Reviews Microbiology*, 8(9), 623–633.
- Fuchslueger, L., Bahn, M., Fritz, K., Hasibeder, R., & Richter, A. (2014). Experimental drought reduces the transfer of recently fixed plant carbon to soil microbes and alters the bacterial community composition in a mountain meadow. *New Phytologist*, 201(3), 916–927.
- Gao, M., Xiong, C., Tsui, C. K., & Cai, L. (2024). Pathogen invasion increases the abundance of predatory protists and their prey associations in the plant microbiome. *Molecular Ecology*, 33(3), e17228.
- George, S., Aguilera, X., Gallardo, P., Farfán, M., Lucero, Y., Torres, J. P., Vidal, R., & O’Ryan, M. (2022). Bacterial gut microbiota and infections during early childhood. *Frontiers in Microbiology*, 12, 793050.
- Getzke, F., Wang, L., Chesneau, G., Böhringer, N., Mesny, F., Denissen, N., Wesseler, H., Adisa, P. T., Marner, M., & Schulze-Lefert, P. (2024). Physiochemical interaction between osmotic stress and a bacterial exometabolite promotes plant disease. *Nature Communications*, 15(1), 4438.
- Gonzales, M., Kergaravat, B., Jacquet, P., Billot, R., Grizard, D., Chabrière, É., Plener, L., & Daudé, D. (2024). Disrupting quorum sensing as a strategy to inhibit bacterial virulence in human, animal, and plant pathogens. *Pathogens and Disease*, 82, ftac009.
- Grainha, T., Jorge, P., Alves, D., Lopes, S. P., & Pereira, M. O. (2020). Unraveling *Pseudomonas aeruginosa* and *Candida albicans* communication in coinfection scenarios: insights through network analysis. *Frontiers in Cellular and Infection Microbiology*, 10, 550505.
- Greenspan, S. E., Migliorini, G. H., Lyra, M. L., Pontes, M. R., Carvalho, T., Ribeiro, L. P., Moura-Campos, D., Haddad, C. F., Toledo, L. F., & Romero, G. Q. (2020). Warming drives ecological community changes linked to host-associated microbiome dysbiosis. *Nature Climate Change*, 10(11), 1057–1061.

- Guan, X., Jia, D., Liu, X., Ding, C., Guo, J., Yao, M., Zhang, Z., Zhou, M., & Sun, J. (2024). Combined influence of the nanoplastics and polycyclic aromatic hydrocarbons exposure on microbial community in seawater environment. *Science of the Total Environment*, 945, 173772.
- Guo, P., Li, C., Liu, J., & Chai, B. (2023). Predation has a significant impact on the complexity and stability of microbial food webs in subalpine lakes. *Microbiology Spectrum*, 11(6), e02411–02423.
- Guzzo, G. L., Andrews, J. M., & Weyrich, L. S. (2022). The neglected gut microbiome: Fungi, Protozoa, and bacteriophages in inflammatory bowel disease. *Inflammatory bBowel Diseases*, 28(7), 1112–1122.
- Hao, L., Zhang, Z., Hao, B., Diao, F., Zhang, J., Bao, Z., & Guo, W. (2021). Arbuscular mycorrhizal fungi alter microbiome structure of rhizosphere soil to enhance maize tolerance to La. *Ecotoxicology and Environmental Safety*, 212, 111996.
- Hartmann, A., Binder, T., & Rothballer, M. (2024). Quorum sensing-related activities of beneficial and pathogenic bacteria have important implications for plant and human health. *FEMS Microbiology Ecology*, 100(6).
- Hu, J., Amor, D. R., Barbier, M., Bunin, G., & Gore, J. (2022). Emergent phases of ecological diversity and dynamics mapped in microcosms. *Science*, 378(6615), 85–89.
- Jiang, F., & Doudna, J. A. (2017). CRISPR–Cas9 structures and mechanisms. *Annual Review of Biophysics*, 46(1), 505–529.
- Jin, Y., Zhang, W., Cong, S., Zhuang, Q.-G., Gu, Y.-L., Ma, Y.-N., Filiatrault, M. J., Li, J.-Z., & Wei, H.-L. (2023). *Pseudomonas syringae* Type III Secretion Protein HrpP Manipulates Plant Immunity To Promote Infection. *Microbiology Spectrum*, 11(3), e05148–05122.
- Kataki, S., Patowary, R., Chatterjee, S., Vairale, M. G., Sharma, S., Dwivedi, S. K., & Kamboj, D. V. (2022). Bioaerosolization and pathogen transmission in wastewater treatment plants: Microbial composition, emission rate, factors affecting and control measures. *Chemosphere*, 287, 132180.
- Khan, S., Srivastava, S., Karnwal, A., & Malik, T. (2023). *Streptomyces* as a promising biological control agents for plant pathogens. *Frontiers in Microbiology*, 14, 1285543.
- Law, S. K. K., & Tan, H. S. (2022). The role of quorum sensing, biofilm formation, and iron acquisition as key virulence mechanisms in *Acinetobacter baumannii* and the corresponding anti-virulence strategies. *Microbiological Research*, 260, 127032.
- Lee, S.-M., Kong, H. G., Song, G. C., & Ryu, C.-M. (2021). Disruption of Firmicutes and Actinobacteria abundance in tomato rhizosphere causes the incidence of bacterial wilt disease. *The ISME journal*, 15(1), 330–347.

- Li, J., Bates, K. A., Hoang, K. L., Hector, T. E., Knowles, S. C., & King, K. C. (2023). Experimental temperatures shape host microbiome diversity and composition. *Global Change Biology*, 29(1), 41–56.
- Li, M., Zhao, J., Tang, N., Sun, H., & Huang, J. (2018). Horizontal gene transfer from bacteria and plants to the arbuscular mycorrhizal fungus *Rhizophagus irregularis*. *Frontiers in Plant Science*, 9, 701.
- Li, N., Ma, W.-T., Pang, M., Fan, Q.-L., & Hua, J.-L. (2019). The commensal microbiota and viral infection: a comprehensive review. *Frontiers in Immunology*, 10, 1551.
- Liu, C., Wang, Y., Zhou, Z., Wang, S., Wei, Z., Ravanbakhsh, M., Shen, Q., Xiong, W., Kowalchuk, G. A., & Jousset, A. (2024). Protist predation promotes antimicrobial resistance spread through antagonistic microbiome interactions. *The ISME journal*, 18(1), wrac169.
- Liu, M., Bjørnlund, L., Rønn, R., Christensen, S., & Ekelund, F. (2012). Disturbance promotes non-indigenous bacterial invasion in soil microcosms: analysis of the roles of resource availability and community structure. *PLOS ONE* 7(10): e45306.
- Liu, X., Le Roux, X., & Salles, J. F. (2022). The legacy of microbial inoculants in agroecosystems and potential for tackling climate change challenges. *Iscience*, 25(3).
- Liu, X., & Salles, J. F. (2024). Lose-lose consequences of bacterial community-driven invasions in soil. *Microbiome*, 12(1), 57.
- Martínez-Arias, C., Witzell, J., Solla, A., Martin, J. A., & Rodríguez-Calcerrada, J. (2022). Beneficial and pathogenic plant-microbe interactions during flooding stress. *Plant, Cell & Environment*, 45(10), 2875–2897.
- Mawarda, P. C., Le Roux, X., Acosta, M. U., van Elsas, J. D., & Salles, J. F. (2022). The impact of protozoa addition on the survivability of *Bacillus* inoculants and soil microbiome dynamics. *ISME Communications*, 2(1), 82.
- Mehmood, M. A., Zhao, H., Cheng, J., Xie, J., Jiang, D., & Fu, Y. (2020). Sclerotia of a phytopathogenic fungus restrict microbial diversity and improve soil health by suppressing other pathogens and enriching beneficial microorganisms. *Journal of Environmental Management*, 259, 109857.
- Mendes, L. W., Raaijmakers, J. M., De Hollander, M., Sepo, E., Gómez Expósito, R., Chiorato, A. F., Mendes, R., Tsai, S. M., & Carrión, V. J. (2023). Impact of the fungal pathogen *Fusarium oxysporum* on the taxonomic and functional diversity of the common bean root microbiome. *Environmental Microbiome*, 18(1), 68.
- Moorcroft, S. C., Roach, L., Jayne, D. G., Ong, Z. Y., & Evans, S. D. (2020). Nanoparticle-loaded hydrogel for the light-activated release and photothermal enhancement of antimicrobial peptides. *ACS Applied Materials & Interfaces*, 12(22), 24544–24554.

- Ogunrinola, G. A., Oyewale, J. O., Oshamika, O. O., & Olasehinde, G. I. (2020). The human microbiome and its impacts on health. *International Journal of Microbiology*, 2020(1), 8045646.
- Palmer, J. D., & Foster, K. R. (2022). The evolution of spectrum in antibiotics and bacteriocins. *Proceedings of the National Academy of Sciences*, 119(38), e2205407119.
- Parmanand, B. A., Kellingray, L., Le Gall, G., Basit, A. W., Fairweather-Tait, S., & Narbad, A. (2019). A decrease in iron availability to human gut microbiome reduces the growth of potentially pathogenic gut bacteria; an in vitro colonic fermentation study. *The Journal of Nutritional Biochemistry*, 67, 20–27.
- Passi, A., Tibocha-Bonilla, J. D., Kumar, M., Tec-Campos, D., Zengler, K., & Zuniga, C. (2021). Genome-scale metabolic modeling enables in-depth understanding of big data. *Metabolites*, 12(1), 14.
- Poppeliers, S. W., Sánchez-Gil, J. J., & de Jonge, R. (2023). Microbes to support plant health: understanding bioinoculant success in complex conditions. *Current Opinion in Microbiology*, 73, 102286.
- Poveda, J., & Eugui, D. (2022). Combined use of *Trichoderma* and beneficial bacteria (mainly *Bacillus* and *Pseudomonas*): Development of microbial synergistic bio-inoculants in sustainable agriculture. *Biological Control*, 176, 105100.
- Proença, D. N., Fasola, E., Lopes, I., & Morais, P. V. (2021). Characterization of the skin cultivable microbiota composition of the frog *Pelophylax perezi* inhabiting different environments. *International Journal of Environmental Research and Public Health*, 18(5), 2585.
- Rocklöv, J., & Dubrow, R. (2020). Climate change: an enduring challenge for vector-borne disease prevention and control. *Nature Immunology*, 21(5), 479–483.
- Rodrigues, C. F., & Černáková, L. (2020). Farnesol and tyrosol: secondary metabolites with a crucial quorum-sensing role in *Candida* biofilm development. *Genes*, 11(4), 444.
- Rusiñol, M., Hundesa, A., Cárdenas-Youngs, Y., Fernández-Bravo, A., Pérez-Cataluña, A., Moreno-Mesonero, L., Moreno, Y., Calvo, M., Alonso, J. L., & Figueras, M. J. (2020). Microbiological contamination of conventional and reclaimed irrigation water: Evaluation and management measures. *Science of the Total Environment*, 710, 136298.
- Sakakibara, H., Kasahara, H., Ueda, N., Kojima, M., Takei, K., Hishiyama, S., Asami, T., Okada, K., Kamiya, Y., & Yamaya, T. (2005). *Agrobacterium tumefaciens* increases cytokinin production in plastids by modifying the biosynthetic pathway in the host plant. *Proceedings of the National Academy of Sciences*, 102(28), 9972–9977.
- Sam, Q. H., Chang, M. W., & Chai, L. Y. A. (2017). The fungal mycobiome and its interaction

- with gut bacteria in the host. *International journal of molecular sciences*, 18(2), 330.
- SanMiguel, A. J., Meisel, J. S., Horwinski, J., Zheng, Q., Bradley, C. W., & Grice, E. A. (2018). Antiseptic agents elicit short-term, personalized, and body site-specific shifts in resident skin bacterial communities. *Journal of Investigative Dermatology*, 138(10), 2234–2243.
- Sarkar, B., Kumar, C., Pasari, S., & Goswami, B. (2022). Review on *Pseudomonas fluorescens*: a plant growth promoting rhizobacteria. *Journal of Positive School Psychology*, 2701–2709.
- Shade, A., Peter, H., Allison, S. D., Baho, D. L., Berga, M., Bürgmann, H., Huber, D. H., Langenheder, S., Lennon, J. T., & Martiny, J. B. (2012). Fundamentals of microbial community resistance and resilience. *Frontiers in Microbiology*, 3, 417.
- Shu, D., Banerjee, S., Mao, X., Zhang, J., Cui, W., Zhang, W., Zhang, B., Chen, S., Jiao, S., & Wei, G. (2024). Conversion of monocropping to intercropping promotes rhizosphere microbiome functionality and soil nitrogen cycling. *Science of the Total Environment*, 949, 174953.
- Silpe, J. E., Bridges, A. A., Huang, X., Coronado, D. R., Duddy, O. P., & Bassler, B. L. (2020). Separating functions of the phage-encoded quorum-sensing-activated antirepressor Qtip. *Cell Host & Microbe*, 27(4), 629–641. e624.
- Suman, A., Govindasamy, V., Ramakrishnan, B., Aswini, K., SaiPrasad, J., Sharma, P., Pathak, D., & Annapurna, K. (2022). Microbial community and function-based synthetic bioinoculants: a perspective for sustainable agriculture. *Frontiers in Microbiology*, 12, 805498.
- Suman, J., Rakshit, A., Ogireddy, S. D., Singh, S., Gupta, C., & Chandrakala, J. (2022). Microbiome as a key player in sustainable agriculture and human health. *Frontiers in Soil Science*, 2, 821589.
- Trivedi, P., Leach, J. E., Tringe, S. G., Sa, T., & Singh, B. K. (2020). Plant–microbiome interactions: from community assembly to plant health. *Nature Reviews Microbiology*, 18(11), 607–621.
- Ujvári, G., Turrini, A., Avio, L., & Agnolucci, M. (2021). Possible role of arbuscular mycorrhizal fungi and associated bacteria in the recruitment of endophytic bacterial communities by plant roots. *Mycorrhiza*, 31(5), 527–544.
- Vacheron, J., Péchy-Tarr, M., Brochet, S., Heiman, C. M., Stojiljkovic, M., Maurhofer, M., & Keel, C. (2019). T6SS contributes to gut microbiome invasion and killing of an herbivorous pest insect by plant-beneficial *Pseudomonas protegens*. *The ISME Journal*, 13(5), 1318–1329.
- Van Elsas, J. D., Chiurazzi, M., Mallon, C. A., Elhottová, D., Křišťůfek, V., & Salles, J. F. (2012). Microbial diversity determines the invasion of soil by a bacterial pathogen. *Proceedings of*

- the National Academy of Sciences, 109(4), 1159–1164.
- Venkatesh, N., & Keller, N. P. (2019). Mycotoxins in conversation with bacteria and fungi. *Frontiers in Microbiology*, 10, 403.
- Vishnevskaya, N., Shakhnazarova, V., Shaposhnikov, A., & Strunnikova, O. (2020). The role of root exudates of barley colonized by *Pseudomonas fluorescens* in enhancing root colonization by *Fusarium culmorum*. *Plants*, 9(3), 366.
- Walder, F., Schmid, M. W., Riedo, J., Valzano-Held, A. Y., Banerjee, S., Büchi, L., Bucheli, T. D., & van Der Heijden, M. G. (2022). Soil microbiome signatures are associated with pesticide residues in arable landscapes. *Soil Biology and Biochemistry*, 174, 108830.
- Wan, P., Zhou, Z., Yuan, Z., Wei, H., Huang, F., Li, Z., Li, F.-M., & Zhang, F. (2024). Fungal community composition changes and reduced bacterial diversity drive improvements in the soil quality index during arable land restoration. *Environmental Research*, 244, 117931.
- Wang, Y., Pruitt, R. N., Nuernberger, T., & Wang, Y. (2022). Evasion of plant immunity by microbial pathogens. *Nature Reviews Microbiology*, 20(8), 449–464.
- Weiland-Bräuer, N. (2021). Friends or foes—microbial interactions in nature. *Biology*, 10(6), 496.
- Wilhelm, R. C., van Es, H. M., & Buckley, D. H. (2022). Predicting measures of soil health using the microbiome and supervised machine learning. *Soil Biology and Biochemistry*, 164, 108472.
- Woodward, S. E., Neufeld, L. M., Peña-Díaz, J., Feng, W., Serapio-Palacios, A., Tarrant, I., Deng, W., & Finlay, B. B. (2024). Both pathogen and host dynamically adapt pH responses along the intestinal tract during enteric bacterial infection. *PLoS Biology*, 22(8), e3002761.
- Xu, L., & Coleman-Derr, D. (2019). Causes and consequences of a conserved bacterial root microbiome response to drought stress. *Current Opinion in Microbiology*, 49, 1–6.
- Yadav, A. K., Espaillet, A., & Cava, F. (2018). Bacterial strategies to preserve cell wall integrity against environmental threats. *Frontiers in Microbiology*, 9, 2064.
- Zaneveld, J. R., McMinds, R., & Vega Thurber, R. (2017). Stress and stability: applying the Anna Karenina principle to animal microbiomes. *Nature Microbiology*, 2(9), 1–8.
- Zhang, T., Yang, X., Guo, R., & Guo, J. (2016). Response of AM fungi spore population to elevated temperature and nitrogen addition and their influence on the plant community composition and productivity. *Scientific Reports*, 6(1), 24749.
- Zhou, Y., Yang, Z., Liu, J., Li, X., Wang, X., Dai, C., Zhang, T., Carrión, V. J., Wei, Z., & Cao, F. (2023). Crop rotation and native microbiome inoculation restore soil capacity to suppress a root disease. *Nature Communications*, 14(1), 8126.

## CHAPTER 2: A host-derived chimeric peptide protects citrus against Huanglongbing without threatening the native microbial community of the phyllosphere<sup>1</sup>

### 2.1 OVERVIEW

**Introduction** The application of host-derived antibacterial peptides has been highlighted as a potential efficacious and safe tool for the treatment of Huanglongbing (HLB), the most devastating disease of citrus. However, pathogenic bacteria such as HLB-causing *Candidatus liberibacter asiaticus* (CLAs) often develop resistance against the host antibacterial peptides. We showed that chimeras containing two different host antibacterial peptides not only retain antibacterial activity but also overcome bacterial resistance and enhance plant defence responses. Also, chimeric peptides can have an off-target impact on the structure and function of plant-associated microbiomes. However, there is a lack of understanding of the impact of the chimeric peptide therapy on the microbial structure in the citrus phyllosphere while reducing the CLAs titre. Here, we aim to evaluate the efficacy of a chimeric peptide (UGK17) to reduce CLAs titre, inducing plant defence response and impacting the microbiome associated with the citrus phyllosphere.

**Material and Method** Leaf samples were collected from orange and grapefruit trees in Texas and identified as old and young leaves according to their maturity. We collected three different types of leaves based on their infection and symptoms: healthy, symptomatic (infected with typical symptoms), and asymptomatic (infected without symptoms). *In planta* assay was

---

<sup>1</sup>Published as “Jeongyun Choi, Supratim Basu, Abigail Thompson, Kristen Otto, Elena V. Sineva, Madhurababu Kunta, Goutam Gupta, Pankaj Trivedi. 2023. A host-derived chimeric peptide protects citrus against Huanglongbing without threatening the native microbial community of the phyllosphere. *Journal of Sustainable Agriculture and Environment* 2(4): 489-499. <https://doi.org/10.1002/sae2.12089>”

Contributions by J Choi: Data collection, formal analysis, Writing-original draft

performed by dipping the leaves in the 0, 5 and 25  $\mu\text{M}$  of UGK17 solutions for 48 h. The quantifications of CLAs titre and pathogenesis-related (*PR*) gene expression were done by quantitative polymerase chain reaction (qPCR) and reverse transcription-qPCR, respectively. Amplicon sequencing was done to evaluate the impact of UGK17 on individual bacterial community structures. In addition, we performed an *ex planta* assay to assess the effect of UGK17 on the growth of bacterial isolates including *Liberibacter crescens* instead of unculturable CLAs predominant in the phyllosphere.

**Result** The UGK17 treatment reduced the CLAs titre in both asymptomatic and symptomatic citrus leaves, regardless of the age of the leaves. The UGK17 application augmented the *PR* gene expression. In *ex planta* assay, the growth of *L. crescens* along with four other strains belonging to the family *Rhizobiaceae*, was significantly inhibited by the UGK17 while the growth of 74 strains were unaffected. Additionally, there was no statistically significant changes in the microbial community structure with UGK17 treatment.

**Conclusion** Our results suggest that the chimeric peptide therapy is a promising solution to combat HLB by targeting mainly Gram-negative pathogens and enhancing the plant immune responses without impairing the indigenous microbial community in the citrus phyllosphere.

## 2.2 INTRODUCTION

Citrus greening or Huanglongbing (HLB), caused by phloem limited and insect (Asian citrus psyllid [ACP]) vectored bacteria, *Candidatus liberibacter* spp. (*Candidatus Liberibacter asiaticus* [CLAs] in Florida) is the most destructive disease of citrus (Blaustein et al., 2018; Wang & Trivedi, 2013). HLB damage to citrus includes weakened root systems, discoloured leaves, premature fruit drop, and bitter juice (Wang, Pierson, et al., 2017; Wang & Trivedi, 2013). While

the disease, or its vector, has impacted all citrus-growing regions of the United States, it has had significant impacts on commercial citrus-growing regions of Florida and Texas. Moreover, the pathogen is poised to expand from residential areas of California to threaten commercial production. In Florida, the harvest for the state's signature plunged to 45.1 million boxes in 2022; an 69% drop from 149.8 million boxes in 2005, the year when HLB was first detected in the state (USDA, 2023). Florida has lost over \$8.0 billion in revenue, 149,338 citrus acres, and over 8000 jobs to HLB (USDA, 2023). If yields continue to decline and trees keep dying, the US citrus industry will lose relevance resulting in serious economic impact over time.

To date, neither a cure nor an economically viable strategy for the management of diseased trees is available to the industry. Producing resistant cultivars through conventional breeding is difficult due to the lack of commercially available resistant rootstock/scion combinations (Dutt et al., 2015). Other strategies used, or in development, for HLB treatment and prevention include: (i) blocking transmission by ACP using insecticides (Boina et al., 2010; Rehberg et al., 2022; Sétamou et al., 2010; Srinivasan et al., 2008) and RNA interference targeted to ACP genes involved in transmission (Britt et al., 2020); (ii) reducing the level of CLAs and maintaining plant growth by thermal, nutritional, and chemical therapy (Hoffman et al., 2013; Li et al., 2019; Li et al., 2016); (iii) killing CLAs by antibiotics (Hu & Wang, 2016; Zhang et al., 2011); (iv) improving soil biodiversity and harnessing beneficial bacteria (Bazany et al., 2022; Stokes et al., 2023; Zhang et al., 2017); and (v) enhancement of the HLB tolerance by transgenic technology (Dutt et al., 2015; Hao et al., 2016; Stover et al., 2013). These disease management strategies have achieved varying degrees of success (Li et al., 2020). However, citrus growers need other and more efficacious, safe, and cost-effective tools for HLB therapy.

The current lack of methods to effectively combat HLB makes the discovery of innovative

therapeutic measures imperative for the survival of the citrus industry. In this regard, host-therapy based on the natural defence genes that constitute pathogenesis-related (*PR*) or defence peptides/proteins has emerged as a potential tool for the treatment and prevention of HLB (Basu et al., 2022; Huang et al., 2021; Weber et al., 2022). The defence peptides or proteins can kill the bacteria cell directly by forming pores in the cell membrane, interacting with nucleic acids, or inhibiting protein synthesis and activity of enzymes (Dandekar et al., 2012; Montesinos, 2007, 2023; Zhang et al., 2021). *PR* proteins or peptides can function as signalling molecules that modulate the action of some components of the plant immunity-signalling pathways, suggesting that some of these peptides may play a fundamental role as components of feedback loops that regulate the duration and intensity of a plant defence response (Allaker, 2008; Basu et al., 2022; Campos et al., 2018). Recently, Huang et al (2021) identified novel peptides from HLB-tolerant citrus cultivars and reported the enhancement of plant immunity in the peptide-injected trees. Stover et al (2013) reported the bactericidal activity of synthetic peptides on *Agrobacterium tumefaciens* and *Sinorhizobium meliloti* which are phylogenetically related to *CLAs*. Previous research has shown that transgenic citrus-expressing peptides reduced both *CLAs* load and HLB symptoms (Soares et al., 2020). While transgenic citrus will offer a complementary strategy that will provide a more sustained solution, this will require significant time for field efficacy studies and regulatory processes before being handed over to the growers (Graham et al., 2020; Su et al., 2023). The combination of two different peptides resulting in a chimera has been showing increase of the therapeutic potential compared to individual peptides (Basu et al., 2022; Gupta & Stover, 2020). For example, Basu et al (2022) designed chimeric helix-turn-helix (HTH) peptides by joining two different helical amphipathic peptide segments involved in the plant's innate immunity. These chimeras not only show bactericidal activity on infected plants but also

augment a plant's innate immune system during infection. Although host-derived peptides are efficient antibacterial agents and are suitable alternatives to antibiotics in citrus production, there are concerns about their unwanted consequences on environmental sustainability and human health.

Plant-associated microbiomes play key roles in plant nutrition, health, and resistance to various biotic and abiotic stresses (Trivedi et al., 2022). Host-derived peptides can directly impact the selected microbial groups acting as toxins and killing the microbes. In addition, the induction of plant defence responses by host-derived peptides can indirectly influence the structure and function of the plant-associated microbiome (Hacquard et al., 2017; Trivedi et al., 2020). The microbiome plays a central role in plant and soil health (Trivedi et al., 2022), so microbial dysbiosis can lead to decreased plant performance. On the other hand, if peptides are selective against the pathogen, their application can restore the microbiome that can benefit plant growth. HLB is known to have significant impacts on both the structure and functions of plant-associated microbiome (Hu et al., 2022; Li et al., 2021; Liu et al., 2023; Trivedi et al., 2016). The HLB-mediated changes in the plant-associated microbiome is postulated to have a detrimental influence in overall citrus health (Trivedi et al., 2012). Little is known about the consequences of host-derived peptide application on the plant-associated microbiome, and the investigation of unintended effects is rarely considered (Lei et al., 2021; Weinhold et al., 2018). A detailed understanding on the molecular and ecological aspects of interactions between host-derived peptides with plant/insect microbiomes and the impact of these interactions on the environmental sustainability of production systems is required to make science-based decisions about the environmental impact of peptide application in the natural environment. However, to the best of our knowledge, no detailed studies have evaluated the nontarget effect impact of the application

of host-derived antimicrobials on plant-associated microbiomes.

The application of host-based therapy shows clear benefits for HLB management and are the only few silver lining for the citrus industry on the verge of destruction due to HLB (Basu et al., 2022; Wang, 2021). Although the application of peptides provides a robust HLB management tool, there are concerns about the off-target effects of the host-derived antimicrobial peptides on the citrus microbiome. Here, we conducted experiments to evaluate: (a) The efficacy of a newly developed host-derived chimeric peptide (UGK17) in reducing CLas titre in the leaves of two citrus varieties showing different symptoms; (b) the impact of peptide application on the augmentation of *PR* genes involved in plant immune response; and (c) the impact of the peptide application on the structure of phyllosphere microbiome. Overall, our results will provide information to promote host-mediated antimicrobial therapy as a promising solution for protecting the citrus industry against HLB without having off-target impacts on citrus-associated microbiome.

## **2.3 MATERIALS AND METHODS**

### **2.3.1 Sample collection**

We collected leaf samples from mature Valencia sweet orange (*Citrus sinensis*) and Rio Red grapefruit (*Citrus paradisi*) trees grafted on sour orange rootstock. These trees are in Texas A&M University-Kingsville's South Research Farm in Weslaco, TX. From each variety, three types of samples were collected: (a) healthy (no symptoms on the entire tree); (b) symptomatic (showing asymmetric leaf mottling); and (c) asymptomatic (samples collected from the same branch as infected but with no symptoms). Samples were collected from 15 trees from each variety. Also, the collected samples were divided into old and young leaves according to their maturity. Four

leaves were taken randomly for each UGK17 treatment from the collected samples. Samples were shipped to the lab at Colorado State University overnight in blue ice.

### **2.3.2 Experimental setup**

Details on the design and synthesis of the chimeric peptide UGK17 used in this study is provided in (Basu et al., 2022). Briefly, UGK17 is a combination of two segments belonging to proteins associated with plant innate immunity. The UGK17 was custom synthesised after performing molecular modelling to construct a library of peptide chimeras by joining two antibacterial  $\alpha/\beta$  segments from citrus proteins. The selection process focused on identifying energetically stable chimeras with a high predicted antibacterial activity. Figure 2.1 illustrates the experimental setup in this study. A previous study (Basu et al., 2022) has shown that UGK17 is effective in CLas clearing at 25  $\mu\text{M}$  UGK17 treatment. Here, in addition to 25  $\mu\text{M}$  concentrations, we examined the effectiveness of UGK17 treatment in reducing CLas titre at a lower concentration (5  $\mu\text{M}$ ). The peptide was diluted in water to make 5 and 25  $\mu\text{M}$  concentrations. Leaf samples belonging to two varieties and different symptoms were placed in individual Petri dishes. The Petri dishes with two leaves were filled with 25 mL of the UGK17 solutions with 5 or 25  $\mu\text{M}$  concentrations or water (control treatment). The Petri dishes were left in room temperature in the dark for 48 h till they absorbed 5–6 mL of the respective solution. Four biological replicates from each treatment were collected, and immediately frozen in liquid nitrogen, and stored at  $-80^{\circ}\text{C}$  for DNA/RNA extraction.

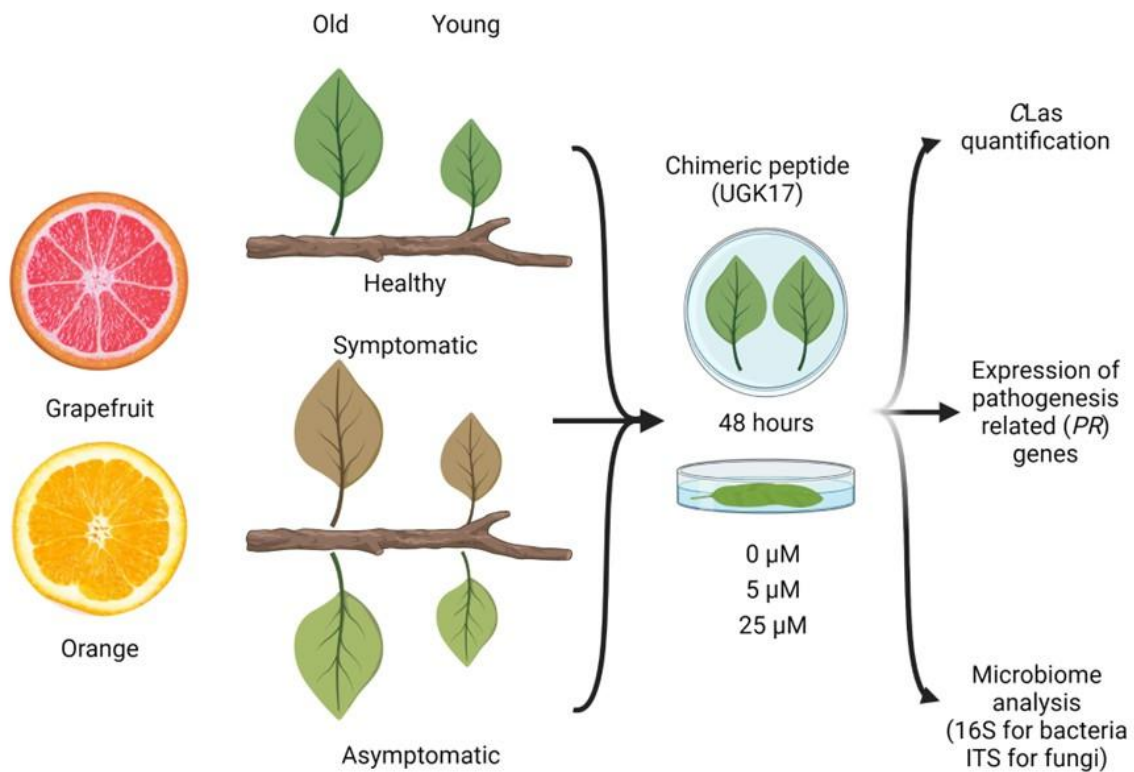


**Figure 2.1.** Experimental setup in this study.

### 2.3.3 DNA/RNA extraction

The frozen samples were grinded using mortar pastel. DNA and RNA were extracted using DNeasy Plant Pro and RNeasy PowerPlant kits (Qiagen), respectively. The extracted DNA/RNA was quantified using NanoDrop 2000 (Thermo Fisher Scientific) and stored at  $-80^{\circ}\text{C}$  for further use.

#### **2.3.4 Quantification of *Clas***

All quantitative polymerase chain reaction (qPCR) assays were performed in a 96-well plate using an ABI Prism 7500 Sequence detection system (Applied Biosystems). Primer set CQULA04F-CQULAP10P-CQULA04R was used to target the  $\beta$ -operon region of *CLAs*, and qPCR reactions were performed according to the conditions described in Trivedi et al (2009). Each individual sample was replicated four times on a 96-well plate and the whole reaction was repeated twice to verify the consistency of the method. Results were analysed using ABI Prism software. Raw data were analysed using the default settings (threshold = 0.2) of the software.

#### **2.3.5 *PR* gene expression**

To determine *PR* gene expression, contamination of genomic DNA was removed by RNA treatment with a Turbo-DNA free kit (Ambion). (Reverse transcription-qPCR) RT-qPCR assays were conducted to determine the expression of three *PR* genes (*PR-1*, *PR-2*, and *PR-5*), using an Applied Biosystems 7500 Fast real-time PCR system, with the QuantiTect SYBR green RT-PCR kit (Qiagen). The PCR conditions were 30 min of reverse transcription at 50°C, followed by 15 min of predenaturation at 95°C and 40 cycles of 15 s of denaturation at 94°C, 30 s of annealing at 55°C, and 30 s of extension at 72°C. The housekeeping gene encoding glyceraldehyde-3-phosphate dehydrogenase-C was used as an endogenous control. Melting curve analysis was conducted to verify the specificity of the RT-qPCR products. The products were run on a 2% agarose gel to confirm the presence of only a single band. Two technical replicates and three biological replicates were used for each gene. The relative fold change in target gene expression was calculated using the formula  $2^{-\Delta\Delta C_t}$  (Livak & Schmittgen, 2001).

### 2.3.6 *Ex planta* bacterial growth assays

The *ex planta* bacterial growth assay was done to investigate the impact of the chimeric peptide application on the growth of individual bacteria from a culture collection maintained in the CSU lab. We selected 81 bacterial isolates that represent dominant microbial groups present in the plant phyllosphere (Trivedi et al., 2020; Trivedi et al., 2011). We also included *Candidatus liberibacter crescens* strain BT-1 (BAA-2481<sup>TM</sup>), which represents the closest culturable relative of CLAs. A precultivated bacterial culture dilution (25  $\mu$ L corresponding to approximately  $1 \times 10^5$ – $2 \times 10^5$  bacterial cells ( $OD_{600} = 0.001$ ]) was mixed with 75  $\mu$ L of Luria-Bertani broth (ATCC medium 2870 for *L. crescens*) with or without 25  $\mu$ M of the UGK17. The bacterial culture was grown in a rotating shaker (200 rpm) at 28°C for 48 h. The cultivation of bacterial strains was replicated three times. The optical density (OD) was measured at 600 nm in 96-well flat-bottom plates (Thermo Fisher Scientific) using the plate reader (Infinite M Nano+; Tecan).

The phylogenetic tree was constructed based on the 16S sequences by using Clustal Omega (Madeira et al., 2022). The heat map was generated based on the z-score of the percentage change of the  $OD_{600}$ . The visualisation of the phylogenetic tree and a heat map was done by ITOL. The significant differences between the cell culture with and without the UGK17 for each strain were determined by Student's t-test at  $p < 0.05$ .

### 2.3.7 Microbiome analysis

The diversity and community structure of bacteria and fungi was determined by amplicon sequencing using an Illumina MiSeq platform. We used the primer sets 515F/806R (Caporaso et al., 2012) and ITS1F/ITS2R (Caporaso et al., 2012) to amplify a portion of the bacterial 16S ribosomal RNA (rRNA) gene and fungal ITS1 region, respectively. The 0.5  $\mu$ M of mitochondrial

peptide nucleic acid and plastid peptide nucleic acid clamps (PNA Bio) per reaction were added to block the 16S rRNA amplification of host mitochondria and chloroplast, respectively. The amplicons were sequenced by an Illumina Miseq platform at the Colorado State University Next Generation Sequencing facility. Bioinformatics processing was performed using a combination of USEARCH (Edgar, 2010) and UNOISE3 (Edgar, 2016). Operational taxonomic units (OTU) tables based on 97% sequence similarity were generated using the USEARCH pipeline. Adapters and primers were removed using cutadapt (Martin, 2011). Then samples were demultiplexed. Paired-end reads were merged, and quality was assessed with fastQC. The merged pairs were discarded if they contained ambiguous nucleotides, had a low ( $Q < 20$ ) quality score, or were short in length ( $< 100$  bp). The representative set database was created using the UCLUST and UPARSE algorithms (Edgar, 2013). Unique sequences were clustered into unique OTUs using DADA2 and DeNoised using uNoise3 as described (Xiong et al., 2021). OTU tables were generated by mapping reads to the representative set database. OTUs were counted at the sample level. Taxonomic identification of bacteria and fungi was obtained against the Silva (Quast et al., 2012) and UNITE database (Nilsson et al., 2019), respectively.

Samples were evaluated separately for bacterial (16S) and fungal (ITS) communities. Samples were rarified to the lowest occupancy of 14,000 and 6800 reads for 16S rRNA and ITS, respectively. We used the R package 'mctools' to analyse microbial community structure (Leff, 2017). To examine beta diversity, Bray–Curtis dissimilarity distances were calculated then ordinated in nonmetric multidimensional scaling (NMDS). Permutational multivariate analysis of variance (PERMANOVA) models were generated to determine significant differences between disease infection, age of the leaves, symptoms, and the UGK17 treatment. To examine alpha diversity, Shannon diversity indexes were calculated and evaluated through general linear

models. Tukey honestly significant difference tests were used to determine the influence of the above variables on alpha-diversity. Using information from the in vitro experiment, we performed random forest (RF) analysis to identify keystone microbes that are affected by the UGK17 treatments (Trivedi et al., 2017). A significance level of  $p < 0.05$  was used for the impact of the UGK17 application on the structure and diversity of the citrus phyllosphere microbiome as compared to the control.

## **2.4 RESULTS AND DISCUSSION**

### **2.4.1 The host-derived chimeric peptides reduces the CLas titre in the citrus leaves**

In this study,  $C_t$  value was used to estimate the quantity of the CLas titre in the samples (Grosdidier et al., 2017). Our results demonstrated that the application of chimeric peptide UGK17 significantly increased the  $C_t$  value, which can be interpreted as a smaller CLas titre (Figure 2.2). The  $C_t$  values of the healthy citrus leaves was higher than 35 regardless of the peptide treatment, indicating the extremely small number of CLas. We found that the UGK17 application decreased pathogen titre in both the citrus varieties with equal effect. Also, we observed that the UGK17 is equally effective in reducing the CLas titre at both the concentrations used in the study. As expected, asymptomatic leaves have less CLas titre compared to symptomatic leaves. However, both 5 and 25  $\mu\text{M}$  of UGK17 treatment increased the  $C_t$  value from the range of 24–35. The increase of  $C_t$  value over five can be interpreted as the decrease of colony forming unit  $\sim 100$ , which is assumed that UGK17 decreased the CLas titre effectively even with low dosage (Grosdidier et al., 2017). Also, the  $C_t$  values from asymptomatic leaves treated with the UGK17 reached 35 indicating the protection of citrus leaves against CLas before the manifestation of symptoms. There are several reports on the design and application of host-derived peptides to provide protection against HLB (Basu et al.,

2022; Huang et al., 2021; Stover et al., 2013). The chimeric peptide used in this study has previously been reported to decrease CLas titre in grapefruit and showed nontoxicity to human and host cells (Basu et al., 2022; Gupta & Stover, 2020). The effectiveness of peptides in suppressing pathogens depends on various factors including disease severity, scion, and age of leaves (Leekha et al., 2011; Moretta et al., 2021). Here we show that the chimeric peptide can efficiently reduce the CLas titre in the citrus leaves and the bactericidal activity might not be affected by host, maturity of leaves, and severity of symptoms. The reduction in CLas titre is comparable to previous reports using the similar (Basu et al., 2022) or other peptides (Huang et al., 2021). Our results suggest that the chimeric peptide can be one of the potential strategies to manage the HLB by reducing the CLas titre effectively in low dosages.

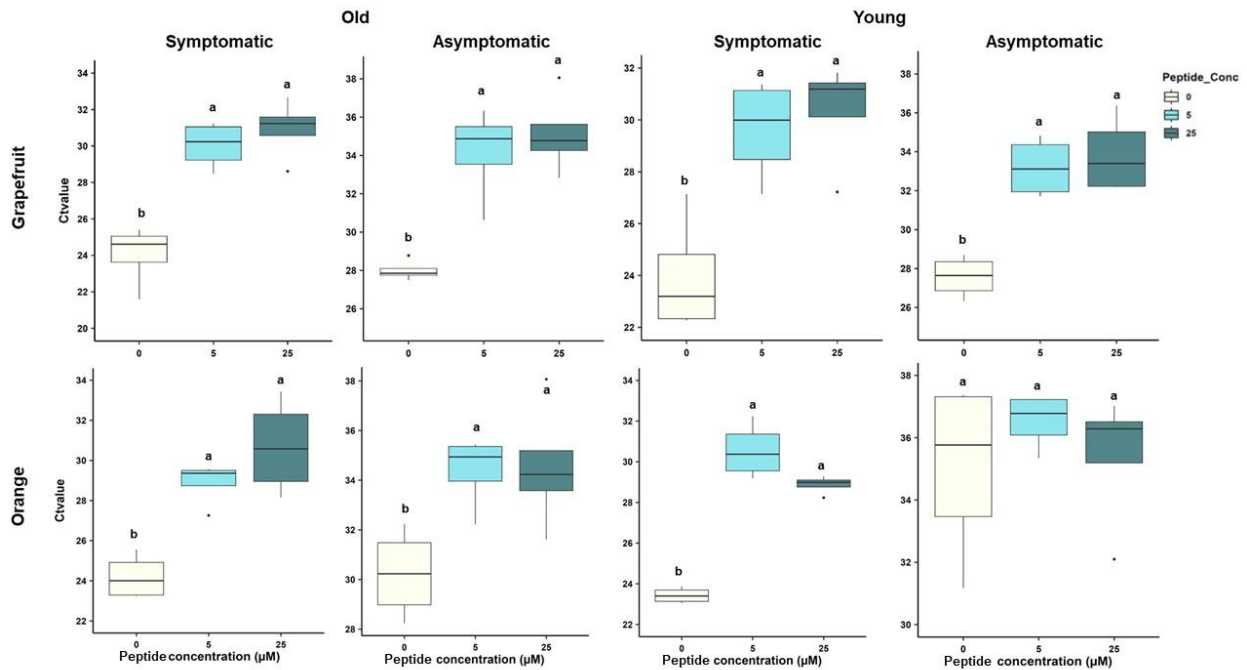


**Figure 2.2.** The  $C_t$  value of the CLas from symptomatic and asymptomatic leaves collected from orange and grapefruit trees under 0, 5, and 25  $\mu\text{M}$  of the UGK17 treatment. The leaves were divided into old and young leaves based on their maturity. Different letters within each peptide treatment in each graph represent significant differences at  $p < 0.05$ .

### **2.4.2 The host-derived chimeric peptide enhance the plant's innate immunity-related gene expression**

Plants recognise pathogens and protect themselves by plant innate immunity composed of pathogen-associated molecular pattern-triggered immunity (PTI) resulting in the activation of the mitogen-activated protein kinase (MAPK), MAPK kinase, and MAPK kinase kinase (Nishad et al., 2020). While pathogens may suppress PTI by using the effector, effector-triggered immunity activated by Nod-like receptor can enhance the disease resistance (Yuan et al., 2021).. Salicylic acid (SA), jasmonic acid, and ethylene are also important signalling hormones as a part of plant innate immunity (Nishad et al., 2020). The activation of plant immune response results to the production of PR proteins which have antimicrobial activity (Ali et al., 2018). As PR proteins are involved in the systemic acquired resistance, they protect plants from reinfection (Durrant & Dong, 2004). It has been proposed that the host antimicrobial peptides may possess the intrinsic ability to directly induce the production of the PR proteins (Jain & Khurana, 2018). We did not test this hypothesis due to the unavailability of the bacteria-free citrus leaves. Here, we monitored the accumulation of *PR* gene transcripts in the asymptomatic and symptomatic leaves of grapefruit and orange in the UGK17 application treatments and compared the expression with the controls to evaluate the augmentation of plant immune response (Figure 2.3). As 5 and 25  $\mu\text{M}$  of UGK17 treatment showed same amount of reduction on *CLas* quantity in Figure 2.1, we considered the expression from the samples treated with 5  $\mu\text{M}$  of UGK17. The results shown are for the young leaves as we were not able to extract high-quality RNA from the old leaves for both the citrus varieties. For the expression of *PR* genes, we tested the expression of the *PR-1*, *PR-2*, and *PR-5* genes, considered markers of plant-immune response (Fu & Dong, 2013; Li et al., 2017; Molinari et al., 2014). The expression of all the *PR* genes increased with the UGK17

application (at a concentration of 5  $\mu\text{M}$ ) for both citrus varieties. We observed higher expression levels of *PR* genes in symptomatic as compared to the asymptomatic samples for both the citrus varieties. Our result indicates the peptide-mediated increases in the plant immune response as a mechanism to reduce CLas titre. CLas produces an active salicylate hydroxylase and the degradation of SA has been reported to decrease the expression of defence-related genes in citrus (Li et al., 2017). Application of exogenous plant defence inducers reduced HLB severity in field trials (Li et al., 2016). Our results suggest that the chimeric peptide is a dual-functional peptide that can reduce CLas titre and suppress disease symptoms in HLB-positive trees and augments plant's systemic defence responses against new infection.

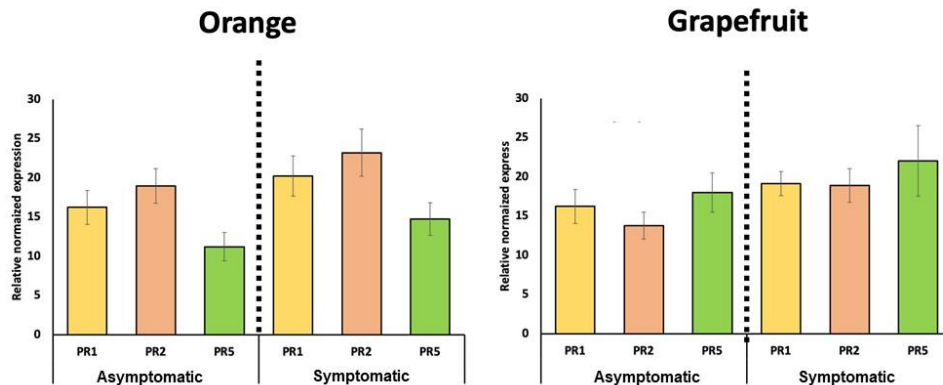


**Figure 2.3.** *PR* gene expression in the young asymptomatic and symptomatic leaves of orange and grapefruit in response to 5  $\mu\text{M}$  of UGK17 application. Relative transcript abundance of the *PR* genes was calculated by calibrating the reverse transcription-quantitative polymerase chain reaction data to a water control. Three biological replicates were performed. Error bars indicate the standard error of mean. *PR*, pathogenesis-related.

### **2.4.3 Host-derived chimeric peptide has a selectively negative impact on the growth of few bacterial isolates**

The HTH peptides prefer to attach to Gram-negative bacterial membranes, particularly pathogens such as CLas (Gupta & Stover, 2020). The bacterial growth assay was done to estimate the specificity of the chimeric peptide to target CLas. In this assay, *Liberibacter crescens* is used as the closest cultured relative of CLas. Most of the strains were not affected by the UGK17 treatment. The OD<sub>600</sub> of the *L. crescens* decreased 58.7% under the UGK17 treatment compared to the control (Figure 4). Four isolates belonging to the family Rhizobiaceae including *S. meliloti*, *Pararhizobium* sp., *Neorhizobium* sp., and *Rhizobium acidisoli* showed significant decrease in growth with the UGK17 treatment compared to control. However, not all the members of family Rhizobiaceae were impacted by the UGK17 treatments. Interestingly, Gram-positive bacterial isolates such as *Streptomyces venezuelae* and *Arthrobacter pascens* showed a significant increase in the growth with the UGK17 treatment compared to the control. Overall, our results suggest that the chimeric peptide will have a direct impact on the growth of pathogen and few related species without impacting the overall bacterial isolates present in the phyllosphere.

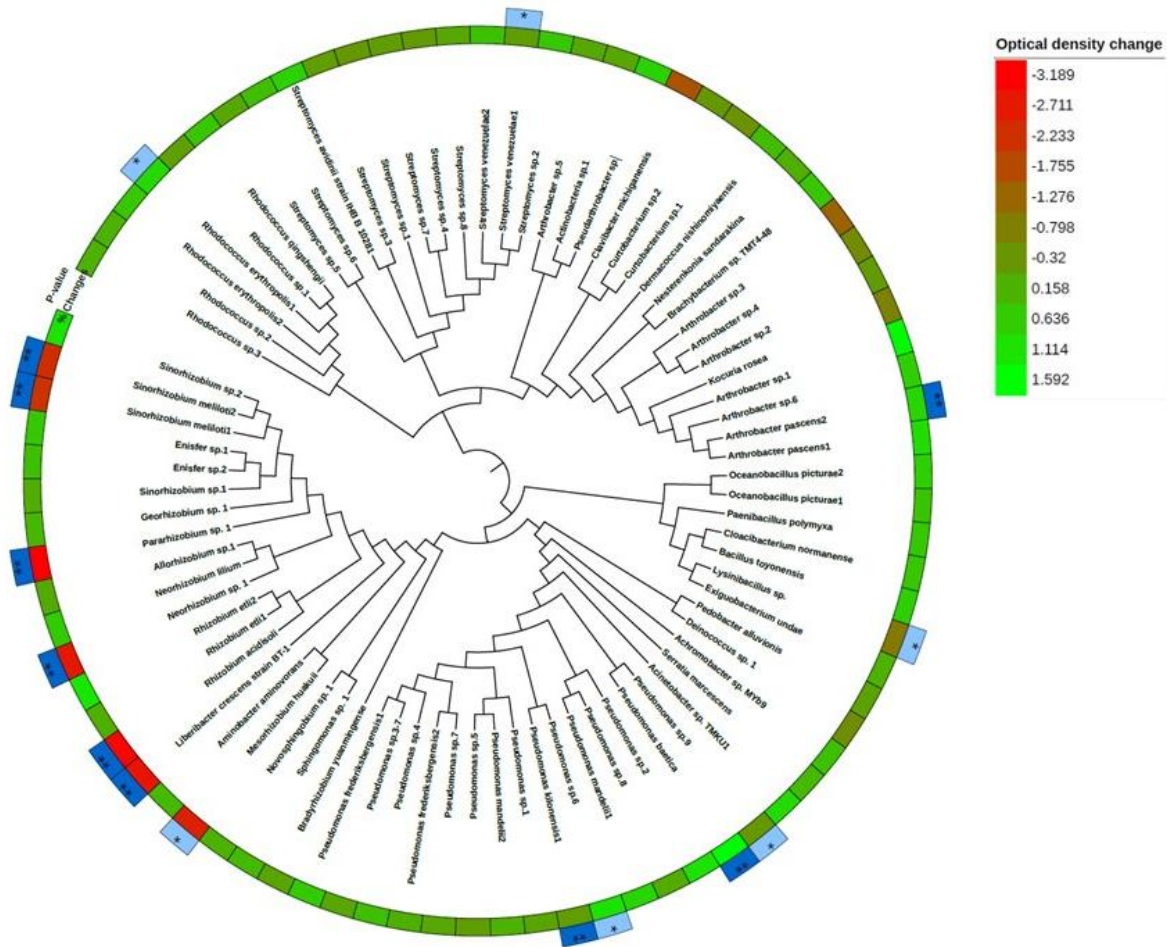


**Figure 2.4.** Heat map showing the optical density changes by the UGK17 and phylogenetic distribution of the bacterial strains. *Liberibacter crescens* highlighted in red box was used as the phylogenetically closest culturable strain with CLAs. The difference of OD<sub>600</sub> of bacterial cell culture were normalised by z-scores. The red indicates the inhibition of bacterial growth with the UGK17 treatment while green indicates the enhancement of bacterial growth with the UGK17 treatment. The star mark indicates the significant difference of the optical density due to UGK17 treatment (\* $p < 0.05$ , \*\* $p < 0.001$ ). CLAs, *Candidatus liberibacter asiaticus*; OD, optical density.

#### **2.4.4 Host-derived chimeric peptide has minimal impact on the phyllosphere microbiome in citrus**

The NMDS analysis showed clear separation (PERMANOVA  $p = 0.001$ ) between healthy and infected (both symptomatic and asymptomatic) phyllosphere-associated bacterial and fungal communities for both the tested varieties with different leaf ages (Figure 5). Thus, our results are per the previous studies that have reported the significant impact of HLB infection and disease severity on leaf microbiome (Srivastava et al., 2022; Wang, Stelinski, et al., 2017; Xu et al., 2018). This is because that HLB causes the imbalanced carbohydrate partitioning and deficiencies of micronutrients such as Fe, Mn, and Zn (Blaustein et al., 2017). As the disease symptom severity is correlated with the CLas titre, the competitive relation between the CLas and native microbiota can affect the microbial community in phyllosphere (Blaustein et al., 2017). The clustering of the UGK17-treated samples at both the concentrations (5 and 25  $\mu\text{M}$  of the UGK17) with the water-treated samples indicated that the UGK17 application has a nonsignificant impact on the bacterial and fungal community associated with the phyllosphere of old and young leaves of citrus and orange (Figure 2.5). The alpha diversity shown as the Shannon index for both bacterial and fungal community was observed to be similar between both the young and old grapefruit and orange leaves (Figure 2.6). For most of the cases our results did not show significant ( $p > 0.05$ ) differences between control and peptide treatments. However, old symptomatic grapefruit leaves had shown a significant decrease in the Shannon index for bacterial and fungal community under the peptide treatment compared to the nontreated leaves. Relative abundance of CLas has been negatively correlated with alpha (Blaustein et al., 2017) therefore decrease in the CLas titre due to the UGK17 treatments can cause increase in microbial diversity in some instances. Machine learning-based RF analysis showed that only three bacterial

species responded to the peptide application (*CLAs*, *Clostridium sensu stricto* and *Clostridium aerotolerans*). The most prominent was *CLAs* (mean decrease accuracy = 0.31). The other impacted bacterial species only constituted less than 0.5% of the relative abundance of the entire bacterial communities. For fungal communities, we did not observe any indicators for the UGK17 treatments. Our observations indicate that the host-derived chimeric peptides have minimal impact on phyllospheric microbial community structure despite the significant shifts of microbial structure by HLB infection. As the chimeric peptide is also a product of the plant's innate immune responses, the induction of plant defence response will have minimal impact on the native microbiota (Trivedi et al., 2020). Consequently, the chimeric peptide derived from the host might target the *CLAs* without impacting on microbial structure in the citrus phyllosphere.

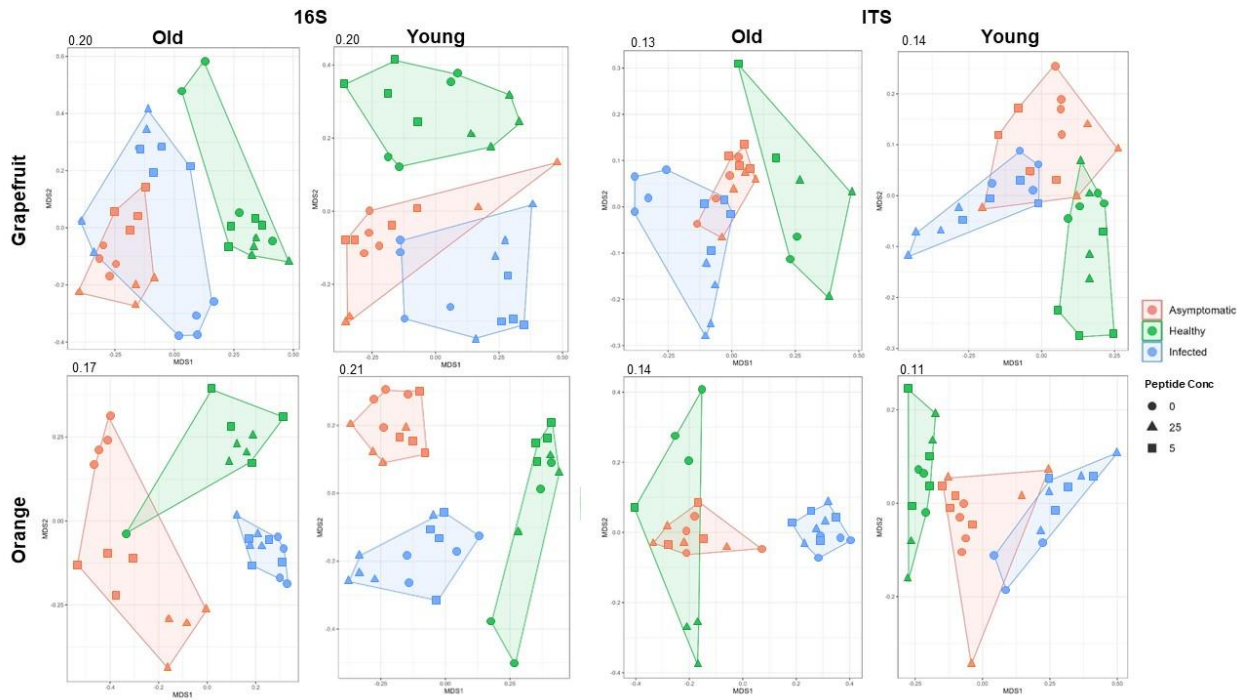


**Figure 2.5.** NMDS plot showing the bacterial (A, B, C, D) and fungal (E, F, G, H) community structural dissimilarity between the disease infection and different concentrations of the UGK17 treatment. The values of the plots indicate the stress values of NMDS. NMDS, nonmetric multidimensional scaling.

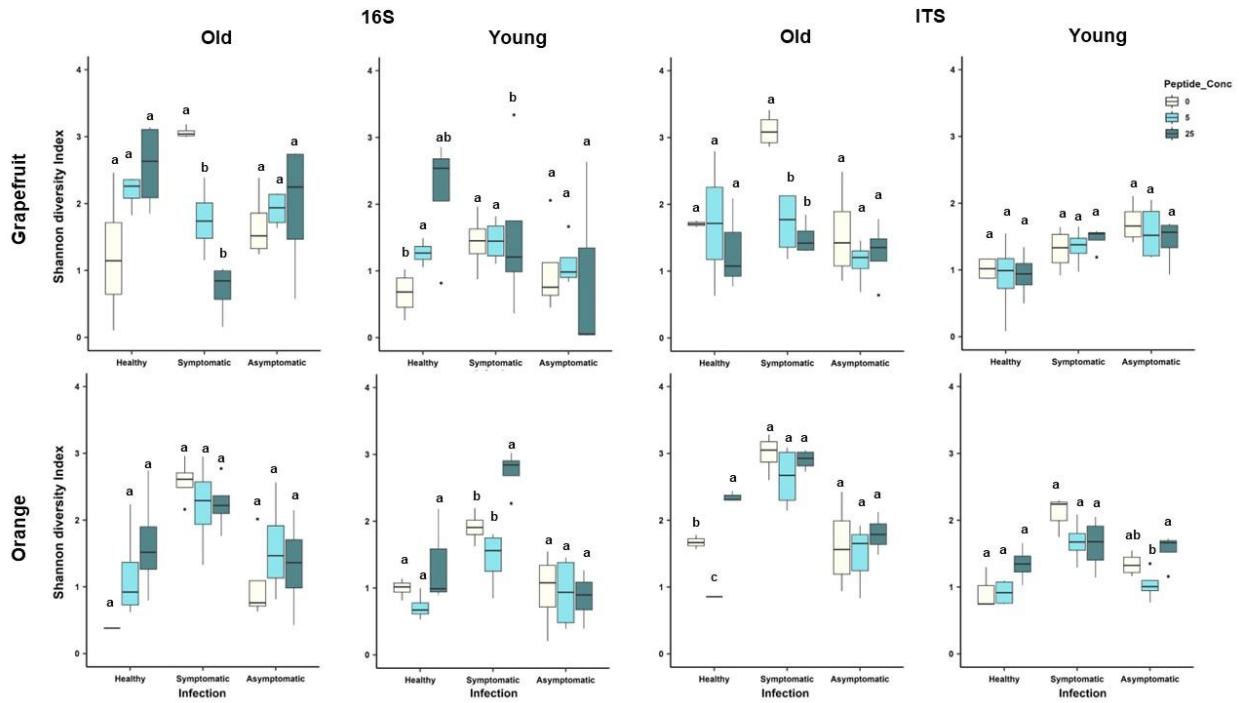


**Figure 2.6.** Shannon diversity index of bacteria (A, B, C, D) and fungi (E, F, G, H) community in the healthy, symptomatic, asymptomatic grapefruit (C, D, G, H) and orange (A, B, E, F) old (A, C, E, G) and young (B, D, F, H) leaves under 0, 5, and 25  $\mu$ M of the UGK17 treatment. Different letter within the same condition of leaves in each graph represents significant differences at  $p < 0.05$  within the condition of leaves.

## 2.5 CONCLUSION

In this study, the chimeric peptide derived from plants had shown effective reduction of CLas regardless of the scion, age of the leaves, and disease symptoms. Also, the augmentation of *PR* gene expression with the peptide treatment showed that the peptide can decrease the pathogen titre by enhancing the plant immune response. Moreover, the chimeric peptide has minimal impact on the microbial community structure in phyllosphere with the promotion of the plant-beneficial microbial growth while it specifically targets the pathogen. These findings provide the possibility of the chimeric peptide as a promising solution to cure the infected citrus trees and/or protect the healthy trees against the HLB in the field conditions. Further, the field study with

different pathogens or practices for the effective uptake will provide the potential of the host-derived chimeric peptide on large-scale agricultural industry for sustainable agriculture.

## REFERENCES

- Ali, S., Ganai, B. A., Kamili, A. N., Bhat, A. A., Mir, Z. A., Bhat, J. A., Tyagi, A., Islam, S. T., Mushtaq, M., & Yadav, P. (2018). Pathogenesis-related proteins and peptides as promising tools for engineering plants with multiple stress tolerance. *Microbiological research*, 212, 29–37.
- Allaker, R. P. (2008). Host defence peptides—a bridge between the innate and adaptive immune responses. *Transactions of the Royal Society of Tropical Medicine and Hygiene*, 102(1), 3–4.
- Basu, S., Sineva, E., Nguyen, L., Sikdar, N., Park, J. W., Sinev, M., Kunta, M., & Gupta, G. (2022). Host-derived chimeric peptides clear the causative bacteria and augment host innate immunity during infection: A case study of HLB in citrus and fire blight in apple. *Frontiers in Plant Science*, 13.
- Bazany, K. E., Delgado-Baquerizo, M., Thompson, A., Wang, J. T., Otto, K., Adair Jr, R. C., Borch, T., Leach, J. E., & Trivedi, P. (2022). Management-induced shifts in rhizosphere bacterial communities contribute to the control of pathogen causing citrus greening disease. *Journal of Sustainable Agriculture and Environment*, 1(4), 275–286.
- Blaustein, R. A., Lorca, G. L., Meyer, J. L., Gonzalez, C. F., & Teplitski, M. (2017). Defining the core citrus leaf-and root-associated microbiota: Factors associated with community structure and implications for managing huanglongbing (citrus greening) disease. *Applied and environmental microbiology*, 83(11), e00210–00217.
- Blaustein, R. A., Lorca, G. L., & Teplitski, M. (2018). Challenges for managing *Candidatus Liberibacter* spp.(Huanglongbing disease pathogen): Current control measures and future directions. *Phytopathology*, 108(4), 424–435.
- Boina, D. R., Rogers, M. E., Wang, N., & Stelinski, L. L. (2010). Effect of pyriproxyfen, a juvenile hormone mimic, on egg hatch, nymph development, adult emergence and reproduction of the Asian citrus psyllid, *Diaphorina citri* Kuwayama. *Pest Management Science: formerly Pesticide Science*, 66(4), 349–357.
- Britt, K., Gebben, S., Levy, A., Al Rwahnih, M., & Batuman, O. (2020). The detection and surveillance of Asian Citrus Psyllid (*Diaphorina citri*)—associated viruses in Florida citrus groves. *Frontiers in Plant Science*, 10, 1687.
- Campos, M. L., de Souza, C. M., de Oliveira, K. B. S., Dias, S. C., & Franco, O. L. (2018). The role of antimicrobial peptides in plant immunity. *Journal of experimental botany*, 69(21),

4997–5011.

- Caporaso, J. G., Lauber, C. L., Walters, W. A., Berg-Lyons, D., Huntley, J., Fierer, N., Owens, S. M., Betley, J., Fraser, L., & Bauer, M. (2012). Ultra-high-throughput microbial community analysis on the Illumina HiSeq and MiSeq platforms. *The ISME journal*, 6(8), 1621–1624.
- Dandekar, A. M., Gouran, H., Ibáñez, A. M., Uratsu, S. L., Agüero, C. B., McFarland, S., Borhani, Y., Feldstein, P. A., Bruening, G., & Nascimento, R. (2012). An engineered innate immune defense protects grapevines from Pierce disease. *Proceedings of the National Academy of Sciences*, 109(10), 3721–3725.
- Durrant, W. E., & Dong, X. (2004). Systemic acquired resistance. *Annu. Rev. Phytopathol.*, 42, 185–209.
- Dutt, M., Barthe, G., Irely, M., & Grosser, J. (2015). Transgenic citrus expressing an Arabidopsis NPR1 gene exhibit enhanced resistance against Huanglongbing (HLB; Citrus Greening). *PLoS One*, 10(9), e0137134.
- Edgar, R. C. (2010). Search and clustering orders of magnitude faster than BLAST. *Bioinformatics*, 26(19), 2460–2461.
- Edgar, R. C. (2013). UPARSE: highly accurate OTU sequences from microbial amplicon reads. *Nature methods*, 10(10), 996–998.
- Edgar, R. C. (2016). UNOISE2: improved error-correction for Illumina 16S and ITS amplicon sequencing. *bioRxiv*, 081257.
- Fu, Z. Q., & Dong, X. (2013). Systemic acquired resistance: turning local infection into global defense. *Annual review of plant biology*, 64, 839–863.
- Graham, J., Gottwald, T., & Setamou, M. (2020). Status of huanglongbing (HLB) outbreaks in Florida, California and Texas. *Tropical Plant Pathology*, 45, 265–278.
- Grosdidier, M., Aguayo, J., Marçais, B., & Ioos, R. (2017). Detection of plant pathogens using real-time PCR: how reliable are late Ct values? *Plant Pathology*, 66(3), 359–367.
- Gupta, G., & Stover, E. (2020). Compositions and Methods for the Treatment of Huanglongbing (HLB) aka Citrus Greening in Citrus Plants. In: Google Patents.
- Hacquard, S., Spaepen, S., Garrido-Oter, R., & Schulze-Lefert, P. (2017). Interplay between innate immunity and the plant microbiota. *Annual Review of phytopathology*, 55, 565–589.
- Hao, G., Stover, E., & Gupta, G. (2016). Overexpression of a modified plant thionin enhances disease resistance to citrus canker and huanglongbing (HLB). *Frontiers in Plant Science*, 7, 1078.

- Hoffman, M. T., Doud, M. S., Williams, L., Zhang, M.-Q., Ding, F., Stover, E., Hall, D., Zhang, S., Jones, L., & Gooch, M. (2013). Heat treatment eliminates ‘*Candidatus Liberibacter asiaticus*’ from infected citrus trees under controlled conditions. *Phytopathology*, 103(1), 15–22.
- Hu, J., & Wang, N. (2016). Evaluation of the spatiotemporal dynamics of oxytetracycline and its control effect against citrus Huanglongbing via trunk injection. *Phytopathology*, 106(12), 1495–1503.
- Hu, Y., Meng, Y., Yao, L., Wang, E., Tang, T., Wang, Y., Dai, L., Zhao, M., Zhang, H.-e., & Fan, X. (2022). Citrus Huanglongbing correlated with incidence of *Diaphorina citri* carrying *Candidatus Liberibacter asiaticus* and citrus phyllosphere microbiome. *Frontiers in Plant Science*, 13, 964193.
- Huang, C.-Y., Araujo, K., Sánchez, J. N., Kund, G., Trumble, J., Roper, C., Godfrey, K. E., & Jin, H. (2021). A stable antimicrobial peptide with dual functions of treating and preventing citrus Huanglongbing. *Proceedings of the National Academy of Sciences*, 118(6), e2019628118.
- Jain, D., & Khurana, J. P. (2018). Role of pathogenesis-related (PR) proteins in plant defense mechanism. *Molecular aspects of plant-pathogen interaction*, 265–281.
- Leekha, S., Terrell, C. L., & Edson, R. S. (2011). General principles of antimicrobial therapy. *Mayo clinic proceedings*,
- Leff, J. W. (2017). *mctoolsr: Microbial community data analysis tools*. R package version 0.1, 1.
- Lei, M., Jayaraman, A., Van Deventer, J. A., & Lee, K. (2021). Engineering selectively targeting antimicrobial peptides. *Annual review of biomedical engineering*, 23, 339–357.
- Li, H., Song, F., Wu, X., Deng, C., Xu, Q., Peng, S. a., & Pan, Z. (2021). Microbiome and Metagenome Analysis Reveals Huanglongbing Affects the Abundance of Citrus Rhizosphere Bacteria Associated with Resistance and Energy Metabolism. *Horticulturae*, 7(6), 151.
- Li, J., Li, L., Pang, Z., Kolbasov, V. G., Ehsani, R., Carter, E. W., & Wang, N. (2019). Developing citrus huanglongbing (HLB) management strategies based on the severity of symptoms in HLB-endemic citrus-producing regions. *Phytopathology*, 109(4), 582–592.
- Li, J., Pang, Z., Trivedi, P., Zhou, X., Ying, X., Jia, H., & Wang, N. (2017). ‘*Candidatus Liberibacter asiaticus*’ encodes a functional salicylic acid (SA) hydroxylase that degrades SA to suppress plant defenses. *Molecular Plant-Microbe Interactions*, 30(8), 620–630.
- Li, J., Trivedi, P., & Wang, N. (2016). Field evaluation of plant defense inducers for the control of citrus huanglongbing. *Phytopathology*, 106(1), 37–46.

- Li, S., Wu, F., Duan, Y., Singerman, A., & Guan, Z. (2020). Citrus greening: Management strategies and their economic impact. *HortScience*, 55(5), 604–612.
- Liu, H.-Q., Zhao, Z.-l., Li, H.-J., Yu, S.-J., Cong, L., Ding, L.-L., Ran, C., & Wang, X.-F. (2023). Accurate prediction of huanglongbing occurrence in citrus plants by machine learning-based analysis of symbiotic bacteria. *Frontiers in Plant Science*, 14, 1129508.
- Livak, K. J., & Schmittgen, T. D. (2001). Analysis of relative gene expression data using real-time quantitative PCR and the 2<sup>-</sup> ΔΔCT method. *methods*, 25(4), 402–408.
- Madeira, F., Pearce, M., Tivey, A. R., Basutkar, P., Lee, J., Edbali, O., Madhusoodanan, N., Kolesnikov, A., & Lopez, R. (2022). Search and sequence analysis tools services from EMBL-EBI in 2022. *Nucleic acids research*, 50(W1), W276–W279.
- Martin, M. (2011). Cutadapt removes adapter sequences from high-throughput sequencing reads. *EMBnet. journal*, 17(1), 10–12.
- Molinari, S., Fanelli, E., & Leonetti, P. (2014). Expression of tomato salicylic acid (SA)-responsive pathogenesis-related genes in Mi-1-mediated and SA-induced resistance to root-knot nematodes. *Molecular plant pathology*, 15(3), 255–264.
- Montesinos, E. (2007). Antimicrobial peptides and plant disease control. *FEMS microbiology letters*, 270(1), 1–11.
- Montesinos, E. (2023). Functional Peptides for Plant Disease Control. *Annual Review of phytopathology*, 61.
- Moretta, A., Scieuzo, C., Petrone, A. M., Salvia, R., Manniello, M. D., Franco, A., Lucchetti, D., Vassallo, A., Vogel, H., & Sgambato, A. (2021). Antimicrobial peptides: A new hope in biomedical and pharmaceutical fields. *Frontiers in Cellular and Infection Microbiology*, 11, 668632.
- Nilsson, R. H., Larsson, K.-H., Taylor, A. F. S., Bengtsson-Palme, J., Jeppesen, T. S., Schigel, D., Kennedy, P., Picard, K., Glöckner, F. O., & Tedersoo, L. (2019). The UNITE database for molecular identification of fungi: handling dark taxa and parallel taxonomic classifications. *Nucleic acids research*, 47(D1), D259–D264.
- Nishad, R., Ahmed, T., Rahman, V. J., & Kareem, A. (2020). Modulation of plant defense system in response to microbial interactions. *Frontiers in microbiology*, 11, 1298.
- Quast, C., Pruesse, E., Yilmaz, P., Gerken, J., Schweer, T., Yarza, P., Peplies, J., & Glöckner, F. O. (2012). The SILVA ribosomal RNA gene database project: improved data processing and web-based tools. *Nucleic acids research*, 41(D1), D590–D596.
- Rehberg, R. A., Trivedi, P., Dooley, G. P., Hageman, K. J., Stokes, S. C., & Borch, T. (2022). Dissipation Rates and Effectiveness of Malathion, Imidacloprid, And Dimethoate at

- Controlling Asian Citrus Psyllids under Field Conditions. *ACS Agricultural Science & Technology*, 2(5), 932–940.
- Sétamou, M., Rodriguez, D., Saldana, R., Schwarzlose, G., Palrang, D., & Nelson, S. (2010). Efficacy and uptake of soil-applied imidacloprid in the control of Asian citrus psyllid and a citrus leafminer, two foliar-feeding citrus pests. *Journal of economic entomology*, 103(5), 1711–1719.
- Soares, J. M., Tanwir, S. E., Grosser, J. W., & Dutt, M. (2020). Development of genetically modified citrus plants for the control of citrus canker and huanglongbing. *Tropical Plant Pathology*, 45, 237–250.
- Srinivasan, R., Hoy, M. A., Singh, R., & Rogers, M. E. (2008). Laboratory and field evaluations of Silwet L-77 and kinetic alone and in combination with imidacloprid and abamectin for the management of the Asian citrus psyllid, *Diaphorina citri* (Hemiptera: Psyllidae). *Florida Entomologist*, 91(1), 87–100.
- Srivastava, A. K., Das, A. K., Jagannadham, P. T. K., Bora, P., Ansari, F. A., & Bhate, R. (2022). Bioprospecting microbiome for soil and plant health management amidst huanglongbing threat in citrus: a review. *Frontiers in Plant Science*, 13, 858842.
- Stokes, S. C., Trivedi, P., Otto, K., Ippolito, J. A., & Borch, T. (2023). Determining soil health parameters controlling crop productivity in a Citrus Greening disease affected orange grove. *Soil & Environmental Health*, 1(2), 100016.
- Stover, E., Stange, R. R., McCollum, T. G., Jaynes, J., Irely, M., & Mirkov, E. (2013). Screening antimicrobial peptides in vitro for use in developing transgenic citrus resistant to huanglongbing and citrus canker. *Journal of the American Society for Horticultural Science*, 138(2), 142–148.
- Su, H., Wang, Y., Xu, J., Omar, A. A., Grosser, J. W., Calovic, M., Zhang, L., Feng, Y., Vakulskas, C. A., & Wang, N. (2023). Generation of the transgene-free canker-resistant *Citrus sinensis* using Cas12a/crRNA ribonucleoprotein in the T0 generation. *Nature communications*, 14(1), 3957.
- Trivedi, P., Batista, B. D., Bazany, K. E., & Singh, B. K. (2022). Plant–microbiome interactions under a changing world: Responses, consequences and perspectives. *New Phytologist*, 234(6), 1951–1959.
- Trivedi, P., Delgado-Baquerizo, M., Trivedi, C., Hamonts, K., Anderson, I. C., & Singh, B. K. (2017). Keystone microbial taxa regulate the invasion of a fungal pathogen in agroecosystems. *Soil Biology and Biochemistry*, 111, 10–14.
- Trivedi, P., He, Z., Van Nostrand, J. D., Albrigo, G., Zhou, J., & Wang, N. (2012). Huanglongbing alters the structure and functional diversity of microbial communities

- associated with citrus rhizosphere. *The ISME journal*, 6(2), 363–383.
- Trivedi, P., Leach, J. E., Tringe, S. G., Sa, T., & Singh, B. K. (2020). Plant–microbiome interactions: from community assembly to plant health. *Nature reviews microbiology*, 18(11), 607–621.
- Trivedi, P., Sagaram, U. S., Kim, J.-S., Brlansky, R. H., Rogers, M. E., Stelinski, L. L., Oswalt, C., & Wang, N. (2009). Quantification of viable *Candidatus Liberibacter asiaticus* in hosts using quantitative PCR with the aid of ethidium monoazide (EMA). *European Journal of Plant Pathology*, 124, 553–563.
- Trivedi, P., Spann, T., & Wang, N. (2011). Isolation and characterization of beneficial bacteria associated with citrus roots in Florida. *Microbial ecology*, 62, 324–336.
- Trivedi, P., Trivedi, C., Grinyer, J., Anderson, I. C., & Singh, B. K. (2016). Harnessing host-vector microbiome for sustainable plant disease management of phloem-limited bacteria. *Frontiers in Plant Science*, 7, 1423.
- USDA. (2023). Florida Citrus Statistics 2021-2022.
- Wang, N. (2021). A promising plant defense peptide against citrus Huanglongbing disease. *Proceedings of the National Academy of Sciences*, 118(6), e2026483118.
- Wang, N., Pierson, E. A., Setubal, J. C., Xu, J., Levy, J. G., Zhang, Y., Li, J., Rangel, L. T., & Martins Jr, J. (2017). The *Candidatus Liberibacter*–host interface: insights into pathogenesis mechanisms and disease control. *Annual Review of phytopathology*, 55, 451–482.
- Wang, N., Stelinski, L. L., Pelz-Stelinski, K. S., Graham, J. H., & Zhang, Y. (2017). Tale of the huanglongbing disease pyramid in the context of the citrus microbiome. *Phytopathology*, 107(4), 380–387.
- Wang, N., & Trivedi, P. (2013). Citrus huanglongbing: a newly relevant disease presents unprecedented challenges. *Phytopathology*, 103(7), 652–665.
- Weber, K. C., Mahmoud, L. M., Stanton, D., Welker, S., Qiu, W., Grosser, J. W., Levy, A., & Dutt, M. (2022). Insights into the mechanism of Huanglongbing tolerance in the Australian finger lime (*Citrus australasica*). *Frontiers in Plant Science*, 13, 1019295.
- Weinhold, A., Karimi Dorcheh, E., Li, R., Rameshkumar, N., & Baldwin, I. T. (2018). Antimicrobial peptide expression in a wild tobacco plant reveals the limits of host-microbe-manipulations in the field. *Elife*, 7, e28715.
- Xiong, C., Zhu, Y. G., Wang, J. T., Singh, B., Han, L. L., Shen, J. P., Li, P. P., Wang, G. B., Wu, C. F., & Ge, A. H. (2021). Host selection shapes crop microbiome assembly and network

- complexity. *New Phytologist*, 229(2), 1091–1104.
- Xu, J., Zhang, Y., Zhang, P., Trivedi, P., Riera, N., Wang, Y., Liu, X., Fan, G., Tang, J., & Coletta-Filho, H. D. (2018). The structure and function of the global citrus rhizosphere microbiome. *Nature communications*, 9(1), 4894.
- Yuan, M., Ngou, B. P. M., Ding, P., & Xin, X.-F. (2021). PTI-ETI crosstalk: an integrative view of plant immunity. *Current opinion in plant biology*, 62, 102030.
- Zhang, M., Powell, C. A., Zhou, L., He, Z., Stover, E., & Duan, Y. (2011). Chemical compounds effective against the citrus Huanglongbing bacterium ‘*Candidatus Liberibacter asiaticus*’ in planta. *Phytopathology*, 101(9), 1097–1103.
- Zhang, Q.-Y., Yan, Z.-B., Meng, Y.-M., Hong, X.-Y., Shao, G., Ma, J.-J., Cheng, X.-R., Liu, J., Kang, J., & Fu, C.-Y. (2021). Antimicrobial peptides: mechanism of action, activity and clinical potential. *Military Medical Research*, 8, 1–25.
- Zhang, Y., Xu, J., Riera, N., Jin, T., Li, J., & Wang, N. (2017). Huanglongbing impairs the rhizosphere-to-rhizoplane enrichment process of the citrus root-associated microbiome. *Microbiome*, 5, 1–17.

## **CHAPTER 3: The elimination of the *Xylella fastidiosa* in the grapevine by using the chimeric antimicrobial peptide and its impact on the native microbiome**

### **3.1 OVERVIEW**

Plant-associated microbiomes play a crucial role in plant health, yet pathogen invasion can disrupt microbial community structure and stability. Understanding how plant microbiomes respond to pathogen suppression is essential for developing disease management strategies that minimize unintended impacts on beneficial microbes. In our previous study, we demonstrated that the chimeric antimicrobial peptide UGK17 selectively targets phloem limited pathogens while causing minimal disruption to the native phyllosphere microbiota under laboratory conditions. In this study, we aimed to evaluate the efficacy of UGK17 against the xylem-limited pathogen *Xylella fastidiosa* (Xf) under field conditions and to examine its impact on the native phyllosphere microbiome.

Leaf and bark from grapevines were sampled across three time points, including healthy plants, Xf infected plants, and infected plants treated exogenously with UGK17. Pathogen abundance was quantified using qPCR and amplicon sequencing, while bacterial and fungal community structures were characterized through 16S and ITS amplicon sequencing. Microbial diversity, community composition, and inter-kingdom co-occurrence networks were analyzed to evaluate microbiome responses to infection and treatment.

UGK17 treatment effectively suppressed the proliferation of Xf over time, while untreated infected plants exhibited significant increases in pathogen abundance. Pathogen infection led to pronounced microbiome dysbiosis, characterized by reduced microbial diversity, increased compositional variability, and altered microbial interaction networks. In contrast, peptide-treated

plants showed bacterial community structures and network architectures that progressively converged toward those observed in healthy plants, suggesting partial microbiome recovery following pathogen suppression. Fungal communities, however, remained primarily influenced by infection status rather than peptide treatment. Overall, targeted pathogen suppression restores bacterial microbiome stability while preserving native community structure, supporting its potential as a microbiome-friendly disease management strategy.

### **3.2 INTRODUCTION**

The plant microbiome has emerged as one of the crucial determinants of plant health, development, and resilience to environmental stressors (Trivedi et al., 2020). This community of bacteria, fungi, and other microorganisms forms complex networks that interact intimately with the host plants, influencing nutrient acquisition, hormone signaling, and immune modulation (Agler et al., 2016; Russ et al., 2023). In recent years, increasing attention has been given to understanding how the inherent or core microbiome contributes to plant productivity and disease resistance. The balance of microbial communities is often essential for maintaining plant fitness under stress. When dysbiosis of the microbial community occurs, plants may experience increased susceptibility to pathogens or reduced tolerance to abiotic stresses (Ketehouli et al., 2024; Paasch & He, 2021).

Pathogen invasion is one of the primary factors that disrupts the equilibrium of the plant microbiome, leading to dysbiosis. The invasion of a pathogen can reshape the microbial structure through competition for resources, secretion of antimicrobial metabolites, or manipulation of host immune responses (Ketehouli et al., 2024; Pfeilmeier et al., 2024; Ping et al., 2024). This disruption can have cascading effects on the overall microbial network, influencing not only disease progression but also plant recovery after infection. Conventional pathogen control

strategies often exert off-target effects on resident microbiota (Noel et al., 2022), making it difficult to disentangle the direct consequences of pathogen removal from collateral microbial disturbance. Therefore, how plant associated microbiomes respond to and recover following pathogen-specific disturbance remains unexplored.

Recent advances in biocontrol and synthetic biology have led to the development of novel antimicrobial strategies designed to target specific pathogens while minimizing collateral damage to beneficial microbiota (Lei et al., 2021; Qi et al., 2024; Tanaka et al., 2024). Among these, antimicrobial peptides (AMPs) are highlighted as novel solutions for combating pathogens. In our previous study, a chimeric antimicrobial peptide was designed to target *Candidatus Liberibacter asiaticus* (CLAs) and *Erwinia amylovora*, which cause Huanglongbing on citrus and Fire blight on apples, respectively (Basu et al., 2022). UGK17, which is used in this study, effectively reduced the titer of CLAs with negligible effect on the citrus phyllosphere microbiome (Choi et al., 2023). These findings suggest that the UGK17 can serve as a selective biocontrol tool capable of suppressing a broad-range of gram-negative pathogens without inducing widespread disruption of the plant microbiome.

Building on these insights, this study explores the effects of the UGK17 on *Xylella fastidiosa* (Xf), a gram-negative, xylem-limited bacterium causing Pierce's disease in grapevine. Xf is transmitted by xylem-feeding insects and colonizes the xylem, obstructing water transport by forming a biofilm and leading to severe wilting and yield loss (Mourou et al., 2025). There are reports that Xf infection alters the microbial community composition and decreases the abundance of beneficial bacteria in endosphere (Anguita-Maeso et al., 2022; Giampetruzzi et al., 2020). This may be due to the shifts in nutrient availability and plant immune signaling. These findings underscore that pathogen colonization can reconfigure plant associated microbiomes far

beyond the infection site, raising questions about the extent to which microbial communities can recover after successful pathogen suppression.

We hypothesized that the application of UGK17 would effectively reduce the Xf titers due to its strong activity against gram-negative pathogens, while exerting minimal effects on the inherent microbiome in grapevine, which also contains gram-negative bacteria. Furthermore, we proposed that Xf infection induces a transient dysbiosis in the microbial community, which may gradually return to a stable state once pathogen pressure is alleviated. To test this, we compared the microbial composition of healthy, infected, and peptide-treated infected grapevines using high-throughput sequencing.

By examining the structure of recovery of the grape phyllosphere microbiome following pathogen infection and peptide treatment, this study provides new insights into the resilience of plant associated microbial communities. Understanding how the microbiome responds to targeted pathogen suppression will advance our ability to design disease management strategies that restore plant health while preserving beneficial microbial networks. Ultimately, this research bridges microbial ecology and plant pathology by addressing how therapeutic interventions shape the ecological balance of plant-microbe systems.

### **3.3 MATERIALS AND METHODS**

#### **3.3.1 Sample collection and chimeric antimicrobial peptide treatment**

Leaf and bark samples were collected from grape vines (*Vitis vinifera*) located in a vineyard in Napa Valley, California. Vines showing symptoms of Pierce's disease were selected for sampling. Healthy controls were selected from the same vineyard row as infected vines, specifically the third asymptomatic vine located next to each infected vine.

Sampling was conducted at three distinct time points. During the initial sampling, leaf and bark samples were collected from both healthy and Pierce's disease-infected vines. Immediately after the first sampling, 10  $\mu$ M chimeric antimicrobial peptide in water was sprayed onto the canopy of half of the infected trees. The leaf and bark samples were again collected from healthy, peptide-treated infected, and untreated infected trees after one month of initial treatment. The chimeric peptide treatment was reapplied to the same previously treated infected trees. One month after the second treatment, a third sampling of leaf and bark was performed from all previously sampled trees. All samples were collected consistently from the same individual trees throughout the sampling. The collected samples were sent to Colorado State University via overnight flight and stored at  $-20^{\circ}\text{C}$  within 24 hours after collection.

### **3.3.2 DNA extraction**

Frozen samples were ground into powder using a mortar and pestle, and the DNA was extracted from the powder using a DNeasy Plant Pro Kit (Qiagen, Valencia, CA) following the manufacturer's protocol. Quantification of DNA was performed using a Nano Drop 2000 spectrophotometer (Thermo Fisher Scientific, Waltham, MA, USA). DNA were subsequently stored at  $-80^{\circ}\text{C}$  until further analysis.

### **3.3.3 Quantitative PCR**

Quantitative PCR (qPCR) was used to quantify Xf titers, as well as total bacteria and fungi. DNA samples were diluted to 10 ng/ $\mu$ L prior to qPCR assays. The qPCR reactions were prepared using the SensiFAST SYBR No-ROX Kit (Bioline, London, UK). Each reaction had a total volume of 10  $\mu$ L, comprising 5  $\mu$ L of master mix from the kit, 0.5  $\mu$ L of each forward and reverse primers, 1  $\mu$ L of DNA, and 3  $\mu$ L of nuclease free water.

Primer sets were HL5 and HL6 for Xf, EUB338 and EUB518 for total bacteria, and ITS1F and 5.8s for total fungi (Table 3.1). The amplification conditions were as follows: initial denaturation at 95°C for 2 min, followed by 40 cycles of 95°C for 15 sec and 60°C for 20 sec. For total bacteria and fungi, amplification conditions included an initial denaturation at 95°C for 2 min, followed by 40 cycles at 95°C for 15 sec and annealing and extension at 54°C for bacteria and 53°C for fungi, for 30 sec. Reactions were performed using an ABI Prism 7500 Sequence Detection System (Applied Biosystems, Foster City, CA, USA), and data were analyzed using the ABI Prism software with default settings (threshold = 0.2). Each sample was replicated 3 times on a 96-well plate, and the entire experiment was conducted twice to ensure reproducibility and method consistency.

**Table 3.1.** Primer sequences used in this study for qPCR

Target	Primer	Sequence (5' – 3')	Reference
<i>Xylella fastidiosa</i>	HL5	AAG GCA ATA AAC GCG CAC TA	Francis et al., 2006
	HL6	GGT TTT GCT GAC TGG CAA CA	
Total bacteria	EUB338	ACT CCT ACG GGA GGC AGC AG	Fierer et al., 2005
	EUB518	ATT ACC GCG GCT GCT GG	
Total fungi	ITS1F	TCCGTAGGTGAACCTGCGG	Fierer et al., 2005
	5.8S	CGCTGCGTTCTTCATCG	

### 3.3.4 Microbiome analysis

Bacterial and fungal community diversity and structure were assessed via amplicon sequencing using the Illumina MiSeq platform. Amplification of the V4 region of the bacterial 16S rRNA gene and the fungal ITS1 region was performed using the primer sets 515F/8086R and ITS1F/ITS2R, respectively (Caporaso et al., 2012). To reduce host-derived sequence contamination, 0.5 mM of mitochondrial (mPNA) and plastide (pPNA) peptide nucleic acid blockers (PNA Bio, CA, USA) were included in each PCR reaction. The library preparation and sequencing were conducted at the Colorado State University Next Generation Sequencing Facility (Fort Collins, CO, USA). Raw sequence data were processed using USEARCH (Edgar, 2010) and UNOISE3 (Edgar, 2016) pipelines. Adapters and primers were trimmed using cutadapt (Martin, 2011), followed by sample demultiplexing. Paired-end reads were merged, and the quality was checked by fastQC. The paired reads containing ambiguous bases, low-quality scores ( $Q < 20$ ), or short length ( $< 100$ bp) were removed. High-quality reads were clustered into the representative set database using the UCLUST and UPARSE algorithm (Edgar, 2013). The unique operational taxonomic units (OTUs) at 97% similarity were inferred using DADA2 and denoised with UNOISE3 (Xiong et al., 2021). Additionally, OTU tables were generated by mapping reads to representative sequence sets, and counts were aggregated per sample. Each OTU was assigned taxonomy using the SILVA database (Quast et al., 2012) for bacterial 16S and the UNITE database (Nilsson et al., 2019) for fungal ITS sequences.

All downstream analyses were conducted in R using the ‘mctoolsr’ and ‘phyloseq’ packages. First, datasets were separated by domain (bacteria and fungi), and then by tissue type (leaf and bark). OTUs present in fewer than four samples were removed. For the bacterial dataset,

sequences classified as chloroplast or mitochondrial cell were excluded to minimize host DNA contamination. Each dataset was then rarefied to the median sequencing depth.

Alpha diversity was calculated using the Shannon diversity index (Shannon, 1948). General linear models (GLMs) followed by Tukey's HSD test were used to assess significant differences among treatments (Healthy, AMP-treated, AMP-nontreated) and sampling time point. Beta diversity was examined using Bray-Curtis dissimilarity and visualized through canonical analysis of principal coordinates (CAP) (Anderson & Willis, 2003). PERMANOVA was performed to determine whether microbial community composition differed significantly across sampling time points and between treatments.

### **3.3.5 Inter-kingdom co-occurrence network**

Co-occurrence networks were constructed to investigate bacterial-fungal associations and compare network structures across treatment groups by using FastSpar (Watts et al., 2019), an implementation of the SparCC algorithm designed for compositional data (Friedman & Alm, 2012). To reduce the influence of low abundance taxa, only OTUs with more than three reads and present in at least 20% of total samples were retained. FastSpar was executed with 100 iterations and 100 bootstrap replicates to assess the statistical significance of correlations. Only strong ( $r > 0.60$ ) and significant ( $p < 0.01$ ) associations were used for network construction for each treatment. Additionally, only correlations between Xf and other bacterial or fungal OTUs were extracted to examine the correlation between the pathogen and other microbial taxa. The networks were visualized in Gephi (version 0.10.1) using the Fruchterman-Reingold layout (Fruchterman & Reingold, 1991).

### 3.4 RESULT AND DISCUSSION

#### 3.4.1 UGK17 treatment suppresses the proliferation of *Xylella fastidiosa* in grape leaves

Xf was quantified in grapevine leaves and bark tissues using both qPCR and amplicon sequencing (Figure 3.1). Although residual pathogen DNA from dead cells may persist in plant tissues, DNA is an appropriate material for estimating pathogen titer in grapevine because Xf is a slow growing bacterium with limited turnover (De La Fuente et al., 2024). To further validate the qPCR-based quantification, pathogen abundance was independently assessed using high-throughput amplicon sequencing by quantifying OTUs aligned with Xf. The consistency between these two independent approaches validated the observed patterns of pathogen abundance across treatments and sampling time points. Since pathogen titers in bark tissues did not show meaningful variation among treatments or sampling time points (Supplimentary Figure S3.1), subsequent analyses focused on leaf tissues.

Quantification of Xf in grapevine leaves showed changes in pathogen abundance temporally and based on the treatment. Healthy grapevine showed negligible pathogen levels by qPCR with the  $C_t$  value consistently around 30 (Figure 3.1A). Also, amplicon sequencing of healthy samples showed no abundance of OTU associated with Xf (Figure 3.1B). In contrast, the  $C_t$  value of Xf in infected grapevines without UGK17 treatment was significantly decreased at the third sampling time compared to the first sampling time, indicating a substantial increase in pathogen titer over time (Figure 3.1A). Consistent with this result, Xf abundance from the same samples increased (Figure 3.1B). However, UGK17 treated grapevine leaves did not show significant temporal changes in Xf quantity by either qPCR or amplicon sequencing.

UGK17 had shown a strong efficacy against the bacterial pathogen causing apple fire blight

and Huanglongbing which colonize extracellular spaces and phloem, respectively (Basu et al., 2022; Choi et al., 2023). In this study, the titer of Xf in UGK17 treated grapevines remained stable over time indicating that UGK17 effectively suppressed the proliferation of Xf. Xf is gram-negative pathogen, as are CLas and *E. amylovora*. Gram-negative pathogens commonly possess negatively charged outer membranes that are susceptible to the cationic AMP (Bechinger & Gorr, 2017).

In addition, AMPs are not restricted to a single tissue or cellular compartment within plants. AMPs synthesized in one cellular compartment can transit across cellular boundaries and potentially influence pathogen defense in distant tissues. For example, AMPs expressed in *Nicotiana benthamiana* have been shown to accumulate in apoplast via the endomembrane secretion system (Chaudhary et al., 2024). Defensin, a plant AMP, has been detected in the xylem of defensin-expressing transgenic rice (Gu et al., 2023).

UGK17 was designed to be very stable relative to many naturally occurring AMPs, which prolongs its persistence and bioactivity within plant tissues (Basu et al., 2022). Together, the conserved gram-negative membrane properties, the effective distribution of AMP, and the enhanced stability of UGK17 enable its sustained activity against Xf, resulting in suppression of pathogen proliferation.

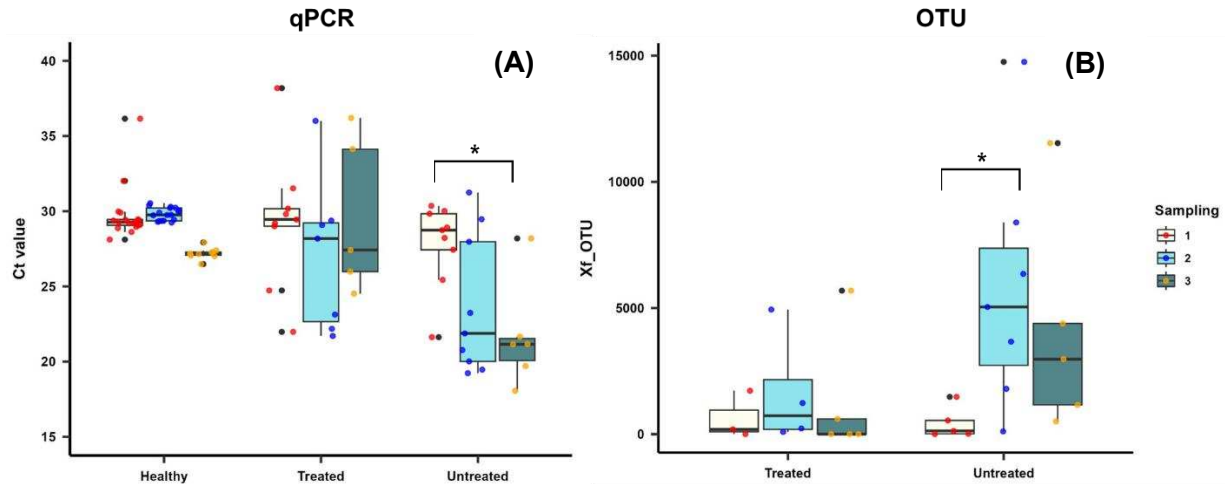


**Figure 3.1.** The quantification of the *Xylella fastidiosa* (Xf) in grapevine leaves. Leaves were collected from the healthy and infected grapevines, and the infected grapevines were divided into two groups with and without treatment of the AMP UGK17. Pathogen quantification was done by the quantitative PCR (A) and counting the operational taxonomic units (OTUs) aligned with Xf (B) from the amplicon sequencing. Significant differences were determined by Tukey HSD ( $p < 0.05$ ). Comparisons are within the same leaf condition.

### 3.4.2 Pathogen-driven disruption of leaf-associated microbial communities

The Shannon diversity index was used to assess alpha diversity of bacterial and fungal communities in grapevine leaves (Figure 3.2). For bacterial communities, Healthy leaves consistently showed the highest Shannon index across all sampling time points, with relatively small variation among replicates, indicating that they maintain a highly diverse and evenly structured bacterial community (Figure 3.2A). UGK17 treated leaves exhibited a reduction in bacterial diversity, whereas untreated leaves showed the lowest Shannon index throughout the sampling period.

A similar pattern was observed for fungal communities (Figure 3.2B). Healthy leaves harbored the highest Shannon index, while Xf infected leaves showed a significant reduction in the fungal Shannon index across sampling time points regardless of UGK17 treatment. To

determine whether these diversity shifts were associated with changes in total microbial abundance, qPCR was used to estimate total bacterial and fungal abundance in grapevine tissues (Supplementary Figure S3.2). In leaf samples, total bacterial abundance remained relatively stable regardless of infection status or sampling time point. In contrast, total fungal abundance did not differ significantly between healthy and infected leaves but showed a marked decrease at sampling time point 3. These findings indicate that the observed changes in microbial diversity were not primarily driven by total microbial abundance, but rather by shifts in community composition and structure, suggesting that pathogen infection alters microbial community without substantially affecting overall microbial load.

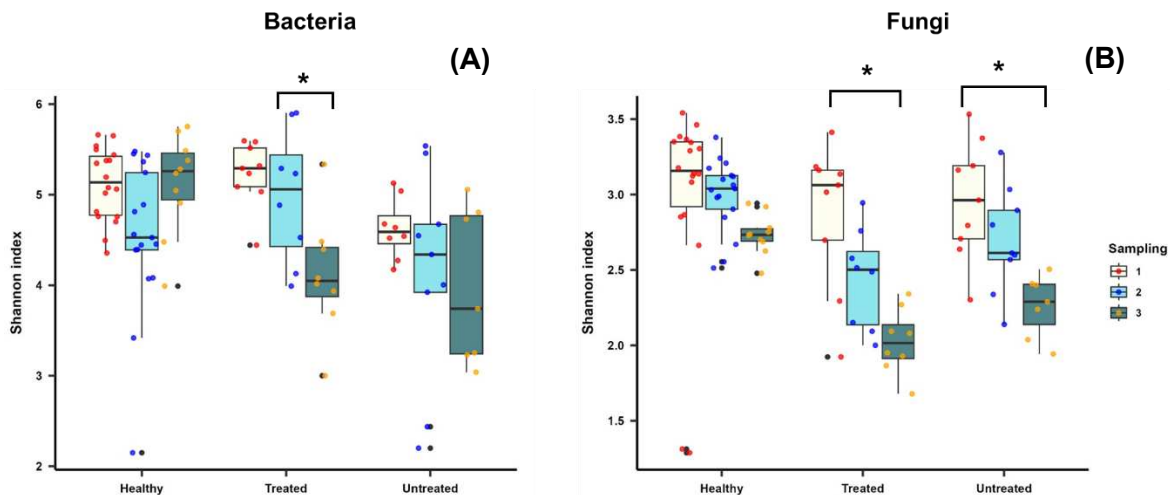


**Figure 3.2.** Shannon diversity index of bacteria (A) and fungi (B) in grapevine leaves. The significant difference between the sampling was determined by Tukey HSD ( $p < 0.05$ ). Comparisons are within the same leaf condition.

In addition to changes in alpha diversity, beta diversity analysis revealed pronounced shifts in microbial community composition in grapevine leaves (Figure 3.3). CAP ordination showed

separation of samples according to AMP treatment for both bacterial and fungal communities. For the bacterial community, healthy samples clustered distinctly from UGK17 untreated samples, while treated samples occupied an intermediate ordination space, partially overlapping with healthy samples (Figure 3.3A). Notably, untreated samples showed a broader dispersion in the ordination space compared to healthy and UGK17 treated samples, suggesting increased compositional variability and reduced community stability. Interestingly, there was a clear distinction between healthy and infected leaves in fungal communities, while UGK17 treated and untreated leaves largely overlapped (Figure 3.3B).

The alpha and beta diversity analyses demonstrate that Xf infection strongly disrupted the phyllosphere microbiome of grapevine, affecting both microbial diversity and composition. The consistent reduction in Shannon index observed in infected leaves indicates a loss of microbial complexity. The separation of bacterial communities in beta diversity analyses between healthy and infected leaves indicates that pathogen infection caused systematic restructuring of microbial assemblages rather than a uniform decline in abundance. Anguita-Maeso et al (2022) reported that Xf infection in Almond trees resulted in reduced Shannon index and reconstructed microbial composition. The low Shannon index of Xf infected leaves may be due to the decrease of evenness caused by the dominance of the pathogen relative to other taxa (Anguita-Maeso et al., 2022). Also, the broader dispersion observed in untreated bacterial communities reflects increased community instability. This pattern is consistent with the Anna Karenina effect, whereby pathogen infection promotes heterogeneous and unstable community structures rather than coordinated assembly (Arnault et al., 2023; Kuang et al., 2023). As a result, untreated samples tend to assemble into distinct, unpredictable, and sample unique bacterial communities instead of converging toward a common community structure.

However, intermediate clustering of treated leaves between healthy and untreated leaves in CAP ordination suggests that pathogen control by UGK17 partially mitigated pathogen-induced shifts in the bacterial community. Notably, the treated samples at time point 3 (square in Figure 3.3A) located closer to healthy samples compared to the treated samples at time point 2 (Triangle in Figure 3.3A). This indicates that restriction of pathogen proliferation helps to restore the disrupted bacterial community composition to healthy status. Larson & Crandall (2023) has reported that the disinfection of fungal pathogen helps the recovery of fungal communities in soil. Also, Jurburg et al (2024) showed that soil and rhizosphere microbiomes exhibit resilience following disturbance, with communities partially or fully recovering their original diversity and composition over time through ecological succession, species reassembly, and the restoration of microbial interactions.

In contrast to the bacterial community, the fungal community appeared to be primarily affected by infection rather than UGK17 treatment. The strong separation between healthy and infected leaves, combined with the overlap between treated and untreated infected leaves, suggests that fungal communities are less responsive to UGK17 mediated effects. Moreover, the trends of the Shannon index reduction throughout the sampling time point were similar among healthy, treated and untreated samples. This may be because fungal communities are more sensitive to environmental and host-associated factors, often exhibiting slower growth rates and stronger niche specialization than bacterial communities (De Vries et al., 2012). In addition, fungal communities typically form more structured and less functionally redundant networks, which increases their vulnerability to disturbance and limits their capacity for recovery following perturbation (Banerjee et al., 2019).

Consequently, these findings indicate that Xf infection leads to both a reduction in microbial

diversity and destabilization of community structure in grapevine leaves. Specific inhibition of pathogen proliferation by AMP treatment appears to alleviate bacterial community disruption but has limited impact on fungal community.

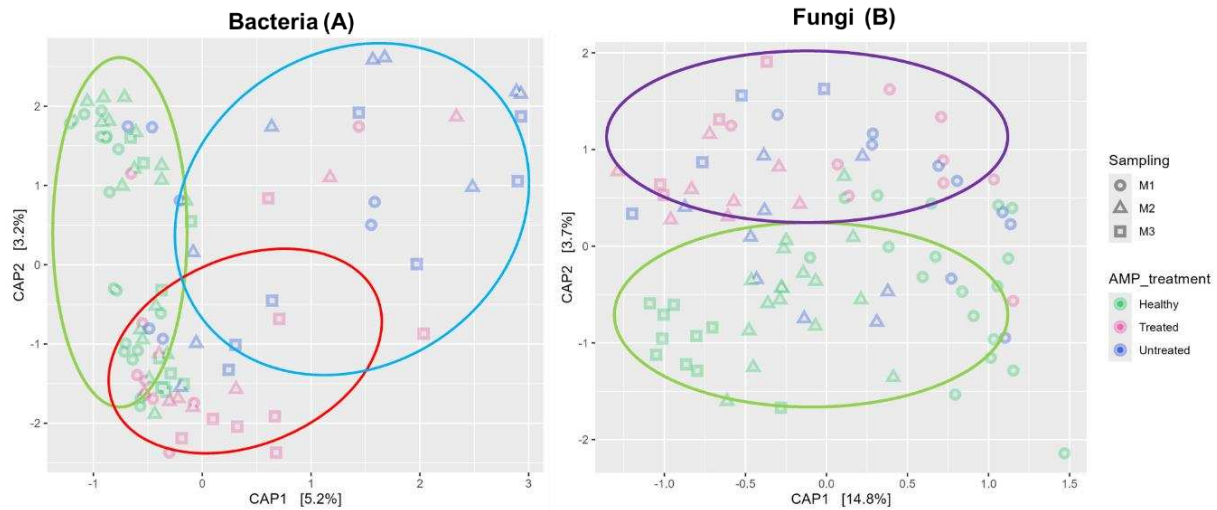


**Figure 3.3.** Canonical analysis of principal (CAP) plot for bacterial (A) and fungal (B) community structures in grapevine leaves. The analysis was performed after the Bray-Curtis distance. Circles represent the approximate clustering regions of each treatment group, highlighting differences in community composition and dispersion among healthy, UGK17-treated, and untreated samples.

### 3.4.3 Targeted suppression of *Xylella fastidiosa* mitigates pathogen-driven shifts in the grapevine leaf microbiome

As *Xf* targeted inhibition by the AMP restored bacterial community structure, we next examined which bacterial taxa were affected by pathogen invasion and subsequently suppressed by the UGK17 treatment. The volcano plot and bar plot with relative abundance showed the significant compositional shifts in bacterial community composition due to *Xf* infection (Figure 3.4). The volcano plot showed that OTU4, taxonomically assigned to *Xf*, was significantly enriched in infected leaves compared to healthy samples at the first sampling time point (Figure

3.4A). This OTU4 exhibited the largest fold change and the highest significance among all detected OTUs, indicating strong pathogen enrichment in untreated infected leaves. In contrast, the abundance of OTU4 was markedly reduced in UGK17 treated samples, with read levels of OTU4 approaching those observed in healthy grapevines. Aside from OTU4, most OTUs displayed small fold changes and non-significant adjusted p-values, suggesting that UGK17 treatment did not broadly perturb bacterial taxa but instead primarily targeted the pathogen-associated OTU. This indicates that UGK17 treatment selectively suppressed Xf while largely preserving the overall bacterial community structure.

At the phylum level, the phylum-level relative abundance bar plot showed distinct compositional differences among healthy, treated, and untreated grapevine leaves across sampling time points (Figure 3.4B). In this plot, we separated the Proteobacteria into family level, as the Proteobacteria is most dominant and common phylum in the bacterial community. Overall, Proteobacteria, Actinobacteria, and Bacteroidetes were the most dominant phylum across the treatment. They are very common phyla in the phyllosphere and the frequency of each taxa can vary depending on the environment (Bashir et al., 2022). Untreated infected leaves exhibited an increased relative abundance of Gammaproteobacteria, reflecting pathogen overrepresentation, as Xf belongs to this group. In contrast, treated leaves maintained a phylum-level composition similar to that of healthy leaves, supporting that suppression of the dominant pathogen allows the bacterial community to revert toward a healthier and more balanced state. Also, the slightly elevated proportion of Cyanobacteria in treated leaves compared to healthy leaves may reflect a recovery-oriented community shift following selective suppression of Xf. Targeted AMP strategies can reduce a dominant pathogen while limiting collateral disruption to resident microbiota (Guo et al., 2015).

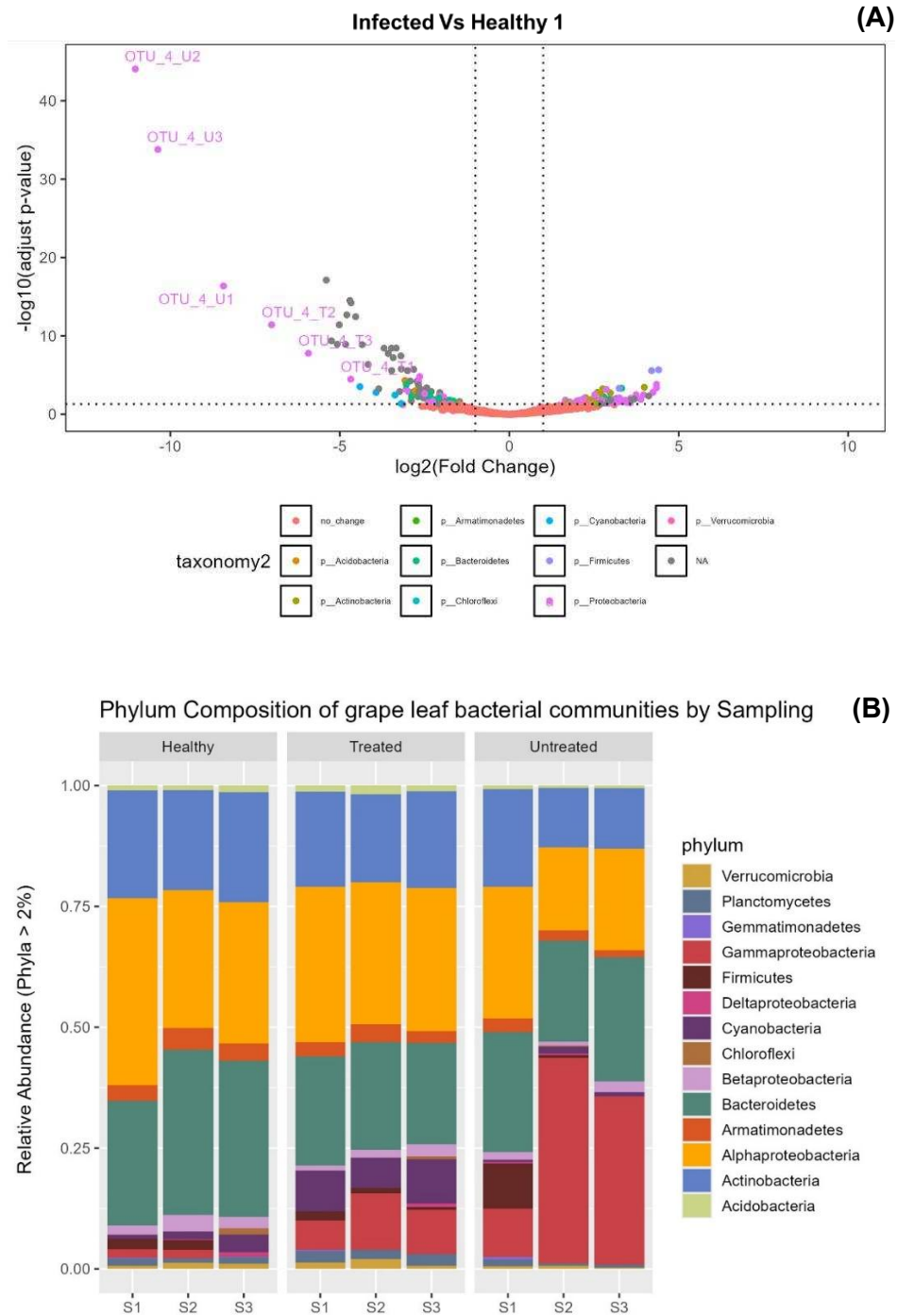


**Figure 3.4.** Differential abundance and taxonomic composition of bacterial communities in grapevine leaves. The volcano plot (A) shows differentially abundant OTUs between healthy grapevine leaves collected at the first sampling and Xf infected leaves. The x-axis represents  $\log_2$  fold change and the y-axis indicates  $-\log_{10}$  adjusted p-values. OTU4 corresponds to the pathogen *Xylella fastidiosa*. Phylum-level composition of bacterial communities in grapevine leaves from healthy, treated, and untreated plants across sampling time points (S1, S2, S3). Stacked bar plots (B) show relative abundances of bacterial phyla with mean abundance  $>2\%$ .

#### **3.4.4 Pathogen-specific treatment is associated with recovery of inter-kingdom co-occurrence network**

As the microbial community composition changes due to infection and UGK17 treatment, an inter-kingdom microbial network was used to evaluate the changes of microbial interactions among healthy, UGK17 treated, and nontreated grapevine leaves (Figure 3.5). Furthermore, we analyzed the correlations between Xf and other microbial taxa in the infected grapevine leaves to investigate the interaction between the pathogen and microbe within the community (Figure 3.6). In healthy grapevines (Figure 3.5A-C), the microbial networks exhibited a balanced and moderately connected structure, characterized by distributed interactions between bacterial and fungal nodes. Also, there was progressive increase in network complexity over time. Such temporal increases in network density and connectivity have been reported in maize and rice and are considered hallmarks of maturity of plant (Peng et al., 2025; Xiong et al., 2021).

In infected grapevine leaves treated with UGK17, the overall network topology closely resembled that of healthy grapevines (Figure 3.5D-F). Particularly, this similarity became clearer at later sampling points, where the treated network architecture converged further toward healthy conditions. In addition, the node aligned with Xf moved away from the hub center, which means that the pathogen had fewer interactions with other microbes in the network. The number of correlation between Xf and other taxa in UGK17 treated leaves decreased over time especially at sampling time point 3 (Figure 3.6A-C). Moreover, the number of positive and negative correlations was balanced, suggesting a constrained and regulated interaction profile between the pathogen and the resident microbiota. This result may indicate that pathogen control by AMP help to not only restore the bacterial composition also support the overall function of microbial community by maintaining the healthy network structure (Zheng et al., 2020; Zhou et al., 2022)

In contrast, infected grapevine leaves without UGK17 treatment displayed a markedly altered network structure (Figure 3.5G-I). These networks were characterized by increased connectivity and a dense clustering of interactions centered around the pathogen node. As sampling progressed, the untreated networks remained structurally distinct from healthy networks, indicating a persistent disruption of microbial community. Also, there was no core taxa except sampling time point 2 (Supplementary Figure S3.3). Similar disease-associated reductions in network complexity and loss of core taxa have been reported in other plant pathosystems, where pathogen invasion disrupts microbiome assembly and weakens stabilizing microbial interactions. For example, disease-induced shifts in plant microbiome assembly have been shown to reduce functional adaptation and network resilience (Gao et al., 2021), while root rot disease destabilizes the rhizosphere of Sanqi, *panax notoginseng*, core fungal microbiome by diminishing negative connectivity among beneficial taxa (Wang et al., 2024). Although these studies were conducted in root-associated systems, similar principles may apply to *Xylella fastidiosa*, a xylem-limited pathogen that disrupts host vascular function and alters the physicochemical environment of leaf tissues. Such changes can interfere with microbial interactions and weaken stabilizing network structures, ultimately leading to increased community instability and reduced resilience in the phyllosphere microbiome. Additionally, Untreated infected leaves exhibited a greater number of correlations between Xf and other taxa particularly at sampling time point 1 and 3 (Figure 3.6D-F). These associations were predominantly positive and mainly involved Proteobacteria, Actinobacteria, and Bacteroidetes. Although Xf is not the core taxa in the network (Supplementary Figure S3.3), the persistence of these positive correlations suggests that, in the absence of pathogen regulation, Xf remains tightly embedded within the microbial network and maintains extensive co-occurrence

relationships with resident microbial groups. This may relax community constraints, potentially facilitating the proliferation of opportunistic or commensal bacteria and increasing the susceptibility of the host to subsequent or secondary pathogenic effects (Zhang et al., 2025).

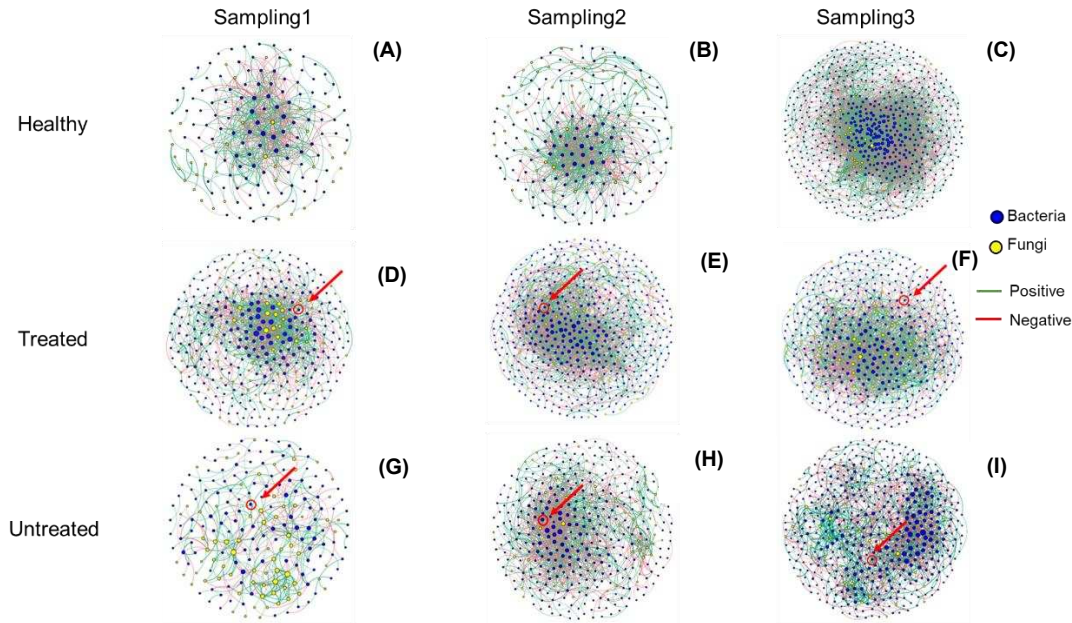


**Figure 3.5.** The inter-kingdom microbial network in leaves collected from healthy grapevines (A, B, C), infected grapevines treated with UGK17 (D, E, F) and infected grapevines without treatment of UGK17(G, H, I). The blue and yellow nodes indicate the bacteria and fungi, respectively. The green and red lines indicate the positive and negative correlation, respectively. The Xf is indicated with a red circle in each network.

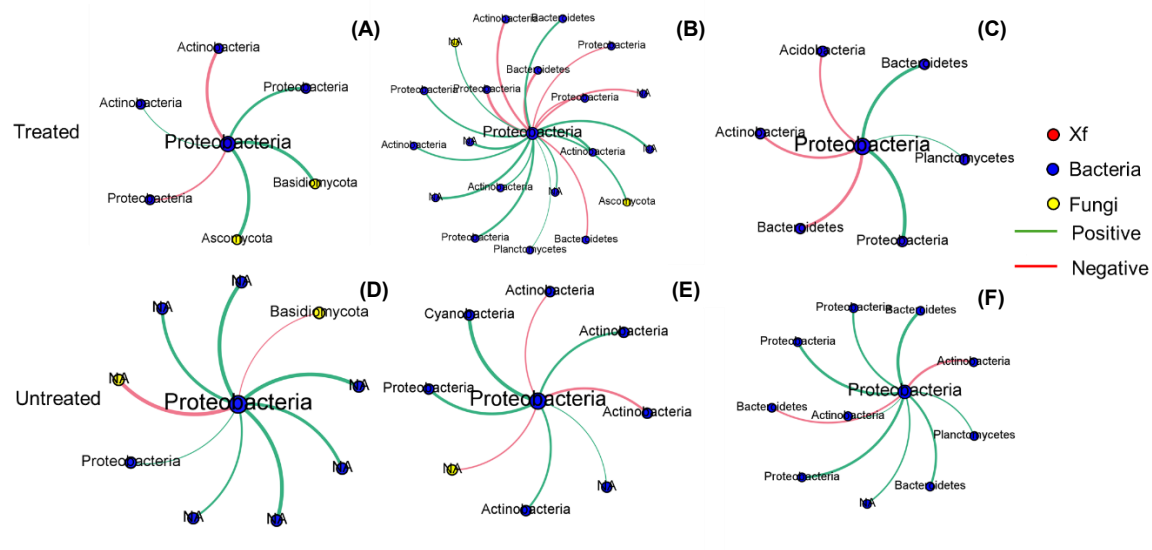


**Figure 3.6.** The correlation between the Xf and microbes in leaves collected from the infected grapevine with and without the UGK17 treatment. The red node in the center indicates the pathogen Xf, and the blue and yellow nodes refers to bacteria and fungi, respectively. The green and red lines indicate positive and negative correlations, respectively.

### 3.5 CONCLUSION

This study demonstrates that targeted suppression of *Xylella fastidiosa* using the chimeric antimicrobial peptide UGK17 effectively limits pathogen proliferation in the field while largely preserving the native grapevine phyllosphere microbiome. Pathogen infection alone induces pronounced microbiome dysbiosis, characterized by reduced diversity, increased community instability, and altered microbial interactions. In contrast, selective pathogen control by the AMP UGK17 allowed recovery of the bacterial community composition and network structure, progressively converging toward a healthy state. Overall, these findings highlight that pathogen-targeted antimicrobial strategies can mitigate disease-driven microbiome disruption and promote microbial community resilience.

## REFERENCE

- Agler, M. T., Ruhe, J., Kroll, S., Morhenn, C., Kim, S.-T., Weigel, D., & Kemen, E. M. (2016). Microbial hub taxa link host and abiotic factors to plant microbiome variation. *PLoS Biology*, 14(1), e1002352.
- Anderson, M. J., & Willis, T. J. (2003). Canonical analysis of principal coordinates: a useful method of constrained ordination for ecology. *Ecology*, 84(2), 511-525.
- Anguita-Maeso, M., Ares-Yebra, A., Haro, C., Román-Écija, M., Olivares-García, C., Costa, J., Marco-Noales, E., Ferrer, A., Navas-Cortés, J. A., & Landa, B. B. (2022). *Xylella fastidiosa* infection reshapes microbial composition and network associations in the xylem of almond trees. *Frontiers in Microbiology*, 13, 866085.
- Bashir, I., War, A. F., Rafiq, I., Reshi, Z. A., Rashid, I., & Shouche, Y. S. (2022). Phyllosphere microbiome: Diversity and functions. *Microbiological Research*, 254, 126888.
- Basu, S., Sineva, E., Nguyen, L., Sikdar, N., Park, J. W., Sinev, M., Kunta, M., & Gupta, G. (2022). Host-derived chimeric peptides clear the causative bacteria and augment host innate immunity during infection: A case study of HLB in citrus and fire blight in apple. *Frontiers in Plant Science*, 13.
- Bechinger, B., & Gorr, S.-U. (2017). Antimicrobial peptides: mechanisms of action and resistance. *Journal of Dental Research*, 96(3), 254–260.
- Caporaso, J. G., Lauber, C. L., Walters, W. A., Berg-Lyons, D., Huntley, J., Fierer, N., Owens, S. M., Betley, J., Fraser, L., & Bauer, M. (2012). Ultra-high-throughput microbial community analysis on the Illumina HiSeq and MiSeq platforms. *The ISME Journal*, 6(8), 1621–1624.
- Chaudhary, S., Ali, Z., Pantoja-Angles, A., Abdelrahman, S., Juárez, C. O. B., Rao, G. S., Hong, P. Y., Hauser, C., & Mahfouz, M. (2024). High-yield, plant-based production of an antimicrobial peptide with potent activity in a mouse model. *Plant Biotechnology Journal*, 22(12), 3392–3405.
- Choi, J., Basu, S., Thompson, A., Otto, K., Sineva, E. V., Kunta, M., Gupta, G., & Trivedi, P. (2023). A host-derived chimeric peptide protects citrus against Huanglongbing without threatening the native microbial community of the phyllosphere. *Journal of Sustainable Agriculture and Environment*, 2(4), 489–499.

- De La Fuente, L., Navas-Cortés, J. A., & Landa, B. B. (2024). Ten challenges to understanding and managing the insect-transmitted, xylem-limited bacterial pathogen *Xylella fastidiosa*. *Phytopathology*, 114(5), 869-884.
- Edgar, R. C. (2010). Search and clustering orders of magnitude faster than BLAST. *Bioinformatics*, 26(19), 2460–2461.
- Edgar, R. C. (2013). UPARSE: highly accurate OTU sequences from microbial amplicon reads. *Nature Methods*, 10(10), 996–998.
- Edgar, R. C. (2016). UNOISE2: improved error-correction for Illumina 16S and ITS amplicon sequencing. *bioRxiv*, 081257.
- Fierer, N., Jackson, J. A., Vilgalys, R., & Jackson, R. B. (2005). Assessment of soil microbial community structure by use of taxon-specific quantitative PCR assays. *Applied and Environmental Microbiology*, 71(7), 4117–4120.
- Francis, M., Lin, H., Rosa, J. C.-L., Doddapaneni, H., & Civerolo, E. L. (2006). Genome-based PCR primers for specific and sensitive detection and quantification of *Xylella fastidiosa*. *European Journal of Plant Pathology*, 115, 203–213.
- Friedman, J., & Alm, E. J. (2012). Inferring correlation networks from genomic survey data.
- Fruchterman, T. M., & Reingold, E. M. (1991). Graph drawing by force-directed placement. *Software: Practice and Experience*, 21(11), 1129–1164.
- Gao, M., Xiong, C., Gao, C., Tsui, C. K., Wang, M.-M., Zhou, X., Zhang, A.-M., & Cai, L. (2021). Disease-induced changes in plant microbiome assembly and functional adaptation. *Microbiome*, 9(1), 187.
- Giampetruzzi, A., Baptista, P., Morelli, M., Cameirão, C., Lino Neto, T., Costa, D., D’Attoma, G., Abou Kubaa, R., Altamura, G., & Saponari, M. (2020). Differences in the endophytic microbiome of olive cultivars infected by *Xylella fastidiosa* across seasons. *Pathogens*, 9(9), 723.
- Gu, T.-Y., Qi, Z.-A., Chen, S.-Y., Yan, J., Fang, Z.-J., Wang, J.-M., & Gong, J.-M. (2023). Dual-function DEFENSIN 8 mediates phloem cadmium unloading and accumulation in rice grains. *Plant Physiology*, 191(1), 515–527.
- Guo, L., McLean, J. S., Yang, Y., Eckert, R., Kaplan, C. W., Kyme, P., Sheikh, O., Varnum, B., Lux, R., & Shi, W. (2015). Precision-guided antimicrobial peptide as a targeted modulator of human microbial ecology. *Proceedings of the National Academy of Sciences*, 112(24), 7569–7574.

- He, T., Moukarzel, R., Fu, M., Yang, M., Du, R., Zhao, J., Liu, J., Wu, J., Deng, W., & Zhu, Y. (2025). Rain-shelter cultivation promotes grapevine health by altering phyllosphere microecology in rainy areas. *Environmental Microbiome*, 20(1), 56.
- Jurburg, S. D., Blowes, S. A., Shade, A., Eisenhauer, N., & Chase, J. M. (2024). Synthesis of recovery patterns in microbial communities across environments. *Microbiome*, 12(1), 79.
- Ketehouli, T., Pasche, J., Buttrós, V. H., Goss, E. M., & Martins, S. J. (2024). The underground world of plant disease: Rhizosphere dysbiosis reduces above-ground plant resistance to bacterial leaf spot and alters plant transcriptome. *Environmental Microbiology*, 26(7), e16676.
- Lei, M., Jayaraman, A., Van Deventer, J. A., & Lee, K. (2021). Engineering selectively targeting antimicrobial peptides. *Annual Review of Biomedical Engineering*, 23, 339–357.
- Martin, M. (2011). Cutadapt removes adapter sequences from high-throughput sequencing reads. *EMBnet. Journal*, 17(1), 10–12.
- Mourou, M., Incampo, G., Carlucci, M., Salamone, D., Pollastro, S., Faretra, F., & Nigro, F. (2025). Insight into biological strategies and main challenges to control the phytopathogenic bacterium *Xylella fastidiosa*. *Frontiers in Plant Science*, 16, 1608687.
- Nilsson, R. H., Larsson, K.-H., Taylor, A. F. S., Bengtsson-Palme, J., Jeppesen, T. S., Schigel, D., Kennedy, P., Picard, K., Glöckner, F. O., & Tedersoo, L. (2019). The UNITE database for molecular identification of fungi: handling dark taxa and parallel taxonomic classifications. *Nucleic Acids Research*, 47(D1), D259–D264.
- Noel, Z. A., Longley, R., Benucci, G. M. N., Trail, F., Chilvers, M. I., & Bonito, G. (2022). Non-target impacts of fungicide disturbance on phyllosphere yeasts in conventional and no-till management. *ISME Communications*, 2(1), 19.
- Paasch, B. C., & He, S. Y. (2021). Toward understanding microbiota homeostasis in the plant kingdom. *PLoS Pathogens*, 17(4), e1009472.
- Peng, Q., Sun, S. e., Ma, J., Chen, S., Gao, L., Du, X., Liu, X., Zhu, F., Peng, W., & Liu, Y. (2025). The effect of developmental stages on microbiome assembly in the phyllosphere and rhizosphere of rice grown in urban area soil. *Environmental Microbiome*, 20(1), 86.
- Pfeilmeier, S., Werz, A., Ote, M., Bortfeld-Miller, M., Kirner, P., Keppler, A., Hemmerle, L., Gäbelein, C. G., Petti, G. C., & Wolf, S. (2024). Leaf microbiome dysbiosis triggered by T2SS-dependent enzyme secretion from opportunistic *Xanthomonas* pathogens. *Nature Microbiology*, 9(1), 136–149.
- Ping, X., Khan, R. A. A., Chen, S., Jiao, Y., Zhuang, X., Jiang, L., Song, L., Yang, Y., Zhao, J., & Li, Y. (2024). Deciphering the role of rhizosphere microbiota in modulating disease resistance in cabbage varieties. *Microbiome*, 12(1), 160.

- Qi, H.-Y., Zhang, D.-D., Liu, B., Chen, J.-Y., Han, D., & Wang, D. (2024). Leveraging RNA interference technology for selective and sustainable crop protection. *Frontiers in Plant Science*, 15, 1502015.
- Quast, C., Pruesse, E., Yilmaz, P., Gerken, J., Schweer, T., Yarza, P., Peplies, J., & Glöckner, F. O. (2012). The SILVA ribosomal RNA gene database project: improved data processing and web-based tools. *Nucleic Acids Research*, 41(D1), D590–D596.
- Russ, D., Fitzpatrick, C. R., Teixeira, P. J., & Dangl, J. L. (2023). Deep discovery informs difficult deployment in plant microbiome science. *Cell*, 186(21), 4496–4513.
- Shannon, C. E. (1948). A mathematical theory of communication. *The Bell System Technical Journal*, 27(3), 379–423.
- Tanaka, T., Sugiyama, R., Sato, Y., Kawaguchi, M., Honda, K., Iwaki, H., & Okano, K. (2024). Precise microbiome engineering using natural and synthetic bacteriophages targeting an artificial bacterial consortium. *Frontiers in Microbiology*, 15, 1403903.
- Trivedi, P., Leach, J. E., Tringe, S. G., Sa, T., & Singh, B. K. (2020). Plant–microbiome interactions: from community assembly to plant health. *Nature Reviews Microbiology*, 18(11), 607–621.
- Wang, B., Geng, Y., Lin, Y., Xia, Q., Wei, F., Yang, S., Huang, X., Zhang, J., Cai, Z., & Zhao, J. (2024). Root rot destabilizes the Sanqi rhizosphere core fungal microbiome by reducing the negative connectivity of beneficial microbes. *Applied and Environmental Microbiology*, 90(3), e02237–02223.
- Watts, S. C., Ritchie, S. C., Inouye, M., & Holt, K. E. (2019). FastSpar: rapid and scalable correlation estimation for compositional data. *Bioinformatics*, 35(6), 1064–1066.
- Xiong, C., Zhu, Y. G., Wang, J. T., Singh, B., Han, L. L., Shen, J. P., Li, P. P., Wang, G. B., Wu, C. F., & Ge, A. H. (2021). Host selection shapes crop microbiome assembly and network complexity. *New Phytologist*, 229(2), 1091–1104.
- Zhang, Y., Hu, D., Sun, H.-x., Chen, J., Yang, J.-h., Li, X.-m., Li, X.-s., Chen, Y., & Yu, F. (2025). Endophytic commensal bacteria capitalize on the AvrPto-FER pathway to enhance proliferation during early stages of pathogen invasion. *The ISME Journal*, 19(1), wraf145.
- Zheng, X., Wang, Z., Zhu, Y., Wang, J., & Liu, B. (2020). Effects of a microbial restoration substrate on plant growth and rhizosphere bacterial community in a continuous tomato cropping greenhouse. *Scientific Reports*, 10(1), 13729.
- Zhou, X., Wang, J., Liu, F., Liang, J., Zhao, P., Tsui, C. K., & Cai, L. (2022). Cross-kingdom synthetic microbiota supports tomato suppression of *Fusarium* wilt disease. *Nature Communications*, 13(1), 7890.

## CHAPTER 4: Interbacterial interactions determine functional shifts in Xylan degradation

### 4.1 OVERVIEW

Microbial communities perform essential ecosystem functions through complex interactions among community members. In natural environments, processes such as the degradation of plant derived polymers are often mediated by extracellular enzymes produced by multiple microbial species. However, functional outputs within microbial communities are not solely determined by the metabolic capacity of individual species but are also shaped by interactions among neighboring microbes. Despite their importance, the extent to which microbial interactions influence functional outputs remains poorly understood. In particular, it is unclear how bacterial interactions alter extracellular enzyme production and metabolic responses during the degradation of complex carbon substrates

To address this question, we used a synthetic microbial community composed of four xylanase producing bacteria: *Bacillus subtilis*, *Arthrobacter agilis*, *Clavibacter michiganensis*, and *Sphingomonas paucimobilis*. *B. subtilis* was used as a model strain and co-cultured with other bacteria in different community combinations. Bacterial growth, extracellular xylanase activity of the community, and *xynA* secretion and *xynA* gene expression in *B. subtilis* were measured to evaluate how bacterial interactions influence functional responses during xylan degradation. Extracellular xylanase secretion varied depending on community composition. *B. subtilis* produced higher levels of xylanase when co-cultured with *S. paucimobilis*, which was associated with the enrichment of carbon metabolism pathways. In contrast, when co-cultured with *A. agilis* and *C. michiganensis*, *B. subtilis* showed reduced xylanase secretion and transcriptional responses associated with competitive interactions. These results suggest that *B. subtilis* adjusts its metabolic strategy depending on the neighboring species within the

community. As microbial community complexity increases, diverse interactions among species may complement each other, resulting in more stable extracellular enzyme activity at the community level.

These findings highlight that microbial functions are emergent properties driven by species interactions rather than individual metabolic potential. Understanding these interaction-driven functional shifts will be important for predicting microbial community behavior and for designing stable microbial consortia for agricultural and environmental applications.

## **4.2 INTRODUCTION**

Microorganisms in natural environments constantly interact with one another through competition, cooperation, and metabolic exchange. These interactions can reshape the functional capacity of microbial communities and generate outcomes that cannot be predicted from the contribution of individual species alone (Bakkeren et al., 2025; Klier & Anantharaman, 2025). The complex interspecies relationships contribute to shaping microbial community structure and function, ultimately influencing host health and ecosystem processes (Bakkeren et al., 2025). However, different bacterial species exhibit distinct ecological strategies and interaction patterns (Pacheco et al., 2019). Giri et al (2021) showed that the extent of cross-feeding between bacterial species varies depending on their metabolic traits and evolutionary relationships. They said that metabolic dissimilarity and phylogenetic distance were identified as key factors influencing the establishment and magnitude of cross-feeding interactions.

Because microbial communities in natural environments are continuously exposed to the introduction of new microorganisms, the invasion of additional bacterial species can modify existing interaction networks. Such bacterial invasion may alter competitive relationships,

metabolic dependencies, or cooperative behaviors, ultimately reshaping both community structure and function (Li et al., 2024; Mickalide & Kuehn, 2019). Changes in microbial interactions can therefore have cascading effects on soil fertility and agricultural sustainability. Despite the importance of these processes, our understanding of how interactions among individual bacterial species influence community-level functions remains limited.

In soil ecosystems, such interactions are particularly important because microbial community dynamics directly influence nutrient cycling, plant health, and crop productivity (Chen et al., 2024; Trivedi et al., 2016; Trivedi et al., 2020). Among the many functions performed by soil microbial communities, the degradation of plant-derived polymers plays a central role in the terrestrial carbon cycle. Xylan, one of the most abundant structural components of hemicellulose in plant biomass, must be hydrolyzed into smaller sugars such as xylose before it can be assimilated. This process relies on extracellular enzymes known as xylanases, which are secreted by specialized microorganisms capable of degrading hemicellulose (Abena & Simachew, 2024). Xylanases are not only ecologically important but are also widely used in industrial applications, including biofuel production, paper processing, and food biotechnology (Phuyal et al., 2023).

Because xylanases are released into the extracellular environment, it can potentially benefit neighboring microbes, serving as a shared resource within microbial communities (Reintjes et al., 2019). When multiple microorganisms capable of producing the same extracellular enzyme coexist, three different stories are possible. Bacteria may cooperate and enhance enzyme production through synergistic interactions, leading to increased degradation efficiency. Alternatively, some species may exploit enzymes secreted by neighboring microbes without investing in their own production, a phenomenon often described as microbial cheating. In other cases, microorganisms may maintain independent metabolic activities with minimal interaction.

These different interaction modes can generate non-additive functional outcomes, where community-level enzyme activity differs from the sum of activities observed in monocultures.

In this study, we used *Bacillus subtilis* as a model bacteria because it is a well-characterized soil bacterium with extensive genetic resources and well known as a xylanase producing bacteria (Ulucay et al., 2022). To investigate how bacterial interactions influence functional outputs related to xylan degradation, we constructed a defined bacterial community composed of four xylanase-producing species: *Bacillus subtilis*, *Arthrobacter agilis*, *Clavibacter michiganensis*, and *Sphingomonas paucimobilis*. These bacteria represent diverse taxa commonly associated with soil environments and possess the capacity to degrade xylan in soil.

Using this system, we examined how bacterial interactions influence both community-level and strain-specific functional outputs during xylan degradation. We quantified total community xylanase activity as well as xylanase specifically produced and secreted by *B. subtilis* under different bacterial combinations. In addition, transcriptomic analysis of *B. subtilis* was performed to investigate how the presence of other bacterial species alters gene expression patterns associated with xylan utilization. By integrating functional assays with transcriptomic profiling, this study provides mechanistic insights into how interspecies interactions reshape microbial functional outputs. Understanding these interaction-driven changes will improve our ability to predict microbiome functions in soil ecosystems and may contribute to the rational design of microbial communities for enhanced plant health and soil carbon cycling.

## **4.3 MATERIAL AND METHOD**

### **4.3.1 Bacterial strais and culture conditions**

A total of 345 bacterial isolates were collected from soil, plant roots, and air samples. Among

these isolates, 104 strains were identified as xylanase producing bacteria based on Congo red assays (Medded-Mouelhi et al., 2014). Xylanase gene sequences from each bacterium were obtained from the Joint Genome Institute (JGI). Sequence comparison revealed that 33 strains possessed unique xylanase gene sequences. From these candidates, we selected *Arthrobacter agilis*, *Clavibacter michiganensis*, and *Sphingomonas paucimobilis* to represent taxonomic diversity and interspecies variability in xylanase producing bacterial communities. *B. subtilis* BWB143 was kindly provided from Dr. Joen Luirink (University of Amsterdam, The Netherlands).

All bacterial strains were initially cultured in Nutrient Broth (NB) at 31 °C until they reached the optical density (OD) measured at 600 nm of 0.8 using 96 well clear plates (Corning, USA) with plate reader (Infinite M Nano+, Tecan, Switzerland). Cells were then inoculated into M9 minimal medium (Mageshwaran et al., 2014) supplemented with 0.5% (w/v) xylan from beechwood (Biosynth, Switzerland) as the sole carbon source. Each strain was washed with autoclaved 0.03 M MgSO<sub>4</sub> and adjusted to an initial OD<sub>600</sub> of 0.05 to standardize the starting cell density. Eleven bacterial combinations were tested (Table 4.1). Cultures were incubated at 31 °C, and samples were collected at 2, 6, 8 h after inoculation. This experiment was independently repeated three times.

**Table 4.1.** Bacterial combination

Community name	Strains composition
B	<i>B. subtilis</i>
A	<i>A. agilis</i>
C	<i>C. michiganensis</i>
S	<i>S. paucimobilis</i>
BA	<i>B. subtilis</i> + <i>A. agilis</i>
BC	<i>B. subtilis</i> + <i>C. michiganensis</i>
BS	<i>B. subtilis</i> + <i>S. paucimobilis</i>
BAC	<i>B. subtilis</i> + <i>A. agilis</i> + <i>C. michiganensis</i>
BAS	<i>B. subtilis</i> + <i>A. agilis</i> + <i>S. paucimobilis</i>
BCS	<i>B. subtilis</i> + <i>C. michiganensis</i> + <i>S. paucimobilis</i>
BACS	<i>B. subtilis</i> + <i>A. agilis</i> + <i>C. michiganensis</i> + <i>S. paucimobilis</i>

#### 4.3.2 Congo red assay for xylanase producing bacteria screening

Bacteria were screened for xylanase production using a Congo red assay (Samanta et al., 2011). Briefly, the isolates were spot inoculated onto agar plates containing beechwood xylan (5 g/L), peptone (5 g/L), yeast extract (5 g/L), MgSO<sub>4</sub>·7H<sub>2</sub>O (0.2 g/L), K<sub>2</sub>HPO<sub>4</sub> (1 g/L), and agar (20 g/L). Plates were incubated at 31 °C for 48 h. After incubation, plates were flooded with 1 % (w/v) Congo red solution and stained for 30 min at room temperature. Excess dye was removed, and plates were destained with 1 M NaCl. Xylan degradation by xylanase was visualized as a clear halo surrounding bacterial colonies against a red stained background.

### **4.3.3 Quantification of total xylanase activity**

Total xylanase activity of the bacterial cultures was quantified using the 3,5-dinitrosalicylic acid (DNS) method following (Miller, 1959) with minor modifications. This assay measured the overall xylanase activity produced by the mixed bacterial cultures rather than activity from individual strains.

Culture samples collected at each time point were centrifuged at 13,000 rpm for 15 min using Eppendorf 5430R centrifuge (Eppendorf, Germany) to obtain the supernatant containing extracellular enzymes produced by the bacterial community. The 60  $\mu$ L of supernatant was mixed with 600  $\mu$ L of 1% xylan solution prepared in 50 mM citrate buffer. The reaction mixture was incubated in water bath at 55 °C for 20 min to allow enzymatic hydrolysis of xylan. After incubation, 1 mL of DNS reagent was added to the reaction mixture, followed by boiling in a 100 °C water bath for 5 min to terminate the enzymatic reaction. The reaction mixtures were cooled to room temperature, and absorbance was measured at 540 nm using a spectrophotometer (Infinite M Nano+, Tecan, Switzerland). The amount of released xylose was calculated using a xylose standard curve. One unit of xylanase activity was defined as the amount of enzyme required to release 1  $\mu$ mol of xylose per minute under the assay conditions.

### **4.3.4 Luminescence assay for *Bacillus subtilis* xylanase secretion**

The secretion of xylanase from *B. subtilis* was quantified using a HiBiT split luciferase detection system (Kes et al., 2024). In *B. subtilis* BWB143, the xylanase protein was fused with a HiBiT tag, allowing detection of secreted proteins through luminescence. Bacterial cultures collected at each time point were kept on ice prior to measurement. The 5  $\mu$ L of culture samples containing secreted HiBiT-tagged proteins were mixed with 5  $\mu$ L of the Nano-Glo HiBiT

extracellular Detection System reagent (Promega, USA) in a black clear bottom 384 well plate (Greiner Bio-One, Austria). The reaction mixture was incubated for 10 min to allow complementation of the HiBiT tag with the luciferase detection reagent. Luminescence signals were measured using a microplate reader (SpectraMax iD3, Molecular Devices, USA) with luminescence optics and an integration time of 2 s. The luminescence intensity reflected the amount of secreted xylanase by *B. subtilis*.

#### **4.3.5 RNA extraction**

Total RNA was extracted from bacterial cultures using RiboZol RNA extraction reagent (VWR, USA) following the manufacturer's instructions. To maintain RNA stability and prevent degradation, all RNA extraction procedures were performed on ice. Briefly, 5 mL of bacterial cultures were centrifuged at 5500 rpm for 25 min using Eppendorf 5430R centrifuge (Eppendorf, Germany) to pellet the cells, and the pellets were resuspended in 1mL of RiboZol reagent to lyse the cells and release RNA. After 10 min of incubation at room temperature, 200  $\mu$ L of chloroform was added to the lysate, followed by vigorous mixing and centrifugation at 12,000 x g for 15 min at 4  $^{\circ}$ C using Eppendorf 5430R centrifuge (Eppendorf, Germany) to separate the mixture into aqueous and organic phases. The upper aqueous phase containing RNA was carefully transferred to a new 1.5 mL microcentrifuge tube. RNA was precipitated by adding 500  $\mu$ L of isopropanol and centrifuging at 12,000 x g for 10 min at 4  $^{\circ}$ C. The pellet was washed with 1 mL of 75 % ethanol, air dried, and resuspended in RNase free water. RNA concentration and purity were determined by nanodrop (Thermo Scientific, USA) and stored at -80  $^{\circ}$ C until downstream analyses.

#### 4.3.6 quantitative real time PCR (qRT-PCR)

Total RNA extracted from bacterial cultures was reverse transcribed into cDNA using the iScript cDNA Synthesis Supermix (BioRad, USA). The reverse transcription reaction was performed with priming at 25 °C for 5 min, followed by reverse transcription at 46 °C for 26 min and a final step at 95 °C for 1 min to terminate the reaction. qRT-PCR was performed using 50 ng of cDNA as the template in each reaction. The reactions were carried out using SensiFAST 2x SYBR No-ROX Mix (Bioline, USA) by using CFX96 Touch Real-Time PCR Detection System (BioRad, USA). Gene expression of the *B. subtilis* xylanase gene (*xynA*) was quantified using the primer pair Forward (5'-AAGGTTGGACTACAGGTTTCGC-3') and Reverse (5'-CGAACACTCCAGTACTGCGT-3'). The qRT-PCR cycling conditions consisted of an initial denaturation at 95 °C for 2 min, followed by 40 cycles of 95 °C for 15 s and 56 °C for 30 s with fluorescence signal acquisition. A melting curve analysis was performed to confirm the specificity of the amplification products. Each reaction was performed with three technical replicates.

#### 4.3.7 RNA sequencing and transcriptomic analysis

RNA-seq was performed at the Colorado State University Next-Generation Sequencing Core (Fort Collins, CO, USA). RNA quality control, library preparation, and sequencing were conducted by the facility. Sequencing libraries were generated from total RNA and sequenced on an Illumina NextSeq to obtain paired-end reads.

Raw sequencing reads were processed for quality control using FastP (v0.24.2). The filtered reads were aligned to the *B. subtilis* 168 reference genome using HISAT2 (v2.2.1) (Kim et al., 2019). The reference genome and gene annotation files were obtained from the NCBI RefSeq

database ([https://www.ncbi.nlm.nih.gov/assembly/GCF\\_000009045.1](https://www.ncbi.nlm.nih.gov/assembly/GCF_000009045.1)). Aligned reads were processed to generate sorted BAM files, and gene-level read counts were obtained using featureCounts (Liao et al., 2014) by assigning reads to coding sequences (CDS) based on locus tags in the annotation file. The resulting count matrix was used for downstream differential gene expression analysis in R (v4.5.2).

Differential gene expression analysis was performed using the DESeq2 package (Love et al., 2014). Genes with fewer than 10 total counts across all samples were removed prior to analysis. Differentially expressed genes (DEGs) were identified by comparing each mixed bacterial community to the *B. subtilis* monoculture. Genes with an adjusted  $p$  value  $< 0.05$  were considered significantly differentially expressed, and DEGs were classified as upregulated or downregulated based on the sign of the log<sub>2</sub> fold change.

To compare DEG overlap among treatments, separate UpSet plots for upregulated and downregulated genes were generated using the UpSetR package (Conway et al., 2017). Functional enrichment analysis of DEGs was performed using the clusterProfiler package (Wu et al., 2021), with upregulated and downregulated gene sets analyzed separately for KEGG pathway enrichment using the *B. subtilis* KEGG database. KEGG enrichment results were visualized as bar plot.

## **4.4 RESULT AND DISCUSSION**

### **4.4.1 Microbial community composition alters bacterial growth dynamics and xylanase activity**

In this study we focused on four representative community combinations: *B. subtilis* alone (B), *B. subtilis* co-cultured with *A. agilis* and *C. michiganensis* (BAC), *B. subtilis* co-cultured

with *S. paucimobilis* (BS), and the four-species community containing all strains (BACS). Results for other community combinations are provided in the supplementary materials.

The growth dynamics of each bacterial species differed depending on community composition (Figure 4.1 A-D). When *B. subtilis* was cultured alone, its abundance remained relatively stable across the sampling period. However, the presence of other bacterial species altered the population dynamics of *B. subtilis*. *B. subtilis* numbers were higher when co-cultured with *A. agilis* and *C. michiganensis* than when it was grown alone or co-cultured with *S. paucimobilis*.

*S. paucimobilis* numbers decreased in the presence of *A. agilis* and *C. michiganensis*, whereas *A. agilis* and *C. michiganensis* maintained their growth when co-cultured with other bacterial species. *B. subtilis* and *A. agilis*, and *C. michiganensis* are gram positive bacteria, whereas *S. paucimobilis* is a gram negative bacteria. These fundamental differences in cell envelope structure may influence how these bacteria interact within microbial communities.

We next examined whether these differences in community composition influenced the functional outcome of the community. Xylanase activity, measured using the DNS assay, differed among the communities and across time points (Figure 4.1 E). The B, BAC, and BS communities showed the highest xylanase activity at 6 h after inoculation, which significantly decreased at 8 h after inoculation. In contrast, the most complex community, BACS, showed consistently high xylan degradation activity across the sampling period compared with the simpler communities. When *B. subtilis* was co-inoculated with one additional species, the pattern of xylanase activity dynamics varied depending on the partner species (Supplementary Figure S4.1). This result suggests that communities with more species exhibit more stable functional outputs.

This can be explained by complementary metabolic interactions during xylan degradation by multiple species. The breakdown of complex polymers such as xylan typically generates intermediate products, including xylo-oligosaccharides and xylose, which can be utilized differently by various microbial species. Such metabolic complementarity and cross-feeding can sustain substrate turnover in complex communities (Pacheco et al., 2019). Because the DNS assay measures reducing sugars released during xylan degradation, the observed activity likely reflects the combined action of multiple enzymes in the xylan degradation pathway, including xylanases and downstream enzymes such as  $\beta$ -xylosidases. As a result, substrate availability may persist longer, sustaining enzyme activity across the community.

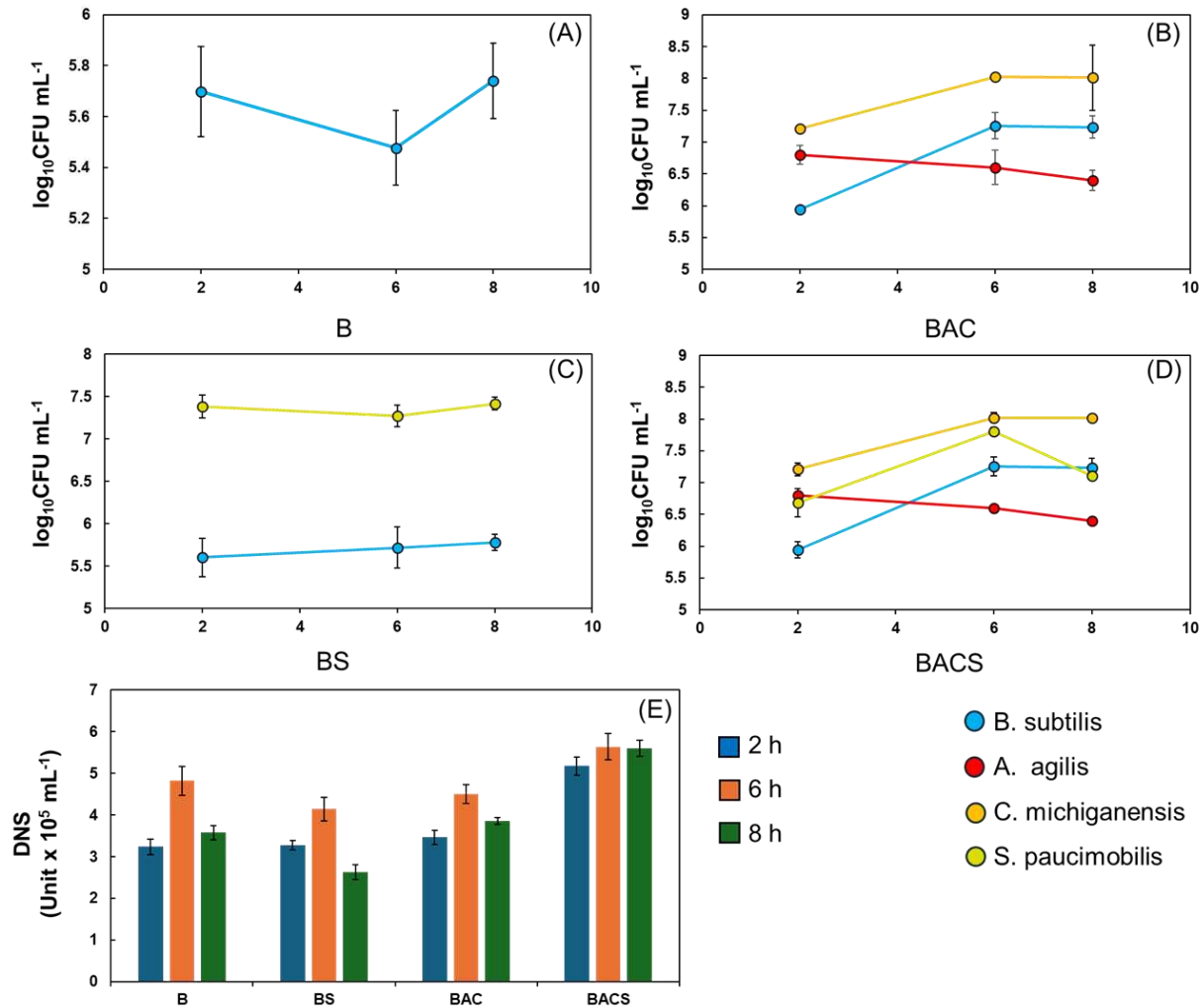


**Figure 4.1.** Growth pattern of individual species (A-D) and xylanase activity (E) in different community composition. Each community composition include *b. subtilis* alone (A), *B. subtilis* with *A. agilis* and *C. michiganensis* (B), *B. subtilis* with *S. paucimobilis* (C), and all four strains (D). Bacterial abundance was quantified a log<sub>10</sub> CFU mL<sup>-1</sup> at 2 , 6, and 8 h after inoculation. Colony forming units (CFU) were determined by plating serially diluted cultures on nutrient agar (NA) plates and counting colonies after 5 days of incubation. Different colors represent bacterial species: Blue indicates *B. subtilis*, Red indicates *A. agilis*, Orange indicates *C. michiganensis*, and Yellow indicates *S. paucimobilis*. Xylanase activity was measured using the DNS assay in cultures with different community compositions at 2, 6, 8 h after inoculation. Dark blue, orange, and green bars represent measurements taken at 2, 6, 8 h after inoculation, respectively. Error bars represent the standard deviation of biological replicates.

#### 4. 4. 2 Xylanase secretion and *xynA* expression of *B. subtilis* in different bacterial community compositions.

To determine the impact of microbial interactions on the functional activity of a single microbe, we monitored extracellular xylanase secretion by *B. subtilis* and the expression of the *xynA* gene across different community combinations. Since bacterial communities showed the highest xylanase activity at 6 h after inoculation (Figure 4.1), samples collected at 6 h were selected for gene expression analysis.

Extracellular xylanase secretion varied depending on bacterial community composition (Figure 4.2A). As community complexity increased, *B. subtilis* generally tended to secrete lower amounts of xylanase. However, the combination with *S. paucimobilis* showed the highest xylanase secretion at 6 h after inoculation, followed by a significant decrease at later time points. In contrast, the combination with *A. agilis* and *C. michiganensis* showed reduced xylanase secretion throughout the sampling period.

The expression of the *xynA* gene at 6 h after inoculation measured by qRT-PCR showed patterns that were different from the observed xylanase secretion (Figure 4.2B).  $C_t$  values for *A. agilis*, *C. michiganensis*, and *S. paucimobilis* were above 35, indicating no detectable amplification. This result confirms that the *xynA* specific primers used in this study are specific to *B. subtilis* and do not amplify homologous sequences from the other bacterial species. Among the treatments, the BS community showed the lowest  $C_t$  value, indicating the highest *xynA* expression. Although the  $C_t$  values for BAC and BACS were not significantly different from those of B, they trended lower than B, suggesting slightly higher *xynA* expression in these communities. However, RNA-seq analysis revealed that the normalized transcript abundance of *xynA* did not differ significantly among B, BS, BAC, and BACS (Figure 4.2C), indicating that

microbial interactions did not strongly alter *xynA* transcription at the whole-transcriptome level.

The differences observed between luminescence based xylanase measurements and transcriptomic analyses likely arise from the distinct biological levels measured by these approaches. Luminescence assays quantify secreted proteins, whereas qRT-PCR and RNA-seq measure mRNA abundance. It is well established that mRNA expression levels do not always correlate with protein abundance (Vogel & Marcotte, 2012). This discrepancy occurs because the production of functional proteins involves multiple regulatory steps beyond transcription, including translation efficiency, protein folding, secretion, and protein stability. Therefore, changes in extracellular xylanase levels may reflect differences in protein production or secretion rather than direct changes in *xynA* transcript abundance.

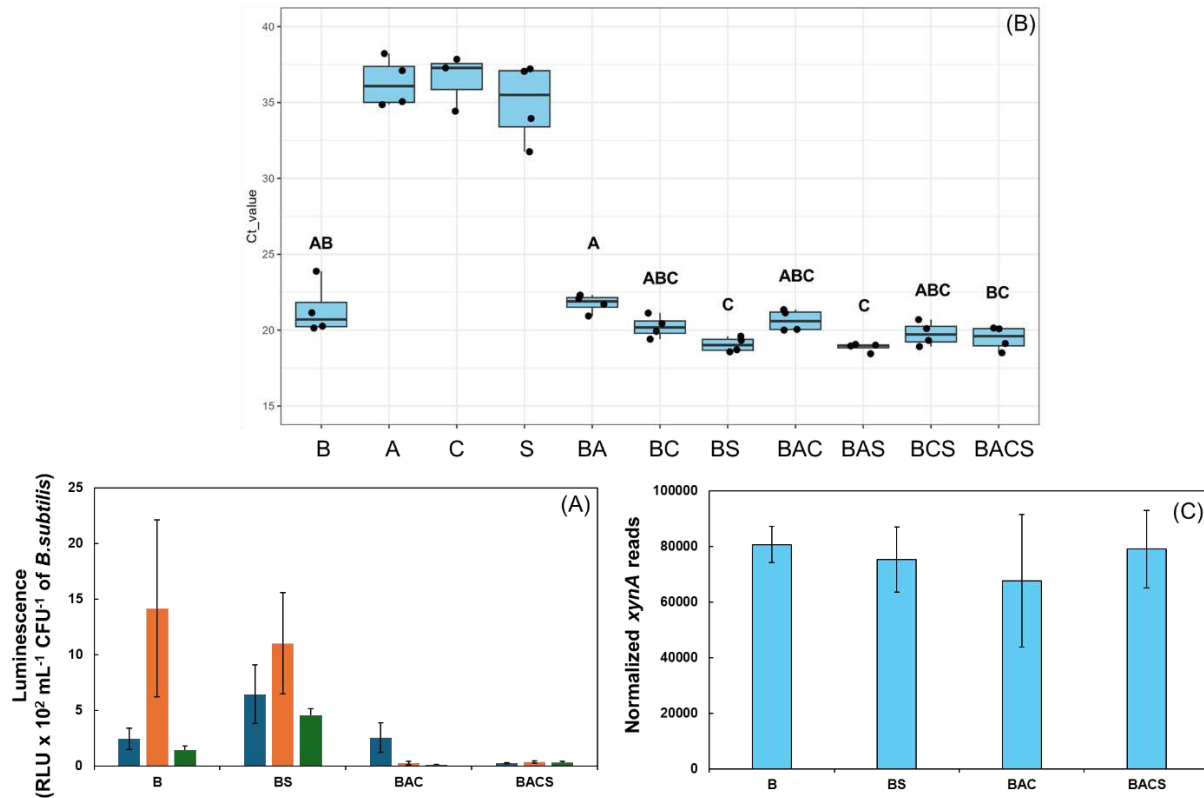


**Figure 4.2.** Detection of extracellular xylanase secreted by *B. subtilis* (A) and *xynA* gene expression at 6 h after inoculation of *B. subtilis* measured by qRT-PCR (B) in different community compositions. Boxplots represent  $C_t$  values across biological replicates. Different letters above the boxplots indicate statistically significant differences among the treatments based on Tukey's HSD test ( $p < 0.05$ ). The relative expression of the *xynA* gene in *B. subtilis* measured by RNA-seq (C) was calculated using DESeq2. Error bars represent the standard deviation of biological replicates

#### 4.4.3 Distinct bacterial communities induce different metabolic responses in *B. subtilis*

To evaluate the potential sequence overlap among bacterial species used in this study, raw RNA-seq reads were mapped separately to the reference genomes of each species (Supplementary Figure 4.3). The mapping results showed that reads mapped to the *B. subtilis* reference genome did not overlap with the reference genomes of the other bacterial species. This

indicates that the reads mapped to the *B. subtilis* reference represent gene expression originating specifically from *B. subtilis*, allowing reliable interpretation of *B. subtilis* transcriptomic responses within mixed bacterial communities.

DEG analysis further revealed that different community compositions induced distinct transcriptional responses in *B. subtilis*. In the BS and BAC communities, *B. subtilis* exhibited unique sets of differentially expressed genes (Supplementary Figure S4.4). The BS community showed 174 uniquely up-regulated genes and 117 uniquely down-regulated genes, whereas the BAC community exhibited 92 uniquely up-regulated genes and 110 uniquely down-regulated genes. These results indicate that the presence of different bacterial species leads to distinct transcriptional responses in *B. subtilis*. To investigate how microbial interactions influence the metabolic activity of *B. subtilis*, KEGG pathway enrichment analysis was performed using differentially expressed genes identified in each community (Figure 4.3).

In the BAC community, up-regulated genes were strongly enriched in pathways associated with biosynthesis of secondary metabolites, ABC transporters, and amino acid biosynthesis. Additional enrichment was observed in pathways such as purine metabolism, arginine biosynthesis, and tryptophan metabolism. These pathways are commonly associated with biosynthetic activity and metabolite production, suggesting that *B. subtilis* increased investment in secondary metabolic processes and transport systems when interacting with the Gram-positive bacterial partners *A. agilis* and *C. michiganensis*.

In contrast, in the BS community, up-regulated genes were more strongly associated with regulatory and metabolic pathways. Enriched pathways included two-component systems, quorum sensing, nitrogen metabolism, glyoxylate and dicarboxylate metabolism, amino sugar and nucleotide sugar metabolism, and starch and sucrose metabolism. Several pathways related

to fatty acid metabolism and amino acid metabolism were also enriched. These pathways indicate that *B. subtilis* adjusted its regulatory networks and central metabolic processes when interacting with *S. paucimobilis*. Meanwhile, several pathways associated with growth-related cellular machinery were enriched among down-regulated genes, including ribosome, nucleotide metabolism, and RNA degradation, suggesting reduced investment in protein synthesis and cellular growth.

The transcriptional patterns suggest that *B. subtilis* adopts distinct competitive strategies depending on the identity of neighboring species. In the BAC community, *B. subtilis* may engage in metabolite-mediated competition with neighboring bacteria. Because *B. subtilis*, *A. agilis*, and *C. michiganensis* are all Gram-positive bacteria, the induction of secondary metabolic pathways may reflect the production of antimicrobial compounds to inhibit competing species occupying similar ecological niches. Previous studies have shown that *B. subtilis* exhibits antagonistic activity against the phytopathogen *C. michiganensis* through the production of antimicrobial metabolites and volatile organic compounds, which can inhibit pathogen growth and cause structural damage to the cells (Jung et al., 2014; Rajer et al., 2017).

In the BS community, *B. subtilis* appeared to adjust its own metabolic state rather than directly inhibiting neighboring bacteria. The enrichment of pathways related to central metabolism and regulatory systems suggests that *B. subtilis* modified carbon utilization and metabolic flux to compete for available resources. This distinct competition strategy may be associated with differences in interspecies communication mechanisms between Gram-positive and Gram-negative bacteria.

Gram-negative bacteria typically use LuxI/LuxR quorum sensing systems with acyl-homoserine lactones (AHLs), whereas Gram-positive bacteria rely on oligopeptide-based two-

component signaling (Li & Tian, 2012). These signaling differences allow bacteria to detect neighboring species and adjust their physiological responses. Thus, the distinct transcriptional responses observed in the BS and BAC communities may reflect species-specific sensing and competition strategies of *B. subtilis*.

These transcriptional responses are consistent with the phenotypic observations described earlier. In the BAC community, the CFU of *B. subtilis* increased compared with the monoculture condition (Figure 4.1), suggesting that competitive inhibition of neighboring bacteria may provide a growth advantage. In contrast, the population size of *B. subtilis* remained relatively stable in the BS community. However, extracellular xylanase secretion was higher in BS than in BAC (Figure 4.2), indicating that *B. subtilis* may enhance extracellular enzyme production to increase resource acquisition under this condition.

Interestingly, the BACS community exhibited intermediate transcriptional patterns between the BAC and BS communities. This suggests that *B. subtilis* does not rely on a single competitive strategy when multiple species are present. Instead, as community complexity increases, *B. subtilis* appears to integrate multiple interaction responses, allowing the bacterium to maintain a more stable presence within complex microbial communities.

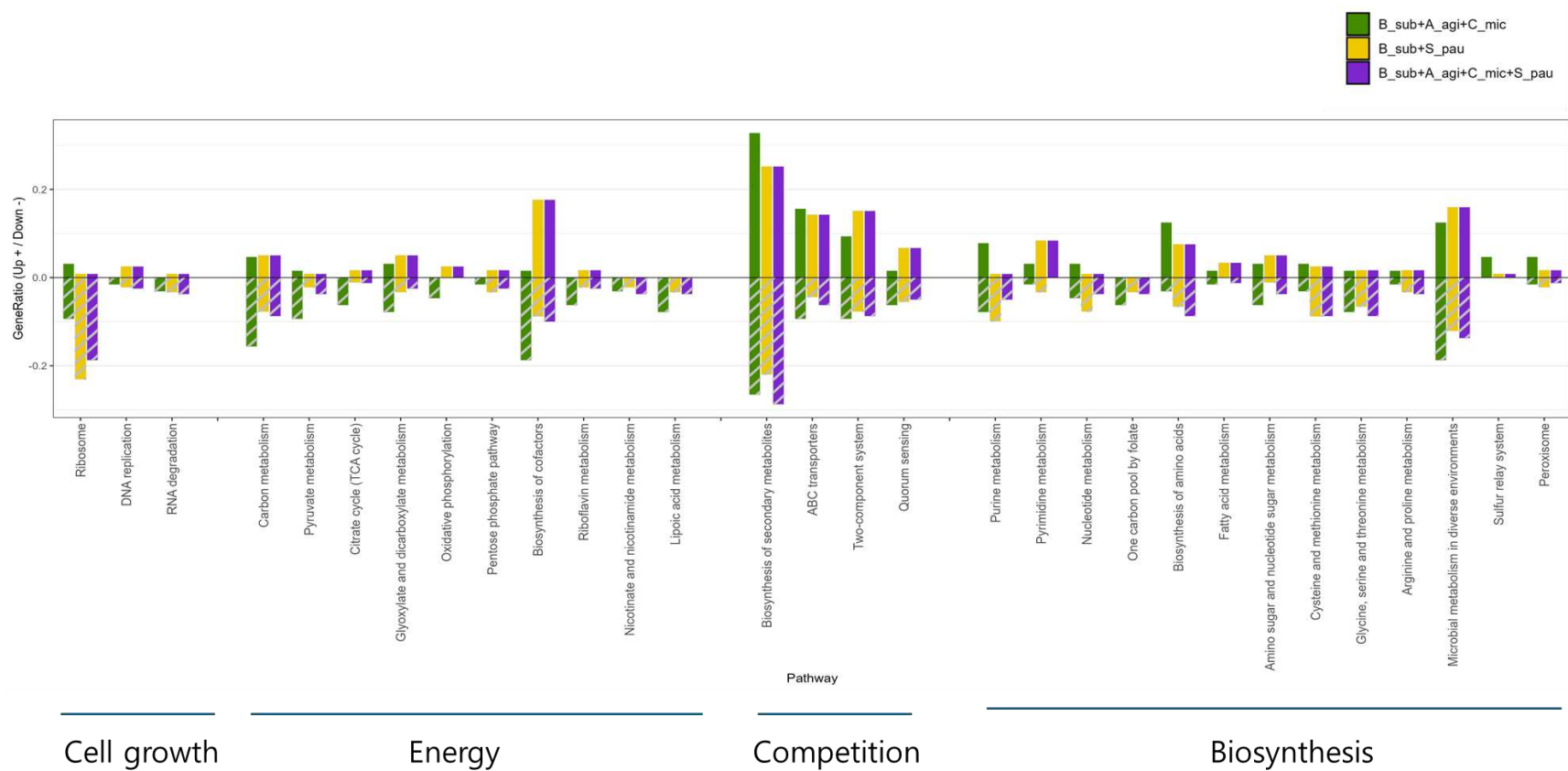


**Figure 4.3.** KEGG pathway enrichment analysis of differentially expressed genes (DEGs) in *B. subtilis* when co-cultured with other bacterial species compared to *B. subtilis* grown alone. The gene ratio in the y axis represent the proportion of DEGs assigned to each pathway. Upward bars indicate the gene ratio of up-regulated genes, whereas downward hatched bars represent the gene ratio of down-regulated genes. Colors represent different community compositions: Green, BAC, Yello, BS, Purple, BACS.

## 4.5 CONCLUSION

This study demonstrates that interbacterial interactions can significantly alter microbial functional outputs during xylan degradation. While all bacterial species in this study were capable of degrading xylan, extracellular xylanase secretion and *xynA* gene expression from *B. subtilis* varied depending on community composition. These findings suggest that microbial interactions reshape metabolic responses rather than simply suppressing competitors. Because bacterial species differ in their physiological and metabolic traits, interactions among more distinct species are likely to generate increasingly divergent functional outcomes in microbial communities. These results highlight that microbial functions are emergent properties driven by species interactions rather than individual metabolic potential. Understanding these interactions will be important for predicting and engineering microbiome functions.

## REFERENCES

- Abena, T., & Simachew, A. (2024). A review on xylanase sources, classification, mode of action, fermentation processes, and applications as a promising biocatalyst. *BioTechnologia*, 105(3), 273.
- Bakkeren, E., Piskovsky, V., & Foster, K. R. (2025). Metabolic ecology of microbiomes: Nutrient competition, host benefits, and community engineering. *Cell Host & Microbe*, 33(6), 790–807.
- Chen, Q., Song, Y., An, Y., Lu, Y., & Zhong, G. (2024). Soil microorganisms: Their role in enhancing crop nutrition and health. *Diversity*, 16(12), 734.
- Conway, J. R., Lex, A., & Gehlenborg, N. (2017). UpSetR: an R package for the visualization of intersecting sets and their properties. *Bioinformatics*, 33(18), 2938–2940.
- Giri, S., Oña, L., Waschina, S., Shitut, S., Yousif, G., Kaleta, C., & Kost, C. (2021). Metabolic dissimilarity determines the establishment of cross-feeding interactions in bacteria. *Current Biology*, 31(24), 5547–5557. e5546.
- Jung, W., Mabood, F., Souleimanov, A., Whyte, L., Niederberger, T., & Smith, D. (2014). Antibacterial activity of antagonistic bacterium *Bacillus subtilis* DJM-51 against phytopathogenic *Clavibacter michiganense* subsp. *michiganense* ATCC 7429 in vitro. *Microbial Pathogenesis*, 77, 13–16.
- Kes, M. B., Wang, B., van Ulsen, P., Hamoen, L. W., & Luirink, J. (2024). Development of a split-luciferase assay to establish optimal protein secretion conditions for protein production by *Bacillus subtilis*. *Microbiology*, 170(6), 001460.
- Kim, D., Paggi, J. M., Park, C., Bennett, C., & Salzberg, S. L. (2019). Graph-based genome alignment and genotyping with HISAT2 and HISAT-genotype. *Nature Biotechnology*, 37(8), 907–915.
- Klier, K. M., & Anantharaman, K. (2025). An updated view of metabolic handoffs in microbiomes. *Trends in Microbiology*.
- Li, C., Chen, X., Jia, Z., Zhai, L., Zhang, B., Grüters, U., Ma, S., Qian, J., Liu, X., & Zhang, J. (2024). Meta-analysis reveals the effects of microbial inoculants on the biomass and diversity of soil microbial communities. *Nature Ecology & Evolution*, 8(7), 1270–1284.
- Li, Y.-H., & Tian, X. (2012). Quorum sensing and bacterial social interactions in biofilms. *Sensors*, 12(3), 2519–2538.

- Liao, Y., Smyth, G. K., & Shi, W. (2014). featureCounts: an efficient general purpose program for assigning sequence reads to genomic features. *Bioinformatics*, 30(7), 923–930.
- Love, M. I., Huber, W., & Anders, S. (2014). Moderated estimation of fold change and dispersion for RNA-seq data with DESeq2. *Genome Biology*, 15, 1–21.
- Mageshwaran, V., Inmann, F., & Holmes, L. (2014). Growth kinetics of *Bacillus subtilis* in lignocellulosic carbon sources. *Int J Microbiol Res*, 6(2), 570–574.
- Meddeb-Mouelhi, Fatma, Jessica Kelly Moisan, and Marc Beauregard. "A comparison of plate assay methods for detecting extracellular cellulase and xylanase activity." *Enzyme and Microbial Technology* 66 (2014): 16-19.
- Mickalide, H., & Kuehn, S. (2019). Higher-order interaction between species inhibits bacterial invasion of a phototroph-predator microbial community. *Cell Systems*, 9(6), 521–533. e510.
- Miller, G. L. (1959). Use of dinitrosalicylic acid reagent for determination of reducing sugar. *Analytical Chemistry*, 31(3), 426–428.
- Pacheco, A. R., Moel, M., & Segrè, D. (2019). Costless metabolic secretions as drivers of interspecies interactions in microbial ecosystems. *Nature Communications*, 10(1), 103.
- Phuyal, M., Budhathoki, U., Bista, D., Shakya, S., Shrestha, R., & Shrestha, A. K. (2023). Xylanase-producing microbes and their real-world application. *International Journal of Chemical Engineering*, 2023(1), 3593035.
- Rajer, F. U., Wu, H., Xie, Y., Xie, S., Raza, W., Tahir, H. A. S., & Gao, X. (2017). Volatile organic compounds produced by a soil-isolate, *Bacillus subtilis* FA26 induce adverse ultra-structural changes to the cells of *Clavibacter michiganensis* ssp. *sepedonicus*, the causal agent of bacterial ring rot of potato. *Microbiology*, 163(4), 523–530.
- Reintjes, G., Arnosti, C., Fuchs, B., & Amann, R. (2019). Selfish, sharing and scavenging bacteria in the Atlantic Ocean: a biogeographical study of bacterial substrate utilisation. *The ISME Journal*, 13(5), 1119–1132.
- Samanta, A., Kolte, A. P., Senani, S., Sridhar, M., & Jayapal, N. (2011). A simple and efficient diffusion technique for assay of endo  $\beta$ -1, 4-xylanase activity. *Brazilian Journal of Microbiology*, 42(4), 1349–1353.
- Trivedi, P., Delgado-Baquerizo, M., Trivedi, C., Hu, H., Anderson, I. C., Jeffries, T. C., Zhou, J., & Singh, B. K. (2016). Microbial regulation of the soil carbon cycle: evidence from gene–enzyme relationships. *The ISME Journal*, 10(11), 2593–2604.
- Trivedi, P., Leach, J. E., Tringe, S. G., Sa, T., & Singh, B. K. (2020). Plant–microbiome interactions: from community assembly to plant health. *Nature Reviews Microbiology*, 18(11), 607–621.

- Ulucay, O., Gormez, A., & Ozic, C. (2022). For biotechnological applications: Purification and characterization of recombinant and nanoconjugated xylanase enzyme from thermophilic *Bacillus subtilis*. *Biocatalysis and Agricultural Biotechnology*, 44, 102478.
- Vogel, C., & Marcotte, E. M. (2012). Insights into the regulation of protein abundance from proteomic and transcriptomic analyses. *Nature Reviews Genetics*, 13(4), 227–232.
- Wu, T., Hu, E., Xu, S., Chen, M., Guo, P., Dai, Z., Feng, T., Zhou, L., Tang, W., & Zhan, L. (2021). clusterProfiler 4.0: A universal enrichment tool for interpreting omics data. *The Innovation*, 2(3).

## CHAPTER 5: CONCLUSION AND FUTURE DIRECTIONS

Microbiomes play essential roles in maintaining ecosystem functions, including nutrient cycling, plant health, and resistance to environmental stressors. In plant-associated environments, microbiomes are continuously shaped by interactions among microbes, host organisms, and external disturbances. Among these disturbances, microbial invasion represents a major force capable of disrupting microbial community structure and altering functions. Understanding how microbiomes respond to invasion, as well as how microbial interactions influence community functions, is essential for developing sustainable strategies for plant and soil health management.

This dissertation investigated how microbial invasions and microbial interactions influence microbiome structure, stability, and functional outputs. By combining studies on pathogen suppression in plant-associated microbiomes with controlled analyses of interbacterial interactions, this work provides insights into the mechanisms through which microbial communities respond to disturbance and reorganize their functional activities.

One major finding of this dissertation is that targeted suppression of plant pathogens can be achieved without disrupting the microbial community. The chimeric antimicrobial peptide (AMP) targeting *Candidatus Liberibacter asiaticus* effectively reduced the pathogen titer by enhancing plant defense responses while at the same time preserved beneficial microbiota. Furthermore, this AMP also targeted a vascular pathogen, *Xylella fastidiosa*, and, due to its inhibition of *X. fastidiosa in planta*, helped to restore the disrupted microbial community into healthy status. These findings indicate that pathogen invasion can destabilize native microbial communities, and that removing the pathogen may allow microbial communities to recover toward a more balanced state. Another finding is that interbacterial interactions can be varied in response to neighboring microbes and complex community can have stable functions

Together, these findings emphasize the importance of considering microbial community context when evaluating microbiome function and designing microbiome based agricultural strategies.

Future directions:

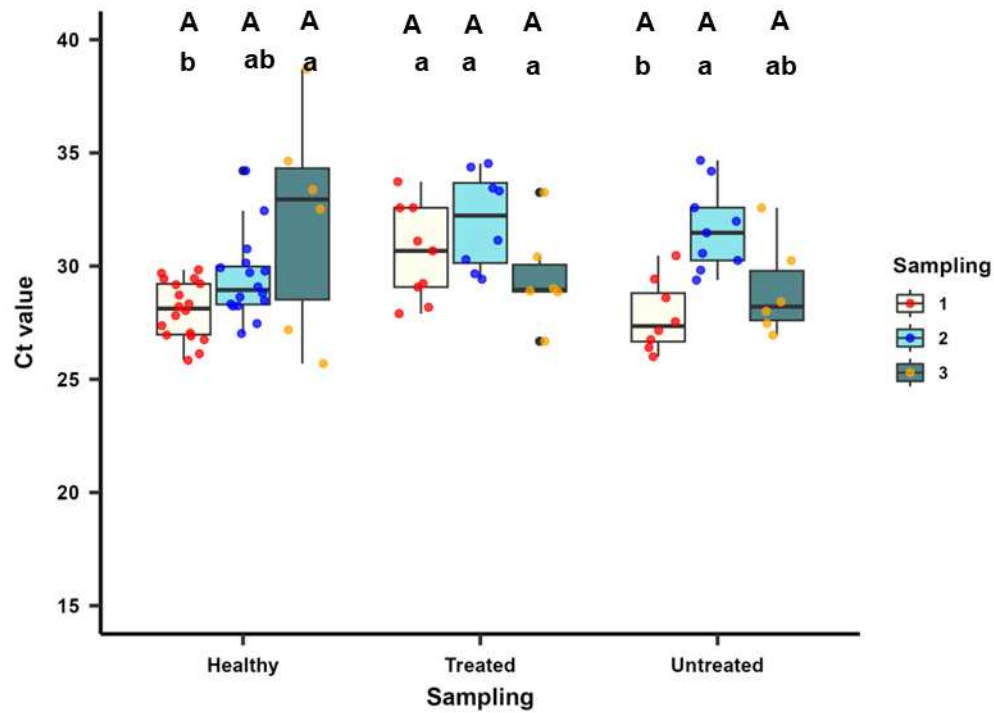
1. Investigating functional shifts in microbiomes following pathogen invasion and suppression. In Chapters 2 and 3, we examined how pathogen invasion and targeted pathogen suppression influence the structure of plant-associated microbial communities. However, the functional consequences of these microbial shifts remain unclear. Future studies should investigate how microbial functional pathways change during pathogen invasion and subsequent pathogen suppression. Approaches such as metagenomics, metatranscriptomics, or metabolomics could be used to identify microbial functions associated with microbiome disruption and recovery.
2. Proteomic analysis to validate functional responses in bacterial interactions. In Chapter 4, transcriptomic analysis revealed that gene expression patterns of *Bacillus subtilis* varied depending on the surrounding bacterial community, and the overlap of expressed genes among species appeared to be limited. However, transcript levels do not always reflect actual protein activity. Future studies could incorporate proteomic analyses to identify enzymes and metabolites actively produced during interbacterial interactions. Such approaches would provide a more direct understanding of the metabolic processes occurring within microbial communities during xylan degradation.
3. Expanding synthetic microbial communities to examine interaction diversity. Chapter 4 investigated bacterial interactions using a four species synthetic community. While this simplified system enabled controlled analysis of microbial interactions, natural microbial

communities are considerably more complex. Future studies could construct additional synthetic communities composed of bacteria with different ecological or phylogenetic relationships. For example, communities consisting of taxonomically closely related species or communities combining Gram-positive bacteria with Gram-negative bacteria capable of responding to similar quorum sensing signals could be used to examine how bacterial traits influence interaction outcomes and functional responses.

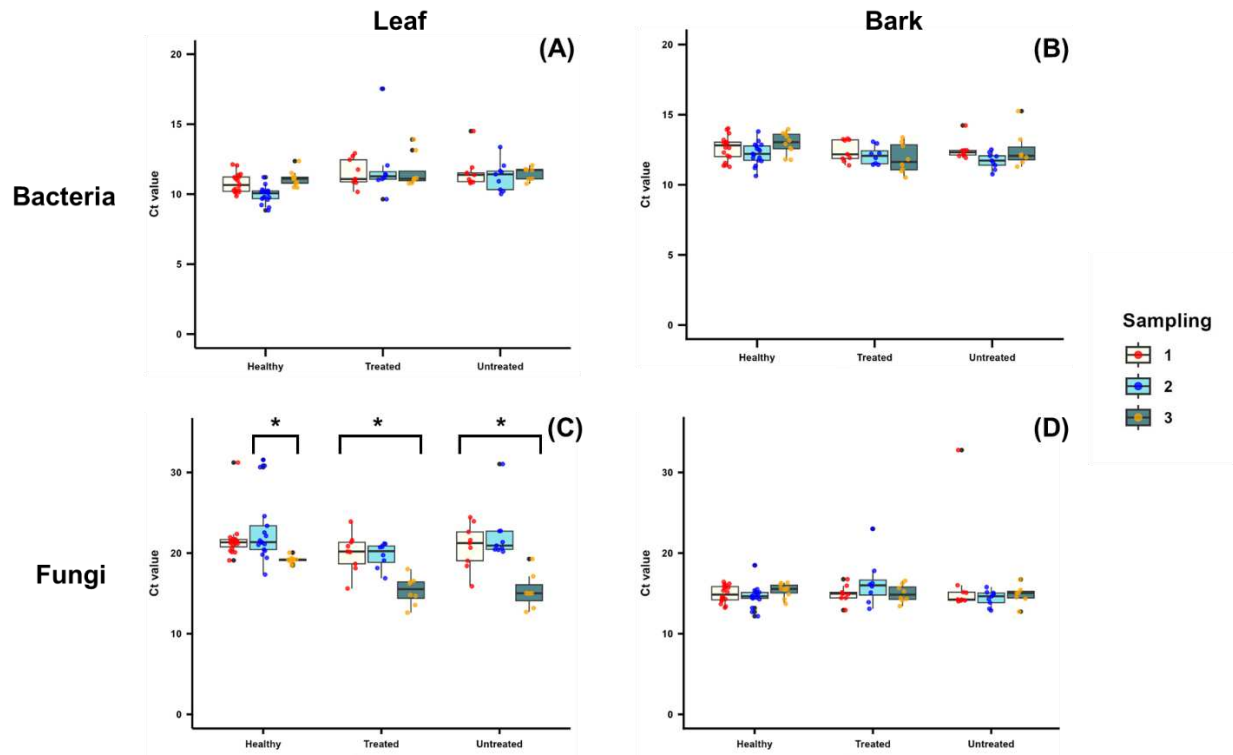
## APPENDIX

### Supplementary Materials

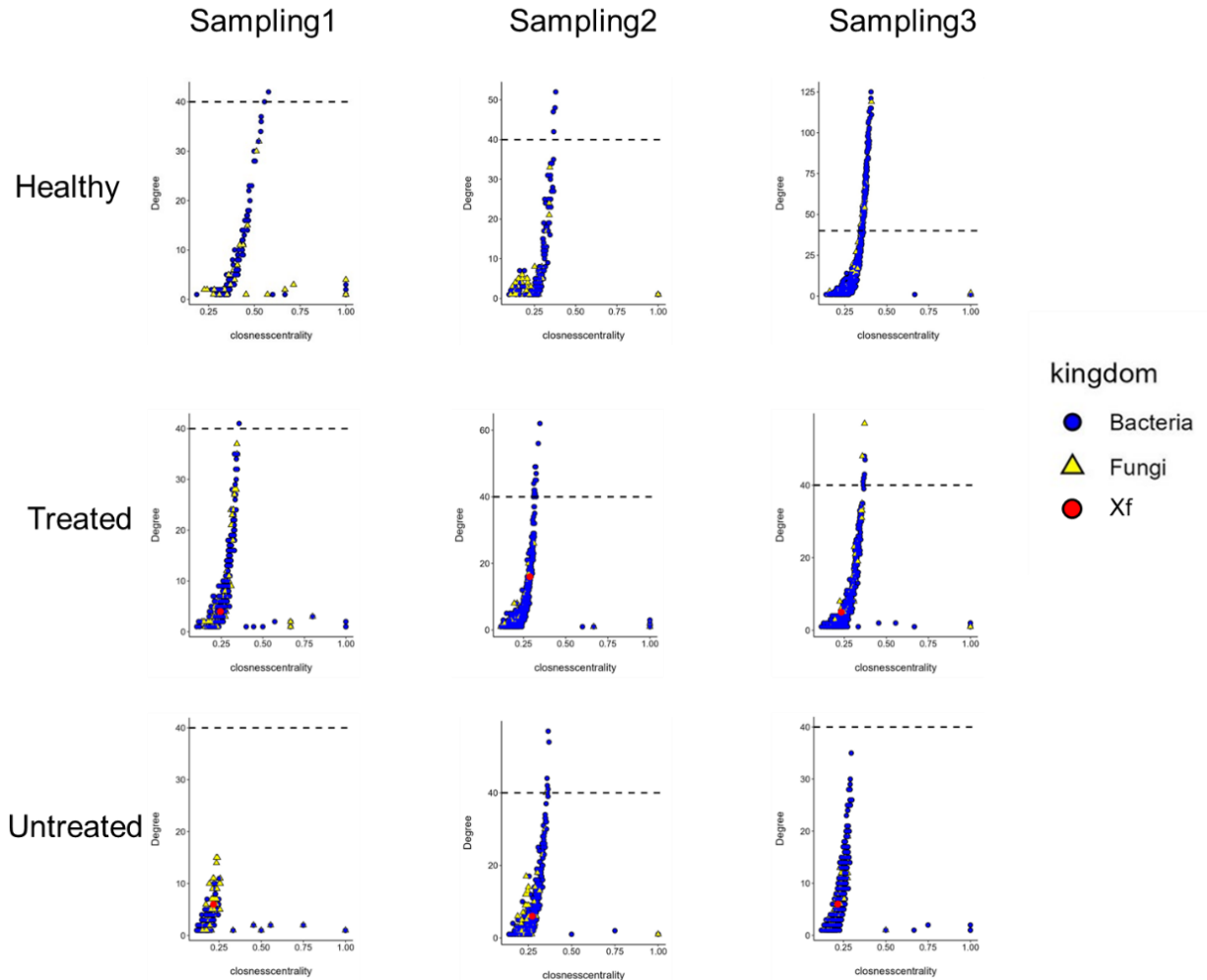
#### Supplementary Materials Chapter 3: The elimination of the *Xylella fastidiosa* in the grapevine by using the chimeric antimicrobial peptide and its impact on the native microbiome



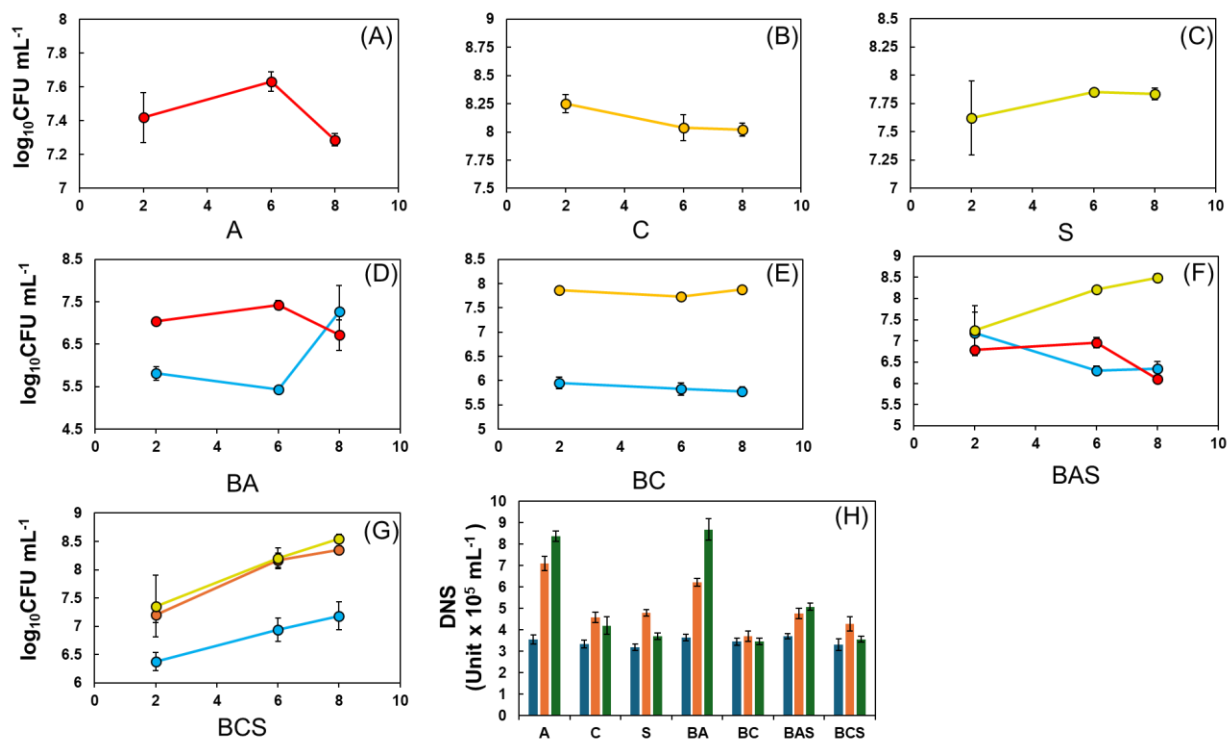
**Supplementary Figure S3.1.** The quantification of the *Xylella fastidiosa* (Xf) in bark tissues of grapevines. The pathogen quantification was done by the quantitative PCR. The significant difference was determined by Tukey HSD ( $p < 0.05$ ).



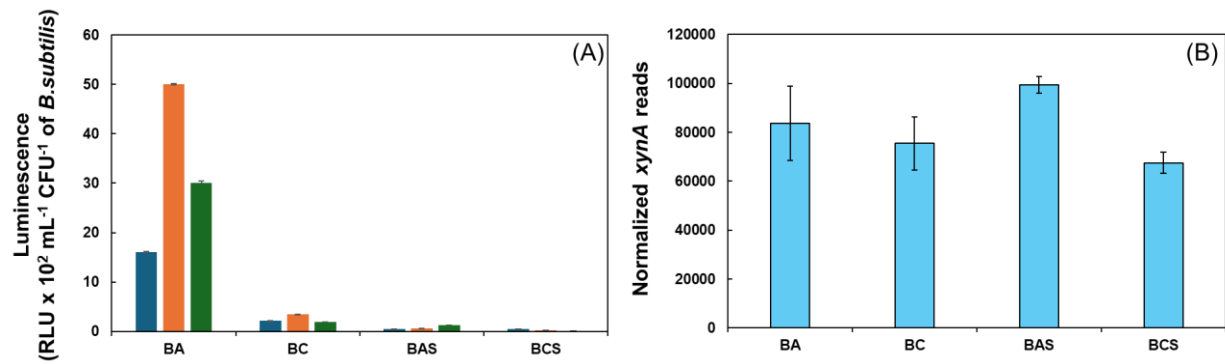
**Supplementary Figure S3.2.** Quantification of total bacteria (A,B) and fungi (C, D) in grapevine leaf (A, C) and bark (B, D). The significant difference was determined by Tukey HSD ( $p < 0.05$ ).



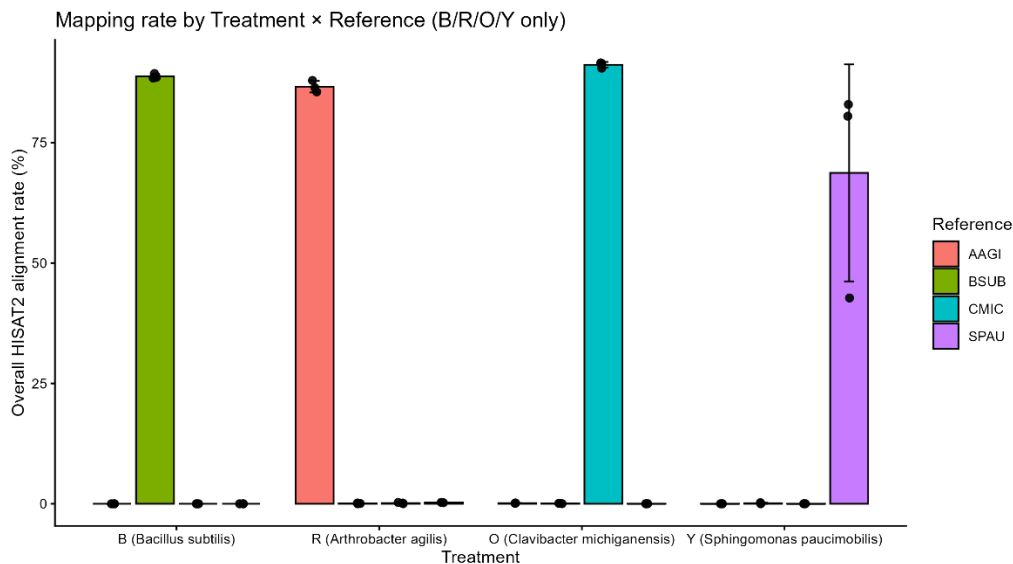
**Supplementary Figure S3.3.** Scatter plots showing the relationship between node degree and closeness centrality in inter-kingdom microbial networks of grapevine leaves across treatments and sampling time points. Each point represents an individual microbial OTU, with bacterial (Blue) and fungal (Yellow) taxa indicated by different symbols and colors. The pathogen is marked as red circle. Dashed horizontal lines denote the threshold (40) used to define highly connected nodes.



**Supplementary Figure S4.1.** Growth pattern of individual species (A-G) and xylanase activity (H) in different community composition. Each community composition include *A. agilis* (A), *C. michiganensis* (B), and *S. paucimobilis* (C) alone, *B. subtilis* co-cultured with *A. agilis* (D) and *C. michiganensis* (E) respectively, *B. subtilis* with *A. agilis*, and *S. paucimobilis* (F), and *B. subtilis* with *C. michiganensis* and *S. paucimobilis* (G). Error bars represent the standard deviation of biological replicates.



**Supplementary Figure S4.2.** Detection of extracellular xylanase secreted by *B. subtilis* (A) and relative expression of the *xynA* gene in *B. subtilis* measured by RNA-seq (C). The relative expression was calculated using DESeq2. Error bars represent the standard deviation of biological replicates



**Supplementary Figure S4.3.** Mapping rate of RNA-seq reads across bacterial monocultures and reference genomes. RNA-seq reads obtained from each bacterial monoculture were mapped against the reference genomes of four bacterial species (*B. subtilis*, *A. agilis*, *C. michiganensis*, and *S. paucimobilis*) to evaluate gene overlap among species. The x-axis indicates the bacterial monoculture from which RNA-seq reads were obtained, and the y-axis represents the overall alignment rate (%) calculated using HISAT2. Bar colors correspond to the reference genome used for read mapping. Error bars represent the standard deviation across biological replicates.

